Dissertation
submitted to the
Combined Faculties for the Natural Sciences and for Mathematics
of the Ruperto-Carola University of Heidelberg, Germany
for the degree of
Doctor of Natural Sciences

Presented by
M.Sc. (Virology) Divija Deshpande
Born in Mumbai, India

Oral-examination: 26th September 2017

Impairment in Proopiomelanocortin – Mu opioid receptor antinociceptive pathway contributes to Painful Diabetic Neuropathy

Referees: Prof. Dr. Ana Martin-Villalba

Prof. Dr. Peter Nawroth

To dearest Harshal, who was my saviour in the darkest of times

To my loving sister Prerana, who stood with me firmly all along

Acknowledgements

I am grateful to Prof. Dr. Dr. Peter Nawroth for giving me the opportunity to work on this project. His timely advice, criticism and praise have truly made the project, as well as me, as a scientist much better. I thank him for believing in me and supporting me financially.

I would like to acknowledge Prof. Dr. Ana Martin-Villalba for her support as a member of my advisory committee and as first referee of my thesis.

I am extremely thankful to Prof. Dr. Rohini Kuner for her tremendous support not only during TAC meeting, but also for carrying out difficult animal procedures. This project would not have been possible without her help.

I would like to also thank Dr. Thomas Fleming, my mentor, for his constant presence and for his fundamental support.

I offer my gratitude to Dr. Damir Krunic and Dr. Andreas Fischer who enabled me to use the Light Microscopy Facility at German Cancer Research Institute.

I would like to thank Dr. Varun Kumar and Dr. Nitin Agarwal for being always willing to share his knowledge with me.

Nadine Gehrig provided me incredible help with mouse DRG injections. I am so grateful to have worked with such a sincere person. Serap Kaymak, Axel Erhardt and Anja Buhl have provided constant support and help with experimental procedures. They made things easier for me and I cannot thank them enough.

I acknowledge the funding provided by my graduate school DIAMICOM and the opportunity to broaden my skills through my second graduate school, HBIGS.

I express my appreciation for my colleagues Alba, Itahisa, Johanna, Rajesh, Elizabeth and Jakob for making this journey easy and fun.

Lastly, I am hugely indebted to Harshal, Prerana, Ranjit, my mother and father, and last but not the least, Kaku, for providing constant encouragement

Abbreviations

APS	Ammonium peroxodisulphate
bp	Base pair
BSA	Bovine serum albumin
CD	Cluster of differentiation
cDNA	Complementary DNA
ChIP	Chromatin immunoprecipitation
CO_2	Carbon dioxide
CT	Cycle of threshold
DMEM	Dulbecco's Modified Eagles Medium
DMSO	Dimethyl sulfoxide
DNA	Deoxyribonucleic acid
dNTP	Deoxynucleotide triphosphate
DOR	Delta opioid receptor
DPN	Diabetic Peripheral Neuropathy
EDTA	Ethylenediaminetetraacetic acid
FCS	Fetal calf serum
FITC	Fluorescein isothiocynate
GPCR	G protein coupled receptor
H_2O_2	Hydrogen peroxide
HRP	Horseradish peroxidase
IF	Immunoflourescence
IHC	Immunohistochemistry
i.p.	Intraperitoneal
KOR	Kappa opioid receptor
kDa	Kilo Daltons
kbp	Kilo base pairs
M	Molar
mRNA	Messenger RNA
MOR	Mu opioid receptor
NADPH	Nicotinamide adenine dinucleotide phosphate-oxidase
NF-κB	Nuclear factor kappa-light-chain-enhancer of activated B cells
n.s.	Not significant
o/n	Overnight
OP	Opioid peptide
OR	Opioid receptor
PBS	Phosphate buffered saline
PCR	Polymerase chain reaction
PFA	Paraformaldehyde
pH	Pondus hydrogenii
qRT-PCR	Quantitative real-time PCR
RNA	Ribonucleic acid
RT	Room temperature
SDS-PAGE	Sodium dodecyl sulphate - polyacrylamide gel electrophoresis
STZ	Streptozotocin
T1D	Type 1 diabetes
T2D	Type 2 diabates
Taq	*Thermus acquaticus*
V	Volt
v/v	Volume to volume
WB	Western blot
WT	Wild type
w/v	Weight to volume

List of Tables

List of Figures

Table of Contents

1. Introduction

Diabetes is a major global epidemic of 21st century and has had a 50% increase in the incidence rate in the last ten years[1]. Yet, due to its virtue of being a '*slow and a silent killer*' it diminishes the alarm raised amongst the medical practitioners, researchers and therefore, most definitely, the pharmaceutical industry. Diabetes manifests initially as a seemingly harmless symptom of hyperglycaemia, and slowly progresses into the nearly irreversible late complications affecting the eyes (retinopathy), the kidney (nephropathy) and the nerves (neuropathy). With around 422 million adults suffering from diabetes around the globe, a risk of doubling this number by 2030[1], [2] and insufficient treatments to manage the devastating late complications, diabetes poses a considerable economic burden on the health services.

1.1 Diabetic peripheral neuropathy

During diabetes, the damage to the microvasculature results in the most debilitating late diabetic complication – diabetic neuropathy. More than 50% of the diabetic patients develop this complication[3]. Diabetic neuropathy can affect the autonomic, motor and sensory nerves of the peripheral nervous system. There is, however, a growing awareness of the damage occurring in the spinal cord and the peripheral nerves.

1.1.1 Clinical symptoms

During diabetes, the microvascular complications occur, which affect the nerves in the extremities leading to a sensorimotor neuropathy (hereon, referred to as diabetic peripheral neuropathy; DPN). DPN is a condition that starts as tingling or weakness in the most distal organs (fingers and more commonly toes) and progresses up the arms or legs in *glove and stocking manner*[4]. The sensory modalities are primarily affected rather than the motor nerves. As the small afferent nerve fibers are affected, the patient shows symptoms of excruciating pain, burning sensation or allodynia; ca.26% of diabetic patients suffer from such chronic painful symptoms[5]. As the disease progresses, large and small afferent nerve fibers are affected in varying degrees resulting in mixture of symptoms such as presence of numbness, loss of cold and vibration sensations and

episodes of sharp pain. However, at the later stages, the damage to the nerve fibers is extensive, while nerve regeneration is minimal, there is a loss of innervation in the limbs leading a continued loss of pain sensitivity[4]. Around 15% of the diabetic patients develop foot ulcers[6] as consequence of this loss in pain sensitivity and the occurrence of neuropathic ulcerations is associated with increased foot amputations and mortality[6,7].

1.1.2 Treatment

Significance of timely intervention is enunciated by the fact that up to 62% of patients suffering from DPN are detected with pre-diabetic condition[5]. However, due to a lack of adequate knowledge of the pathomechanisms underlying DPN, there exists no treatment that can address the sensory deficits. Thus, DPN can only be managed indirectly to some extent.

Since diabetes is characterized by hyperglycaemia, a control of blood glucose continues to be the primary treatment option for controlling DPN. However, the drawback of intensive glycemic control is the increased occurrence of episodes of hypoglycaemia with a risk of brain injury and even death. Moreover, normalizing blood glucose is not effective in reducing the incidence of neuropathic symptoms in type 2 diabetic patients and can only marginally restore the abnormal nerve functions in type 1 diabetic patients[3,8,9]. In fact, development of DPN in prediabetic patients shows that glucose control does not target the pathogenesis of DPN and hence is an ineffective treatment by itself. In addition, Gaede P. *et al* showed that a multifactorial intervention against hypertension, dyslipidemia and smoking along with aspirin and antioxidants was only effective against diabetes related cardiovascular disease, while no improvement in DPN was noted[10].

At present, only symptomatic relief in the form of analgesics, such as gabapentin, pregabalin and duloxetine, are available for the control of DPN. However, they do not show uniform effect in all DPN patients. Many patients are resistant to one or more analgesics [11]. Therefore, a combination of analgesics is prescribed, such as, gabapentin with opioids or nortryptiline. Yet, whether as a monotherapy or in combination, such drugs have shown a non-uniform effectiveness[12]. Moreover, these drugs have adverse

side effects of nausea, vomiting, CNS depression[13]. In addition, a sudden reduction in Hba1c due to the medications, can even precipitate a condition called 'treatment induced neuropathy' with severe anatomic and sensory defecits[14].

Thus, rather than managing the symptoms of DPN, it is crucial to develop therapeutic approaches targeting the pathogenesis of the condition. Understanding the mechanisms contributing to DPN is therefore of utmost importance.

1.2 Endogenous Opioid System

The metabolic disturbances caused by hyperglycaemia also have many consequences with inflammation being the most proximal one[15]. As such, attention has traditionally been focused on increased pro-algesic and pro-inflammatory mediators, such as cytokines, chemokines, and prostaglandins. However, there exists an innate system to counter pain and inflammation, known as the endogenous opioid system. The endogenous opioid system consists of an opioid receptor and an endogenous opioid ligand. Classically, three genetically distinct endogenous opioid precursors peptides have been identified: pro-opiomelanocortin (POMC), pro-enkephalin (PENK) and pro-dynorphin (PDYN). Upon proteolytic cleavage, these precursors produce opioid peptides which bind with highest affinity to the mu opioid receptor (MOR), delta opioid receptor (DOR), and kappa opioid receptor (KOR) respectively [16]. Three additional opioid peptides have been discovered; the endomorphin-1 and -2, which bind to MOR[17] and nociceptin, which binds to an opioid orphan like receptor 1[18]. In general, inflammatory cytokines, namely IL-1ß, cellular stress and increased neuronal excitation induce pathways that culminate in release of endogenous opioids. The classical opioids have a common N terminus, Tyr-Gly-Gly-Phe, which interacts with the opioid receptor. Binding of the endogenous ligand to its cognate opioid receptor triggers the anti-nociceptive signaling. The endogenous opioids are also important for protection against neuronal damage[16] and improve neuronal survival[19].

1.2.1 Endogenous opioids

(a) Pro-opiomelanocortin (POMC):

Gene and regulation: The POMC gene encodes a complex, multifunctional precursor peptide to many biologically active peptides with neuroendocrine modulatory activities, such as MSH, ACTH and ß-endorphin. The POMC gene was first discovered and cloned by Nakanishi in 1976[20]. Thereafter, using POMC gene deletion studies, the role of POMC and its derived peptides in food intake, regulation of body weight, adrenal function, and opiate activity was shown. Initially, it was thought that given the various functions assigned to POMC, there must exist more than one copy of the gene in the genome. However, only a single functional copy was isolated per haploid genome of human[21], cow[22], rat[23] and mouse[24].

Several POMC gene regulation studies were carried out in pituitary derived AtT-20 cell line. The POMC gene consists of three exons, with exon two and three coding for the precursor protein and N terminal signal sequence. One of the major regulators of POMC promoter is corticotropin-releasing hormone (CRH). CRH can activate POMC expression in multiple ways. CRH, by binding to its own receptor in the cell membrane, is able to indirectly stimulate POMC expression through recruitment of POMC activators. CRH-CRHR interaction activates adenyl cyclase, which increases cAMP level, in turn activating PKA. ERK signaling pathway is triggered by PKA, which recruits multiple POMC activators such as Nur, Tpit, and SRC family of co-activators. Additionally, CRH can also stimulate POMC gene expression by directly binding to the POMC promoter[25]. There are not many known negative regulators of POMC promoter, however, glucocorticoid has been confirmed as a suppressor[26], whilst NF-kB remains a much debated candidate[27,28].

POMC precursor processing and ß-endorphin: A 241 amino acid prohormone from human POMC gene is transcribed (235 in mouse; 78% sequence similarity). Following translation in the endoplasmic reticulum, POMC is packaged into vesicles and transported through the regulated secretory pathway, through trans golgi network. During this transport, different prohormone convertases cleave POMC at the basic residues, in a cell and tissue-specific manner. POMC derived peptides were associated

with different physiological activities using POMC$^{-/-}$ mice, *e.g.* N-POMC (48 amino acids) with mitogenic activity, MSH (13 amino acids) with a role in food intake, ACTH (17 amino acids) has a steriodogenic activity, whilst ß-endorphin (31 amino acids) shows analgesic properties [29]. (Figure 1)

When ß-endorphin was discovered in 1976, Feldberg *et al* showed that the opiate activity of ß-endorphin was so remarkable, it was hundred times more potent than the exogenous opioid, morphine[30]. The half life of ß-endorphin (37 minutes) being much longer[31] than any of the classical endogenous opioid peptides (less than 1 minute)[32,33]. But whilst being a highly potent analgesic effector, it can also induce *tolerance*.

(b) Pro-enkephalin (PENK)

Gene and regulation: Lewis *et al* discovered PENK in 1980 in the adrenal glands[34]. PENK gene is expressed during embryogenesis. Its expression is regulated developmentally and in a tissue specific manner. PENK gene expression is restricted upon terminal differentiation. The full-length precursor peptide is expressed by 4 exons, and includes an N terminal signal sequence.

In the 1980s, studies showed the PENK gene expression was regulated by change in electrical activity of adrenal cells. Potassium chloride treatment induced depolarization or calcium influx, elevated the PENK mRNA levels. This shows that neurotransmitters which increase the electrical activity, indirectly act as POMC promoter activators [35]. Calcium induced cAMP elevation, and thus, activated CREB binding to the promoter acts as a positive regulator for PENK[36]. Secondary messengers such as, calcium influx, cAMP and also PKC activation critically influences PENK gene regulation. It can also be transactivated by AP1 proteins including Fos and Jun[37]. On the other hand, factors that reduce excitability or induce cell differentiation (TGFß in osteoblasts) repress PENK gene[38].

PENK precursor processing and enkephalin: Human full length PENK is a 267 amino acid opioid peptide precursor (268 in mouse; 91% sequence similarity). This precursor contains a copy of leu-enkephalin and 4 copies of met-enkephalin (5 amino acids each). The enkephalins are produced from protelytic cleavages in the C terminal region of

PENK. The half-life of these pentapeptides is very short, and hence, a predominance of their larger, metabolically more stable predecessor peptides is often found [39]. Differential processing by prohormone convertases and furin, depending on the cell type and therefore variable levels of PENK intermediates can be found in different organs[40].

(c) Prodynorphin (PDYN):

Gene and regulation: The PDYN gene codes for the precursor prodynorphin (PDYN). The canonical form of PDYN mRNA consists of 4 exons, which encode the full-length protein. PDYN expression is found to be at negligibly low level in the neural component. In cell lines, basal PDYN expression was lower than *in vivo*, making it difficult to understand the regulatory mechanisms for PDYN gene. Therefore, mechanisms studied *in vivo* have revealed that the transcription factors AP-1 [41], CREB[36], cJun[42] are amongst the known factors that can activate PDYN gene expression whilst glucocorticoids and DREAM are negative regulators. NF-kB, as for POMC, can activate or repress the gene expression depending upon the subunits that bind the promoter [43]. While the cell lineage specific expression of PDYN is controlled by the transcription factors Ptf1a, Pax2, Lbx1 and others [44].

PDYN precursor processing and dynorphin: The human PDYN precursor protein is 254 amino acids in length (248 in mouse; 72% sequence similairty). Similar to POMC and PENK precursor peptides, PDYN protein undergoes a series of proteolytic cleavages by prohomone convertases and carboxypeptidase at the basic residues within PDYN to generate dynorphin A (17 amino acids) and dynorphin B (13 amino acids) and α neo-endorphin [45]. PDYN is also a potential precursor of leu-enkephalin, but it is interesting to note that in the cells expressing PDYN, dynorphins are detected but hardly any leu-enkephalin is detected. This indicates that each opioid precursor is cleaved preferentially, and not at every possible cleavage site [46]. Dynorphins have been known to possess opiate activity upon binding to opioid receptors, but also shows non-opioid functions such as modulation of reward response induced by addictive substances, motor regulation, and stress induced behavioral responses.

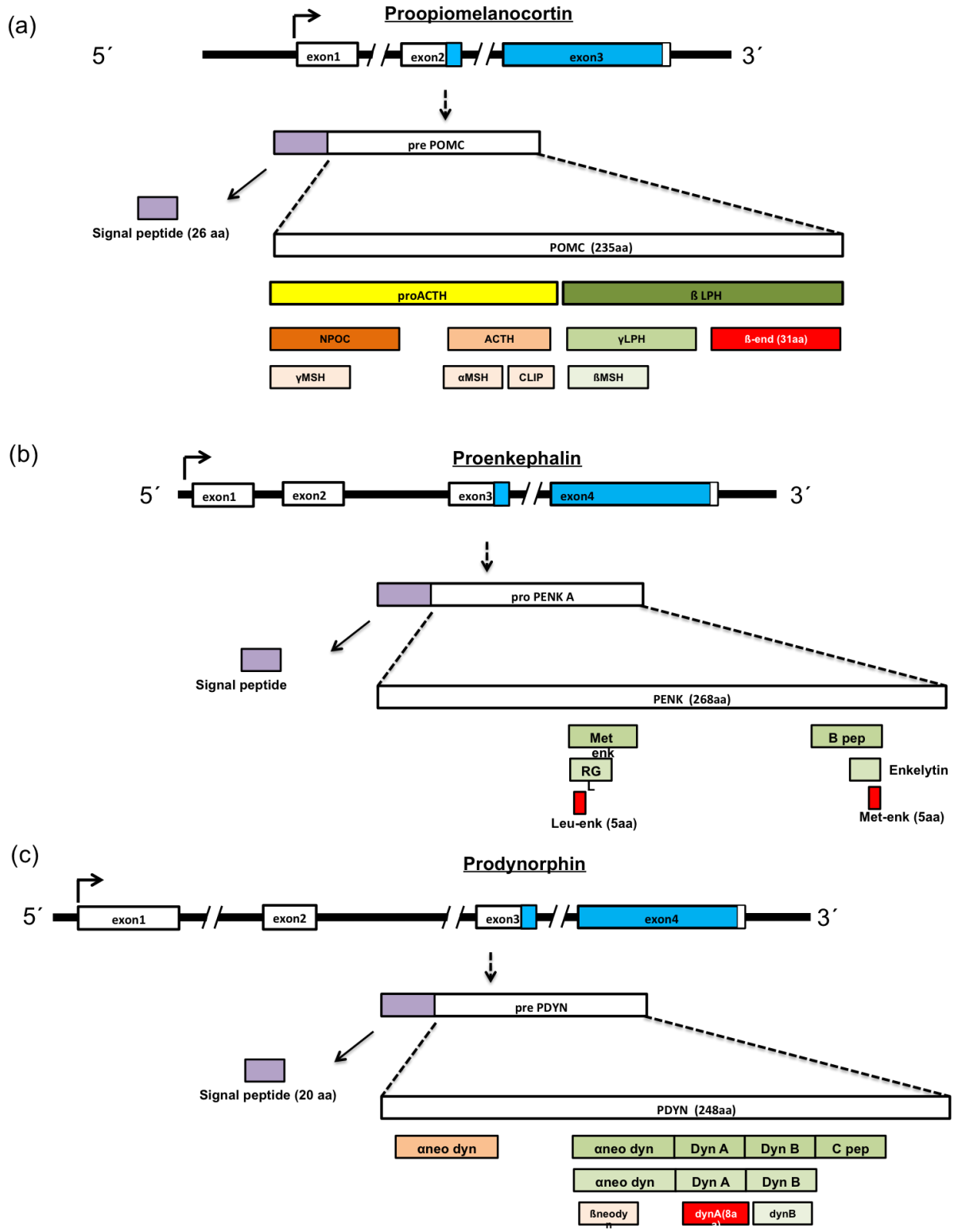

Figure 1: Precursor processing of opioid peptide precursors The opioid peptide precursors POMC, PENK and PDYN are transcribed from 3 different genes. The precursor peptides each consist of a signal peptide for sorting to the endoplasmic reticulum. The precursors are then packaged into secretory vescicles where they undergo proteolytic cleavages by the enzyme prohormone convertases to produce the mature opioid peptides ß-endorphin, leu and met-enkephalin and dynorphin respectively. *Modified from J Rossier; Biosynthesis of peptides; Neuropsychopharmacology; 1988*. Diagram not to scale.

1.2.2 Opioid receptors

There are 3 main types of opioid receptors –mu, kappa and delta receptors (abbreviated as MOR, KOR and DOR respectively). ε, σ and orphanin have also been described as non-classical opioid receptors[47]. Additional pharmacological subtypes may result from alternative splicing, post-translational modifications or receptor oligomerization[48].

MORs is transcribed from OPRM1 gene (324kbp-mouse & 307kbp-human). There are 18 known isoforms of MOR have found to exist as a result of alternate splicing. While many of the isoforms have no known cellular activity, other variants, such as MOR1D, underlie different behaviors, such as itching. However, MOR1 is the only isoform required for morphine induced analgesia, and hence, MOR1 the isoform of interest in the context of DPN [49]. The endogenous agonist for MOR is ß-endorphin.

KOR is transcribed from the gene OPRK1 (44kbp-mouse & 67kbp-human). OPRK1 gives rise to 6 mature mRNA variants. To date, only one KOR cDNA has been cloned[50]. KOR binds with highest affinity to dynorphin opioid peptide and also has some affinity to ß-endorphin[16].

DOR is transcribed from the gene OPRD1 (23kbp-mouse and 34kbp-human). DOR binds enkephalins with highest affinity [16].

The opioid receptors are expressed by central and peripheral nervous system, immune and ectodermal cells. The opioid receptors belong to the family of seven transmembrane G protein coupled receptors (GPCR).

1.2.3 Opioid receptor signaling

Upon binding to its respective ligand, opioid receptors trigger several downstream pathways that have varying effects, depending on the tissue in which the receptor is located. In context of DPN, the analgesic downstream signaling pathways by opioid receptor activation are of consequence. In principle, opioid receptor signaling is similar in all opioid receptors, however, there are certain differences pertaining to the regulation of signaling. Since most of the opioid analgesics used to treat painful diabetic

neuropathy exert their effect by binding to MOR, this thesis will have specific focus on understanding the signaling cascade of MOR and its regulation.

In the peripheral nervous system, MOR1 is localized in the soma of DRG neurons, dendrites and nerve terminals. MOR is said to be functional when it is present on the cell membrane, capable of binding to its ligands. In general, when an agonist (endogenous or exogenous) binds to a MOR, the receptor undergoes a conformational change that activates the heterotrimeric G proteins and signaling effectors at the plasma membrane. The Gβγ subunits then interact directly or indirectly to inhibit cAMP production by inhibition of adenylyl cyclise, inhibit Ca++ channels (N-, T- and P/Q type) and activate K+ channels (GIRKs – G protein coupled inwardly rectifying K+ channels). This leads to attenuated excitability of the neurons in the soma and reduced neurotransmitter release from the nerve terminals. For instance, release of substance P and CGRP is inhibited, both of which are proinflammatory and pro-nociceptive neuropeptides. Activation of peripheral opioid receptor also suppresses tetrodotoxin-resistant Na^+ channels[51], purinergic 2X receptor mediated currents [52], as well as TRPV1 currents [52].

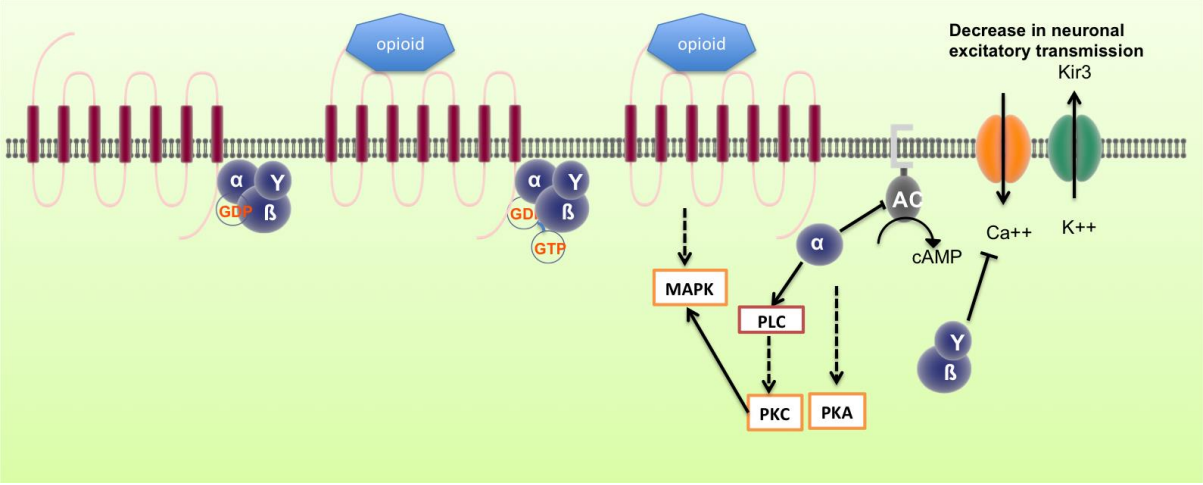

Figure 2: MOR signaling Under resting condition, MOR is associated with an inactive G protein. When an agonist binds to opioid receptor, G protein is phosphorylated, and α subunit is dissociated from ß, Y. A subunit then inhibits cAMP production while ßY subunits modulate the ion channels, which result in inhibition of pain and inflammation. Also other pathways such as, PKC, PKA and MAPK cascades are triggered upon activation of opioid receptors. *Modified from Hasani et al; Anaesthesiology; 2011.*

1.2.4 Regulation of opioid receptor function

MOR protein level is controlled by rate of transcription of the gene, but more relevant to pain related pathways, is the agonist-mediated regulation of receptor expression and its signaling efficiency. Depending on the type of the agonist and the length of exposure to it, the pharmacological properties of MOR can change. This change of functionality is mediated by MOR phosphorylation and it's sorting to intracellular compartments. For instance, following a short-term exposure of few seconds, the above-mentioned G protein coupled signaling pathways is triggered. However, upon a longer exposure of a few minutes to highly efficacious MOR agonists, such as ß-endorphin[53] or enkephalin[54] MOR is phosphorylated at the C terminal tail by G protein receptor kinase 2/3. This results in binding of ß-arrestin to the C terminus, which in turn leads to internalization of MOR into an endosome, via clathrin coated pit[55]. The receptor, now absent from the cell surface and unavailable to bind to ligands, is now said to be functionally desensitized. Since, phosphorylation of MOR by GRK requires a receptor conformational change induced by binding to its own ligand, this type of desensitization is termed as *homologous desensitization.*

Once inside the endosomes, MOR has two possible fates. First, the receptor can be dephosphorylated and recycled back to the surface, referred to as *resensitization*. The resensitized receptor is shown to be more potent in terms of cellular responsiveness to repeated or long exposure of opioids [56]. Second, following an exposure to excessive levels of agonist or a long term exposure (several hours), the recycling event described becomes impaired and the constantly desensitized MOR is eventually trafficked to the lysosomes anddegraded[54]. This reduces the total number of MOR present in a cell and therefore results in a prolonged attenuation of cellular responsiveness to the agonist. Persistent desensitization followed by presence of excessive levels or chronic exposure to an agonist is termed as *tolerance*. Resensitization protects the cell from excessive signaling by continued presence of the agonist and offers protection against tolerance [57].

However, MOR can also be phosphorylated without binding to its ligand. This is called *heterologous phosphorylation*. When binding to its ligand activates a GPCR proximal to

MOR, it triggers downstream signaling cascade. Kinases activated due to this GPCR can phosphorylate MOR and cause its desensitization. For example, Pfeiffer *et al*, showed that cross-phosphorylation and cross-internalization of MOR occurs when a co-expressed GPCR NK1 is activated[58]. This crosstalk is mediated by direct phosphorylation of MOR by protein kinase C (PKC). Involvement of PKC in agonist independent MOR desensitization was confirmed by Illing *et al* by showing that PKC activation by phorbol esters causes phosphorylation at the residue Threonine 370 in C terminus of MOR, while an exposure to exogenous MOR agonist DAMGO does not[59].

The regulation of MOR by agonist dependent and agonist independent pathways complicates the understanding of the MOR signaling in pain related pathways, but explains the non-uniform results given by different opioid analgesics.

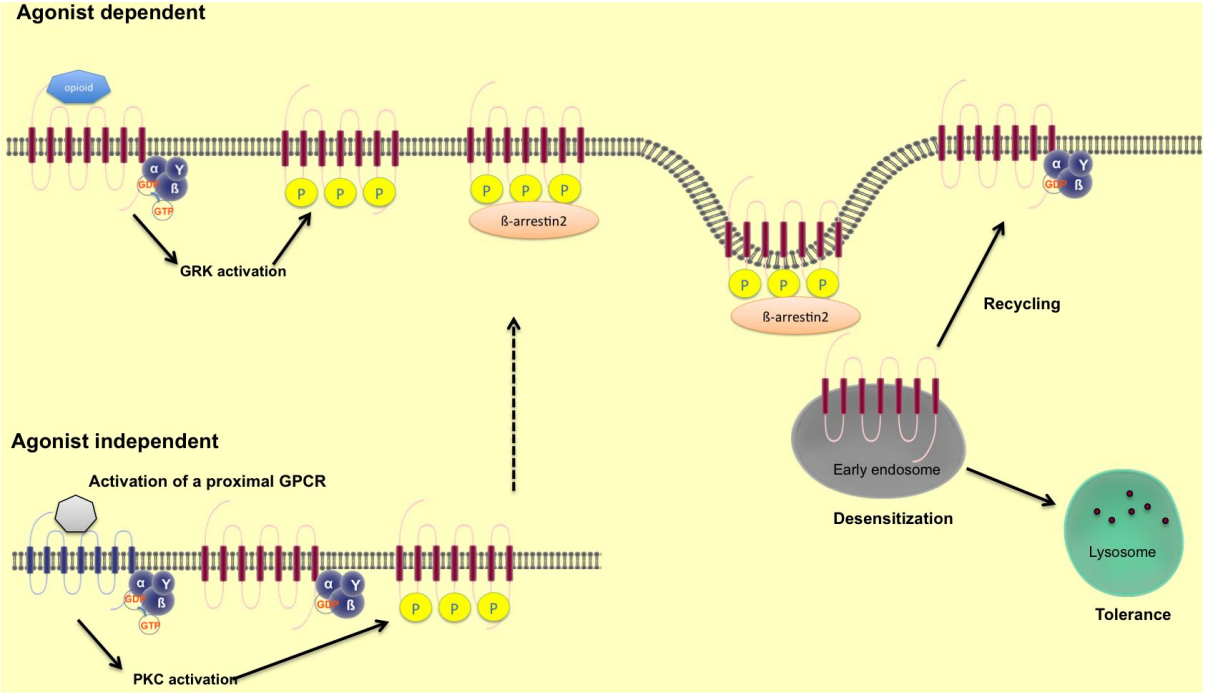

Figure 3: MOR trafficking Depending upon whether MOR is activated due to binding to its own agonist or because of activation of a proximal GPCR, MOR is phorphorylated by GRK or PKC respectively. After being phosphorylated, MOR is internalized due to arrestin binding. The desensitized MOR can now be recycled back to the surface or is degraded in lysosomes. MOR is traffickied to lysosomes in presence of excess of MOR agonists or prolonged exposure to the same. *Modified from Williams et al; Pharmacological Reviews; 2013.*

1.3 Tissue distribution of opioids, receptors and their physiological role

The endogenous opioid system has a widespread localization in different tissues and organs of the body. The endogenous opioids are located in the central nervous system, peripheral nervous system, immune cells, enteric nervous system, heart and skin. Depending upon the cell and tissue type, the opioids and receptors are differentially regulated and have specific functions.

1.3.1 Central nervous system

Within the brain and spinal cord, there is a differential organization of the endogenous opioid pathways. The ß-endorphin synthesizing neurons, designated as POMC neurons, are present predominantly in hypothalamus and dorsal medulla. PENK and PDYN are expressed locally in the multiple areas of the brain including the neocortex, hippocampus, hypothalamus, basal ganglia and superficial layers of dorsal horn and trigeminal nucleus caudalis. Similarly, opioid receptors too are differentially expressed in the cerebral cortex, limbic system, basal ganglia, brainstem, dorsal horn and dorsal root ganglia. Each individual opioid signaling pathway regulates different functions in the brain apart from supraspinal and spinal mechanisms of pain pathways. For instance, POMC plays a major role in glucose sensing, food intake, satiety[60]. MOR signaling also infleunces reward releated behavior[61], fear conditioning response[62] and anxiety behavior in rats[63]. Enkephalin- DOR pathway play an important role in neuroprotection from excitotoxicity[64]. Dynorphin-KOR signaling is implicated in stress pathways, anxiety and emotional distubances[65].

1.3.2 Peripheral Nervous System

It is been widely accepted that the majority of endogenous opioid peptide expression is only found in the central nervous system. Although, this remains correct, there have been studies, which have shown that endogenous opioids gene expression occurs in the dorsal root ganglia (DRG) and peripheral sensory nerves. mRNAs for all three opioids have been detected in DRGs[66–68], however there are few studies showing presence of opioid peptides in the DRG, but only one has looked at the functional contribution of opioid peptide(dynorphin)[69–71]. The MOR, DOR and KOR are expressed by neuronal cell

bodies located in the dorsal root ganglia (DRG) and transported to the nerve endings. The endogenous opioid receptor signaling in the peripheral nervous system is only and widely studied in the context of peripheral analgesia (discussed in section 1.4).

1.3.3 Immune cells

Opioid peptides, as well as receptors are also expressed in different immune cell populations, such as, granulocytes, monocytes/macrophages and lymphocytes. Several studies have shown that leukocytes express only a truncated form of POMC mRNA, but a mature mRNA expression could be induced under inflammatory conditions or by application of CRH. Liou *et al* showed that $Ly6G^+$ leukocytes, $CD3^+$ T cells and $Mac2^+$ macrophages expressed enkephalin. This study also showed colocalization of $CD45^+$ leukocytes with all three opioid peptides[72]. Opioid receptors are also expressed on the immune cells. Few studies have shown that all three opioid receptors are found to be expressed in the T and B lymphocytes. An evidence for occurrence of opioid receptor signaling in monocytes/macrophages, dendritic cells and even NK cells is shown via application of exogenous opioid receptor agonists [73]. Although, some studies argue that while expression of opioid receptors at an mRNA level is observed in the immune cells, detection of proteins is not certain due to lack of specific receptor antibodies[74].

Since the discovery of opioids in immune cells, focus has been on neuro-immuno crosstalk for modulation of pain sensitivity in the peripheral nervous system (section 1.4). However, recent evidence is emerging showing that exogenous opioid agonists have an immunomodulatory effect. Exogenous agonists are able to elicit immunomodulatory effects to varying degrees. A strong immunomodulation effect is afflicted by methadone, morphine, fentanyl while oxcycodone, tramadol and buprenorphine, not so much. The reason for this inconsistent effect is not well understood. Application of exogenous opioids has shown to affect splenic and thymic weight of rodents, T cell viability and function, leukocyte migration, number of macrophages, leukocyte-endothelial adhesion, cytokine production, superoxide production and activity of NK cells[74]. However, the exact reason for the expression of endogenous opioids in immune cells and their effect on immune system is not studied.

1.3.4 Peripheral organ systems

Cardiovascular system: All the three opioids have been detected in heart. They are present in the myocardial cells as well as the sympathetic innervation of the heart[75–77]. Activation of MOR signaling in the heart has been shown to modulate cardiovascular function leading to suppression of stress induced blood pressure and heart rate, urination and inhibition of systemic arterial pressure. While DOR and KOR activation protects the heart against ischemic injury[78].

Gastrointestinal system: Opioids and the receptors are primarily localized in the enteric nervous system and can regulate the digestion process. The release of opioids in the gut and binding to their respective receptors, results in the control of gut motility and digestive secretions. The gut opioid system is complex. It is able to provoke excitatory neural circuits or induce the inhibitory circuits. As a result, activation of opioid receptor signaling may either result in gut muscle relaxation or spasms[79].

Skin: Opioid expression is found in skin melanocytes and keratinocytes. The cutaneous opioid system is able to regulate epidermal cell proliferation. It can also regulate epidermal homeostasis. The wound healing process is also influenced by activation of opioid signaling[80].

1.4 Neuropathic pain modulation by endogenous opioid system

Neuropathic pain is a chronic pain triggered by conditions that directly affect the functioning of the somatosensory system. It can be caused by nerve injury due to trauma, such as amputations or peripheral nervous system diseases, such as diabetes or herpes zoster. The characteristic of neuropathic pain is that it is able to persist long after the cause has ceased. It hence can be considered as a disease in its own right. The pathophysiology has been considered to be the consequence of persistent inflammation at the site of nerve injury and dysfunctional transmission of nerve impulses.

Immune system activation and mobilization is closely associated with inflammation. Due to the inflammatory signals expressed at the site of injury (ICAM-1 upregulation),

immune cells are recruited to the site of inflammation and infiltrate the tissue. Subsequently, these immune cells become activated and secrete chemotactic factors resulting in the attraction and infiltration of more immune cells to the site of inflammation. Immune cells secrete pro-inflammatory (IL-1ß, IL-6 etc.) and anti-inflammatory (IL-10, IL-4) cytokines, which can modulate pain sensitivity in the peripheral nervous system. The involvement of immune system in neuropathic pain was proposed to contribute to neuropathic pain.

However, a direct neuro-immune crosstalk in neuropathic pain was revealed upon the discovery of endogenous opioid expression in immune cells. Animal models with peripheral nerve injury have been used to show that cells of the activated immune system can infiltrate the peripheral nerves in response to inflammatory signals released by the damaged nerve. Schafer *et al* showed for the first time that CRH and IL-1ß treatment releases the endogenous opioids from immune cells *in vitro*[81]. Thereafter, Liou *et al* showed that nerve injury causes release of CRH, which in turn in able to induce opioid release from infiltrating immune cells[72]. Endogenous opioids released by the immune cells are able to act as analgesic mediators, relieving painful symptoms. Several studies have reported the presence of immune cell derived opioids in the injured nerve and a correlation with reduction of thermal and mechanical hyperalgesia [72,82–84].

Immune cells have therefore been the primary focus in nerve injury models as the major source of opioids. However, evidence of expression of opioids in the DRGs also exists. Few studies however have addressed the significance of neuron-derived opioids in neuropathic pain models. In 2009, Obara *et al* showed that PENK mRNA was downregulated in the DRGs or mice with hindpaw inflammation. The study also showed increase in PDYN following chronic constriction injury [68]. The importance of neuron-derived opioid was asserted by reduction in thermal hyperalgesia and improved locomotion upon overexpressing PENK in DRG cells of polyarthritic rats [67]. However, the importance of neuron-derived endogenous opioids in neuropathic pain models without a direct physical injury to the nerves remains unknown.

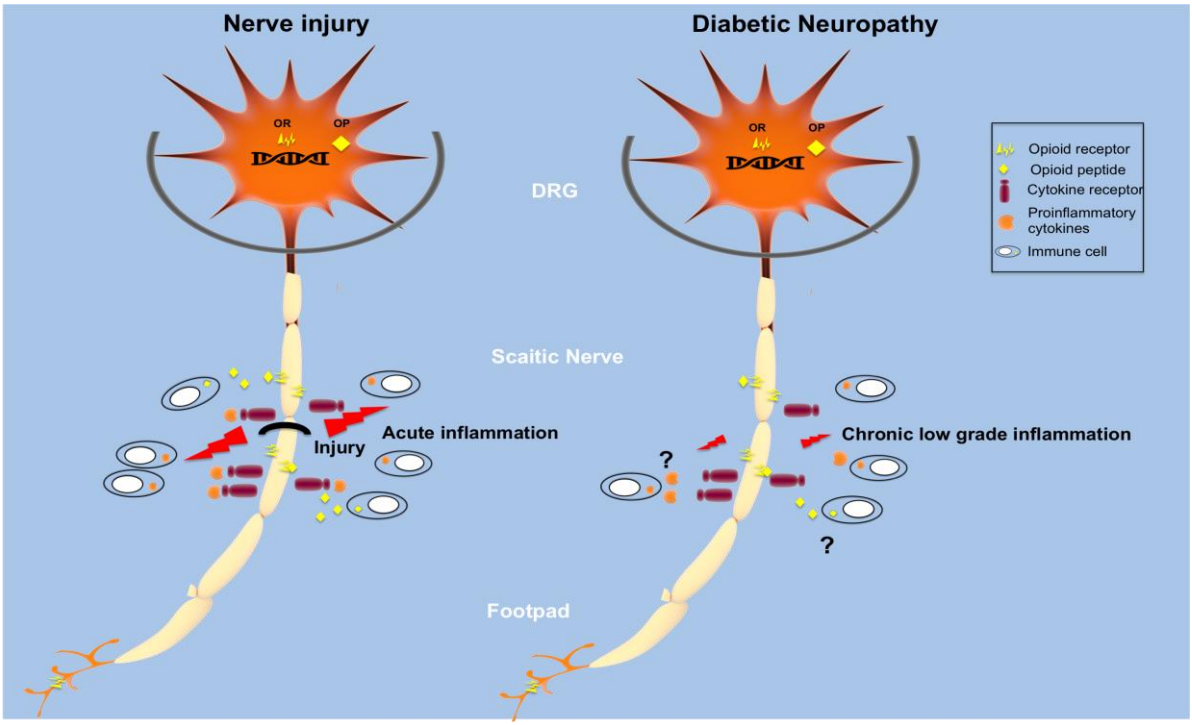

Figure 4: Neuroimmune crosstalk during neuropathic pain In Injury induced neuropathic pain models, there is an acute inflammation leading to recruitment of immune cells from blood vessels to the site of injury. Using overexpressed ICAM-1 receptor, immune cells infiltrate the injured nerve trunk. The immune cells secrete proinflammatory cytokines and also opioid peptides, which bind to the cytokine receptors and opioid receptors respectively. DPN is metabolic model for neuropathic pain. A persistent low-grade inflammation due to metabolic disturbances is present during diabetes. Whether opioid/cytokine containing immune cells are able to influence DPN remains unknown. *Modified from Stein et al; Pharmacological Reviews; 2011.*

1.5 Endogenous opioid system, diseases and implications in diabetes

Endogenous opioids and their respective receptors have diverse physiological roles in different organ systems. The deficiency or an excess of any component of the opioid system would not only translate into aberrant pain sensitivities but also result significant pathophysiological consequences.

POMC deficiency caused by mutations in the gene causes seizures, excessive feeding and severe obesity beginning from first year after birth. The resulting adrenal insufficiency can have severe life threatening consequences. A similar phenotype has been noted in POMC$^{-/-}$ mice[85]. A decrease in POMC derived ß-endorphins in leukocytes contributes to systemic inflammation in Crohn's disease[86] In fact, there are implications of ß-endorphin in autoimmune disorders. ß-enorphins and enkephalins have also been implicated in the pathophysiology Parkinson's disease[8788], Huntington chorea[89], RLS[90]

and Tourette's[91] patients. Imbalance in the opioid system in the gut, specially, enkephalin, underlies the pathology of opioid bowel syndrome with symptoms of idiopathic constipation or diarrhoea and abdominal pain[92].

Excessive opioid signaling is also detrimental. Increased level of dynorphins, and therefore, increased KOR signaling, is thought to contribute to the pathogenesis of Alzheimer's disease impairing cognition and inducing neurodegeneration [93]. Increased POMC expression is associated with Addison's disease, polycystic ovarian syndrome[94] autism[95].

1.5.1 Endogenous opioids and diabetes

Until the 1990s, there were several studies in experimental diabetes models showing changes in the endogenous opioid system during diabetes. Nearly all of them have measured opioid levels in the plasma or in the central nervous system. Forman *et al* showed that after 4 weeks of STZ injection (type 1 diabetes model), there was a significant decrease in the pituitary and hypothalamus of female rats. The decrease was not attributed to an STZ injection effect because the authors argued that STZ was not administered intracerebrovetricularly [96]. The same group showed persistence of low ß-endorphin levels 8 weeks post STZ induction in the plasma of female rats[97]. Both Taylor *et al* and Cheung *et al* showed that male mice showed lower ß-endorphin levels in the anterior pituitary and neurointermediate lobe after 1 week of STZ injection. The males and female mice showed different degrees of the lowering effect of STZ on ß-endorphin[98]. Similar changes were also shown in enkephalin and dynorphin in non-STZ diabetic mouse models.

Greenberg *et al* showed changes in met-enkephalin in pituitaries of male db/db mice[99]. Timmers *et al* showed that in the db/db mice, enkephalin and endorphin level in pituitary and pancreas respectively, decreased in the initial weeks, but as the obesity set in, the opioid levels were higher than the lean littermates[100].Dynorphins were shown to be higher in the brains of STZ treated male rats[101].

There also were studies translating the results observed in mouse and rat models into humans. Fallucca *et al* reported a decreased met-enkephalin level in the plasma of

diabetic patients with neuropathy, even if the neuropathy was asymptomatic. The authors reasoned the effect of plasma met enkephalin in metabolic disturbances rather pain modulation during diabetes[102]. Tsigos *et al* showed that ß-endorphin levels were decreased in diabetic patients regardless of neuropathy symptoms. It was also shown that CSF ß-endorphin levels did not correlate with pain sensitivity.

From the existing data, one can conclude that although changes in the endogenous opioids may be expected during diabetes, in order to understand the relevance of endogenous opioids in pain modulation, the expression of opioids must be studied in the peripheral nervous system rather than in the plasma or brain. Juranek *et al* showed that STZ mice, upon nerve crush injury, shown an increase in infiltrating immune cells in the nerves. These immune cells were reported to be pro-inflammatory macrophages[103]. Another report by Liou *et al*, has studied opioid expression in diabetic nerves after crush injury. The authors demonstrated that the infiltrating immune cells in the nerves of NOD mice after injury, expressed of opioid peptides and helped alleviate pain[72]. A single study, to date, exists showing increased basal dynorphin level and KOR in the peripheral nervous system of STZ treated female rats without an external injury[78].

MOR expression in the PNS during diabetes has been studied in order understand the poor efficiencies of exogenous opioid analgesics. [104–106]. MOR is reported to be upregulated in the PNS during inflammation and injury induced neuropathic pain [107]. Surprisingly, in DPN, there are some reports that show decreased MOR signaling, increased G protein uncoupling and desensitization[106,108].

Thus far, it is evident that though there is a vast knowledge on opioid expression post nerve injury, there is very little information on the changes in endogenous opioid system in the nerves during diabetes.

1.6 Aims of the project

Given that endogenous opioids can modulate pain sensitivity and that the CNS derived peptides may not directly influence peripheral pain sensitivity, it is worthwhile to investigate, the yet unclear, relevance of endogenous opioid system to the pathogenesis of DPN.

Opioid expression in the PNS has always been studied within the context of nerve injury in animal models, wherein, infiltrating immune cells are the source of opioids. In order to study the endogenous opioids system in context of DPN, first it was important to establish whether the opioids peptides are expressed in the PNS in absence of external nerve injury. The next objective was to determine if immune cells in the sciatic nerve are the source of endogenous opioids in DPN, as during nerve injury.

If the presence of opioids was detected in the PNS in diabetic mice, the most important question was whether a change in expression of any of the opioids and their receptor was observed and what is the mechanism that may contribute to the alterations. Lastly, it was crucial to determine the functional consequences of changes in the endogenous opioids in diabetic peripheral neuropathy.

2. Materials & Methods

2.1 Materials

2.1.1 Chemicals and Reagents

Agarose, Ultra Pure	Roth, Karlsruhe, Germany
Ammonium Hydroxide	Sigma-Aldrich, Taufkirchen, Germany
Bovine Serum Albumin (BSA)	Promega, Mannheim, Germany
Bovine Serum Albumin, fraction V	Sigma-Aldrich, Taufkirchen, Germany
Bradford reagent	Biorad, Taufkirchen, Germany
Chloroform	Sigma-Aldrich, Taufkirchen, Germany
Corticotropin releasing hormone (CRH)	Sigma-Aldrich, Taufkirchen, Germany
DNAseI	Sigma-Aldrich, Taufkirchen, Germany
2´-Deoxynucleoside 5´-triphosphates (dNTPs)	Fermentas, St. Leon-Rot, Germany
Dimethyl Sulfoxide (DMSO)	Roth, Karlsruhe, Germany
EDTA	Sigma-Aldrich, Taufkirchen, Germany
Ethanol	Sigma-Aldrich, Taufkirchen, Germany
Ethidium Bromide	Sigma-Aldrich, Taufkirchen, Germany
Glycerol	Sigma-Aldrich, Taufkirchen, Germany
Gö6983 (PKC kinase inhibitor)	Santa Cruz Biotechnology, HD, Germany
Vent DNA polymerase	NEB, Mannheim, Germany
Isopropanol	Sigma-Aldrich, Taufkirchen, Germany
KCl (potassium chloride)	Roth, Karlsruhe, Germany
Low range DNA ladder,	Fermentas, St. Leon-Rot, Germany
Magnesium Chloride	Sigma-Aldrich, Taufkirchen, Germany
Mass Ruler, 1 Kb DNA Ladder,	Fermentas, St. Leon-Rot, Germany

2-Mercaptoethanol	Sigma-Aldrich, Taufkirchen, Germany
Methanol	Roth, Karlsruhe, Germany
Micrococcal nucelase	Cell signaling, Denver, USA
Milk Powder	Roth, Karlsruhe, Germany
NaCl (sodium chloride)	Sigma-Aldrich, Taufkirchen, Germany
Na-deoxycholate	Sigma-Aldrich, Taufkirchen, Germany
Na-fluoride	Sigma-Aldrich, Taufkirchen, Germany
Na-orthovandate	Sigma-Aldrich, Taufkirchen, Germany
Nonidet-p40 (NP-40)	Sigma-Aldrich, Taufkirchen, Germany
Pre-stained protein marker	Invitrogen, Karlsruhe, Germany
Phenol	Roth, Karlsruhe, Germany
Phosphatase inhibitor	ThermoScientific, Waltham , USA
PMSF	Sigma-Aldrich, Taufkirchen, Germany
Primers	MWG, Germany
Proteinase K	Sigma-Aldrich, Taufkirchen, Germany
Protein A/G agarose beads	Santa Cruz Biotechnology, HD, Germany
Protease Inhibitor Cocktail	Sigma-Aldrich, Taufkirchen, Germany
Sodium Acetate	Sigma-Aldrich, Taufkirchen, Germany
Sodium Chloride	Sigma-Aldrich, Taufkirchen, Germany
Sodium Dodecyl Sulfate (SDS)	Sigma-Aldrich, Taufkirchen, Germany
TEMED	Sigma-Aldrich, Taufkirchen, Germany
Tween-20	Roth, Karlsruhe, Germany
Tris-base	Roth, Karlsruhe, Germany
TRIZOL	Invitrogen, Karlsruhe, Germany

Table 1: Chemicals and reagents

2.1.2 Mouse Models

C57BL/6; females; streptozotocin induction (T1D mouse model)	Charles River Laboratories, Inc., Wilmington, MA, USA

Table 2: Mouse model

2.1.3 Cells

AtT20 cells	Sigma-Aldrich, Taufkirchen, Germany
Primary DRG culture from WT C57Bl/6 mice	Generated by our group
HEK293T Cells	Sigma-Aldrich, Taufkirchen, Germany

Table 3: Cell lines and primary cells

2.1.4 Cell culture medium components

DMEM with L-glutamine	Life Technologies, Darmstadt, Germany
Ham's F10 Nutrient medium	Life Technologies, Darmstadt, Germany
DMEM/F10 with L-glutamine	Life Technologies, Darmstadt, Germany
1x Dulbecco's PBS without Ca and Mg	Sigma-Aldrich, Taufkirchen, Germany
Foetal calf Serum Std Quality, EU approved	PAA laboratories, Pasching, Austria
Horse serum, EU approved	Sigma-Aldrich, Taufkirchen, Germany
100x Penicillin / Streptomycin	PAA laboratories, Pasching, Austria
0.05 % Trypsin and 0.05 % EDTA	PAA laboratories, Pasching, Austria

Table 4: Cell culture medium components

2.1.5 Cell Culture Media

AtT20 culture media

Ham'sF10	500ml
Horse serum	15%
FCS	2.5%
Penicillin/streptomycin	50 µg/ml
Amphotericin B	50 µg/ml

L-glutamine	2mM

Table 5: AtT20 cell culture medium preparation

HEK 293 culture media

DMEM 1gm/l Glucose	500ml
FCS	10%
NEAA	1%
Pencillin/streptomycin	50 µg/ml
Amphotericin B	50 µg/ml
L-glutamine	2mM

Table 6: HEK 293 cell culture medium preparation

DRG culture media

DMEM/F10 4.5gm/l Glucose	500ml
Horse serum	10%
NEAA	1%
Pencillin/streptomycin	50 µg/ml
Amphotericin B	50 µg/ml
L-glutamine	2mM

Table 7: Primary DRG culture medium preparation

2.1.6 Antibodies

Antibody	Species	Supplier	Application
ß-actin	Rabbit	4967 (Cell signaling)	WB
CD11b-Biotin	Rat	101203 (Biolegend)	IF
CD45	Rat	103101 (Biolegend)	IF
Endorphin	Rabbit	AB5028(Chemicon)	IF
Enkephalin	Rabbit	T-4293 (Peninsula)	IF
Dynorphin	Rabbit	Ab82509 (Abcam)	IF
Iba-1	Rabbit	019-19741 (Wako)	IF
Lamp1	Rat	12601 (Biolegend)	IF
MOR	Rabbit	RA10104 (Neuromics)	IF, WB
mCherry	Goat	AB0040-20 (Sicgen)	IF
NF-kB p65	Goat	Sc-109x (Santa Cruz)	EMSA
NF-KB p65	Goat	100-4165 (Rockland)	ChIP, WB
NF-kB p52	Rabbit	Sc-848x (Santa Cruz)	EMSA
NF-kB p52	Rabbit	Ab175192 (Abcam)	ChIP, WB

NF-kB p50	Rabbit	Sc-114x(Santa Cruz)	EMSA
NF-kB p50	Rabbit	Ab32360 (Abcam)	ChIP, WB, IF
NF-kB cRel	Rabbit	Sc-70x (Santa Cruz)	EMSA, WB
NF-kB cRel	Rabbit	PA5-47370 (Invitrogen)	ChIP
NF-kB Rel B	Rabbit	Sc-226 (Santa Cruz)	ChIP
Pan PKC	Rabbit	SAB4502356 (Sigma)	IF
Pan opioid	Mouse	MAB5276 (Millipore)	IF, WB
PGP9.5	Rabbit	AB5925 (Millipore)	IP
PGP9.5	Guinea	GP101014 (Neuromics)	IF
POMC	Goat	PA5 18368 (Thermo	IF, WB
RNA polymerase	Mouse	8WG16/MMS-126R	ChIP
Tuj1	Rabbit	T2200 (Sigma)	IF
Secondary antibodies			
Anti Goat-HRP	Donkey	sc-2033 (Santa cruz)	WB
Anti Rabbit IgG-HRP	Goat	7074(Cell Signaling)	WB
Anti mouse IgG-HRP	Horse	7076 (Cell signaling)	WB
Anti Goat-Alexa-647	Donkey	Ab150139 (Abcam)	IF
Anti-Goat-FITC	Donkey	705-095-003 (Jackson)	IF
Anti-Goat-TRITC	Donkey	705-025-003 (Jackson)	IF
Anti mouse-Alexa-647	Donkey	4410 S (Cell signaling)	IF
Anti-mouse-Alexa-488	Goat	A11001 (Thermo Fischer)	IF
Anti Rabbit-Alexa-555	Donkey	Ab150074 (Abcam)	IF
Anti Rabbit-Alexa-488	Goat	4412S(Cell signaling)	IF
Anti-Rabbit-Alexa-647	Goat	4410S (Cell signaling)	IF
Anti-Guinea Pig-Alexa-	Goat	SAB 4600180(Sigma)	IF

Table 8: Primary and secondary antibodies

2.1.7 Kits

ChIP kit	EMD Millipore Corporation, Billerica, MA
ELISA kit	Phoenix Pharmaceuticals, Arizona, USA
ECL reagent	GE Healthcare EU GmbH, Freiburg, Germany
PKC kinase activity kit	Enzo Lifesciences, Lörrach, Germany
QIAGEN Plasmid Plus Maxi and Mini Kit	Qiagen, Hilden, Germany
GenElute™ Gel Extraction Kit	Sigma-Aldrich, Taufkirchen, Germany

Table 9: Kits

2.1.8 Buffers and solutions

(a) Western Blotting

RIPA buffer for whole tissue lysates

Tris-Cl(pH=8)	50mM
NP 40	1%
Na deoxycholate	0.5%
NaCl	150mM
Dithiothreitol	0.1mM
PMSF	10 μg/ml
Benzonase	1 unit/ml

SDS stacking gel buffer

Tris-Cl	1.5M
SDS	0.4%

**Adjust pH to 6.8

SDS resolving gel buffer

Tris-Cl	1.0M
SDS	0.4%

**Adjust pH to 6.8

5x SDS running buffer

Tris	25M
SDS	5%
Glycine	1.25mM

1x SDS sample buffer

Tris-Cl(pH=6.8)	62.5mM
SDS	2%
Glycerol	10%
Bromophenol blue	0.01%
Dithiothreitol	50mM

Transfer buffer

Tris	20M
Methanol	20%
Glycine	150mM

Blocking buffer

PBS	100ml
Milk powder	5g
Tween20(v/v)	0.05%

Washing buffer

PBS	100ml
Tween20(v/v)	0.05%

2.1.8 Equipment

BioDoc Station	Biometra, Goettingen, Germany
Blot chamber	Trans-Blot Electrophoretic Transfer Cell, Biorad Laboratories, Germany
Cell culture flasks and dishes	Becton Dickinson, Heidelberg, Germany
Cover slips for cell culture	Paul Marienfeld GMBH & Co.KG, Lauda-Königshofen, Germany
Centrifuge-labofuge-400R	Heraeus, M & S laborgeräte GMBH, Wiesloch, Germany
CF 100 pulse generator	Biochemical Laboratory Service, Budapest, Hungary
Developer (for western blot)	CURIX 60, Agfa
Neon Electroporation unit	Thermo Fischer Scientific, Waltham, USA
Hettich-Table Centrifuge	GMI, Inc, Minnesota, USA
High speed ultracentrifuge	Beckman Coulter GMBH, Krefeld, Germany
Hotplate	Ugo Basile, Monvalle, Italy
Hargreaves	Ugo Basile, Monvalle, Italy
Immobilon-P Transfer Membrane	Millipore Corporation, Billerica, MA
Mechanical Plantar Anaesthesiometer	Ugo Basile, Monvalle, Italy
Microscope, flourescence	Nikon, Amsterdam, Netherlands
Microscope, confocal: LSM700, LSM780	Carl Zeiss NTS, Oberkochen/Germany
Microplate reader	BMG Labtech, Ortenberg, Germany
Power supply unit	Biorad Laboratories, Germany
Pipettes	Gilson Pipetman, Gilson, Germany
Pipettes, pipette tips and falcon tubes	Finnpipp, Germany
Spectrophotometer	BIO-TEK-Instruments, Inc, Vermont, USA
T3000 Thermocycler	Biometra, Goettingen, Germany
Von Frey filaments	Stoelting, Illinois, USA
X-ray film	GE Healthcare EU GmbH, Freiburg, Germany

Table 10: Instruments

2.1.9 DNA oligonucleotides

Name	Application	Sequence
Actin_forward	qPCR	GGC TGT ATT CCC CTC CAT CG
Actin_reverse	qPCR	CCA GTT GGT AAC AAT GCC ATG T
18srRNA_forward	qPCR	GTA ACC CGT TGA ACC CCA TT
18srRNA_reverse	qPCR	CCA TCC AAT CGG TAG TAG CG
POMC_forward	qPCR	ATGCCGAGATTCTGCTACAGT
POMC_reverse	qPCR	TCCAGCGAGAGGTCGAGTTT
PENK_forward	qPCR	TGCGCTAAATGCACGTACC
PENK_reverse	qPCR	TCCCAGATTTTGAAAGAAGGCAG
PDYN_forward	qPCR	CTCCTCGTGATGCCCTCTAAT
PDYN_reverse	qPCR	AGGGAGCAAATCAGGGGGT
MOR_forward	qPCR	TCCGACTCATGTTGAAAAACCC
MOR_reverse	qPCR	CCTTCCCCGGATTCCTGTCT
NF-kB consensus	EMSA	E329a (Promega)
POMC promoter_forward	ChIP	AGTTCTTCCTAACCACCAGCGCC
POMC promoter_reverse	ChIP	TATACTTGCAGGGTTGGGTGGGTG
GAPDH_forward	ChIP	CAGCCGGAGTTCTTAACCAG
GAPDH_reverse	ChIP	CTGCCAATCCTGATGGACTAA
FlagMOR_forward	Cloning	ACGTACGAATTCTGATTCGAGCTCGCCCCGCCCCCAG
FlagMOR_reverse	Cloning	GATCCGCGG GGGCAATGGAGCAGTTTCTGCTTCCGCA

Table 11: Oligonucucleotide sequences

2.2. Methods

2.2.1 Animal Experimentation

(a) 3.1.1 Animals

C57/Bl6 female mice, obtained from Charles River, USA were used throughout this study. The mice were housed in groups of four and a 12h/12h light / dark cycle with always exposed to free access to food and water. The procedure of the experiments was approved by the Animal care and use committees at the Regierungsspräsidien Tubingen and Karlsruhe, Germany (35-9185.81/G-90/0435-9185.81/G-182/08).

(b) 3.1.2 Experimental groups, diabetes induction and monitoring

Diabetes was induced in the 8 weeks old mice by intra-peritoneal administration of Streptozotocin (50mg/kg) on 6 subsequent days. Insulin supplementation was started as soon as the blood glucose levels reached 300mg/dL. An initial time course study was conducted in order to study the expression of all three endogenous opioids. For this, 4, 8 and 12 weeks post STZ induction were chosen as the time points of interest. For each time point, 4 diabetic and 4 age matched non-diabetic mice were included. There onwards, each study was conducted at 12 weeks post STZ induction. For each study at this time point included 5-6 mice in the diabetic and 5-6 mice in the control group. The mice were continuously monitored by measuring blood glucose levels and body weight. Intradermal insulin (Lantus, Aventis) injections were given when the glucose levels were more than 350mg/dL. Blood glucose, body weights and Hba1c measurements were used as parameters to verify diabetic status of the mice. At the desired time point, the mice were sacrificed, perfused and organs (lumbar DRG, sciatic nerves and footpads) were dissected for further analysis.

(c) 3.1.3 Behavioral testing

Before sacrificing the mice, thermal and mechanical hyperalgesia were measured. Thermal pain sensitivity was measured using hotplate and Hargreaves, while Von Frey filaments were used to measure mechanical pain sensitivity.

Hotplate: The mouse was dropped on a hotplate at 50°C. A stopwatch was immediately started. The mouse was closely monitored for signs of distress, such as, licking of paw or lifting of paw. As soon as these signs were seen, the stopwatch was stopped and the

mouse was lifted from the hotplate. The timings were recorded for each mouse thrice[109].

Hargreaves: The mice were placed in the chambers of the Hargreaves apparatus for an hour for three consecutive days for acclimatization. On the fourth day, Hargreaves measurements were carried out after fifteen minutes of acclimatization. The laser beam was placed under the left paw and the timing was recorded until the mouse its paw. The same was recorded for the right paws. Five readings were taken per mouse, per paw[110].

Von Frey filaments: The mice were dropped in the mechanical pain testing apparatus-transparent cages with a wire mesh at the bottom. After acclimatization for an hour, each paw of the mice was stimulated with filaments of the strengths 0.16g, 0.4g, 0.6g, 1.4g, 2g. Each paw was stimulated five times[111].

For each test, the mean recording of diabetic group was compared with those of the control group. Student's t-test was used as the statistical measure to determine the significance of the difference.

2.2.2 Ex vivo methods

(a) Western blotting

Lysate preparation: After sacrifice and perfusion of the mice with ice-cold PBS, lumbar DRGs(n=12) , sciatic nerves(n=2), footpads(n=2) from each mouse were snap frozen in liquid nitrogen. The organs were then crushed mechanically using the glass pestle, also frozen in liguid nitrogen. Once a powder was obtained, upto 100 µl of ice cold RIPA buffer was added to the the tubes. The tubes were incubated on ice for 60 minutes. The lysates were then centrifuged at 20,000g for 30 minutes at 4°C. The supernatant containing proteins was carefully pipetted out into a new tube and placed immediately on ice. The proteins were then quantified using the Bradford assay.

Immunoblotting: Equal amount of protein samples were electrophoretically separated on SDS Polyacrylamide gels and transferred to PVDF membranes. Following blocking, (room temperature, 1 hour) the membrane was incubated with primary antibody at appropriate dilution made in blocking buffer (4°C, overnight) with continuous shaking. The membrane was washed with washing buffer and was incubated with appropriate secondary HRP conjugated antibody at diluted in blocking buffer (room temperate, 1

hour). Unbounded antibodies were removed by washing and signals were developed using ECL kit according to manufacturer's instructions (GE Healthcare, Germany).

Analysis: The bands obtained were scanned and quantified by densitometry using ImageJ software. The band intensities were compared between control and diabetic groups and significance determined by Student's t-test.

(b) Immunoflourescence staining, microscopy and image analysis

Tissue fixation and embedding: After perfusion, the lumbar DRGs and sciatic nerves were dissected, fixed in 4% paraformaldehyde and cryoprotected in 30% sucrose solution overnight. The tissues were then embedded in Tissue-tek (Sakura, Japan). The DRGs and sciatic nerves were cut at a thickness of 10µm thick sections on a cryostat, while 16 µm thick sections were cut for footpad samples. The sections were dried at RT for two hours and then stored at -20°C until staining.

Immunoflourescence staining: Each fifth section from every mouse in the group was used for staining. The sections were thawed at RT for 2 hours. They were then fixated in acetone at -20°C for 10 minutes. After air drying the sections at T for 15 minutes, the sections was washed with 50mM Glycine for antigen retrieval and permeabilized using 0.1% aqueous solution of Saponin for 30 minutes at room temperature. These permeabilized sections were then washed extensively with Phosphate buffered saline/ 0.2% Triton X100 (TBS-T) for 5 mins x 3 times. The sections were then blocked with 10% horse serum in PBS-0.2% Triton X100 for 45 minutes at room temperature. After incubation respective antibodies were diluted in the blocking buffer and incubated at 4°C overnight. The sections were then washed with PBS-T (10 minutes x 3 times). Fluorochrome conjugated respective secondary antibodies were then used to detect the signal. The sections finally were washed to remove excess secondary antibody, stained with DAPI(nuclear stain) and mounted with Permaflour mountant medium (Thermo Fischer Scientific)

Image analysis: Images were acquired by a fluorescence microscope (Nikon) using 20x and 60x optics or confocal microscope (Zeiss) using 63x objective. Image analysis was performed using ImageJ software. The Mean Flourescence Intensities (MFI) were

measured or number of positive cells for respective protein were counted and then compared amongst the diabetic and non diabetic groups.

(c) ELISA

Extraction of ß-endorphin: From each mouse, 12 lumbar DRG, 2 sciatic nerves and 2 footpads were dissected and snap frozen in liquid nitrogen. The organs were then crushed using frozen glass pestle. 1M acetic acid was added to the crushed tissue and incubated for 15 minutes at room temperature for 15 minutes and then at 95°C for another 15 minutes. The samples were cooled by placing them on ice for 5 minutes and later centrifuged at 4000g for 15 minutes at 4°C. The supernatant containing ß-endorphin was collected. To preclear the supernatant of endogenous biotin, 10µl of avidin coated magnetic beads washed with 1M acetic acid were added to each sample. The samples were then tumbled for 30 minutes at 4°C and the beads were separated using a magnetic rack. The precleared supernatants were then lyophilized and resuspended in 1X assay buffer.

ELISA: To quantify the ß-endorphin levels, ELISA kit (Phoenix Pharmaceuticals, USA) was used. The 50µl of each sample was added in duplicates to a 96 well plate coated with a secondary antibody. Diluted primary antibody specific for ß-endorphin was added to each well, except 'Blank' and incubated overnight at 4°C. Here onwards, all incubation steps were carried at room temperature with continuous shaking. Unbound antibody and proteins were removed by washing. Biotinylated peptide was later added to the wells for competitive binding and incubated for 2 hours, followed by another washing step. After which, substrate was added to the wells and incubated for 1 hour and finally, colour was developed using tetramethylbenzidine substrate (TMB). 2N HCL was used to stop the reaction. The absorbance was measured at 450 nm in a microplate reader.

Analysis: Omega software was used to interpret the readings. A standard curve was constructed by plotting the known concentrations of standard peptide on the log scale (X-axis), and its corresponding O.D. reading on the linear scale (Y-axis). 4 parameter logistics was used to quantify the concentration of standard peptide. The standard

curve showed an inverse relationship between peptide concentrations and the corresponding absorbance. As the standard concentration increases, the yellow color decreases, thereby reducing the O.D. absorbance. The measured concentration was adjusted according to quantity of protein added per well and ß-endorphin concentration per mg or protein was determined for each sample. The means of groups were compared and significance was determined using the Student's t-test.

(d) PKC kinase activity

Lysate preparation: To determine the activity of PKC kinase in the DRGs, protein lysates were prepared from freshly isolated DRGs (not frozen in liquid nitrogen). The lysate preparation is described in 2.2.2(a). The lysates were immediate used for the kinase activity determination.

Kinase activity assay: PKC kinase activity kit was used for this purpose (Enzo Lifesciences, UK). A 96 well plate and the buffers were thawed at room temperature. The wells were washed once with Kinase Dilution Buffer and equal quantities of protein were added per well. Each sample was added in triplicates. Diluted ATP was added to all wells and incubated at 30°C for 90 minutes. The kinase reaction was terminated by emptying the wells and a phosphospecific substrate antibody was added to the wells, which bind specifically to the phosphorylated peptide substrate. Unbound antibody as removed by washing. The phosphospecific antibody is subsequently bound by a peroxidase conjugated secondary antibody. The assay was developed with TMB substrate. A color development proportional to PKC phosphotransferase activity is observed. The color development was stopped with acid stop solution and the intensity of the color was measured in a microplate reader at 450 nm. The mean absorbance of the diabetic group was compared with the control group and Student's t-test was used to determine the significance.

(e) Chromatin immunoprecipitation (ChIP)

To determine whether POMC promoter is bound with NF-kB subunits, a ChIP assay kit (EMD Millipore, USA) was used. The lumbar DRGs and snap frozen in liquid nitrogen were gently thawed on ice before beginning the assay. To each tube containing 12 DRGs, freshly prepared 18.5% formaldehyde was added and incubated at room temperature

for 20 minutes for crosslinking of protein-DNA. Adding glycine to a final concentration of 0.125M terminated the crosslinking. The DRGs were then washed with ice-cold PBS and mechanically dissociated in Cell Lysis buffer using a glass pestle to release the nuclei. The lysate was incubated on ice for 15 minutes and centrifuged (800g, 5 minutes, 4°C) to pellet nuclei. The nuclei were then suspended in MN buffer(10mM TrisCl pH=7.5, 4mMMgCl_2, 1mM$CaCl_2$, PIC). Micrococcal nuclease was added to each tube and incubated at 37°C for 10 minutes to fragment the chromatin. Adding EDTA to the tubes and incubating on ice for 10 minutes terminated the nuclease activity. The fragmented chromatin was pelleted by centrifugation (10,000g, 1 minute, 4°C). The pellet was resuspended in Nuclear Lysis Buffer. Each sample was sonicated (20 seconds, 3 pulses, 20%power) to break the nuclear membrane. The samples were then centrifuged (10,000g, 10 minutes, 4°C) to separate the debris. The samples were then precleared using 10 µl protein A/G magnetic beads. µl from these precleared chromatin-protein preparations were used to check whether the DNA is fragments are appropriately sized. To these 25µl, proteinase K was added, incubated for 2 hours at 62°C and the purified using columns provided in the kit. The sample was electrophoretically separated on 2% agarose gel. The bands were expected to be between 200bp-900bp. If the appropriate digestion was achieved, 20 - 60µg chromatin was transferred to tubes for each immunoprecipitation reaction. Appropriate NF-kB subunit antibody at a predefined concentration was added to the tubes, along with magnetic protein A/G beads. The immunoprecipitation reaction was allowed to proceed overnight at 4°C on a rotor. The beads bound with antibody and the chromatin was separated using a magnetic rack and further washed to remove excess unbound material. Finally, the DNA fragments were eluted in Elution Buffer and proteins were degraded by Proteinase K treatment. The quantification of POMC promoter fragments specific for NF-kB binding sites were quantified using specific primers (listed in section 2.1.9) in a quantitative real time PCR (described below).

(f) Quantitative real time PCR

RNA isolation from DRGs: RNA was isolated from DRGs snap frozen in liquid nitrogen using the Trizol reagent (Invitrogen, Germany). The frozen DRGs were gently thawed on ice and homogenized mechanically in Trizol reagent. The homogenates were incubated at room temperature for 5 minutes and vortexed. One-fourth volume of chloroform was

then added, properly mixed by inverting and then centrifuged (20,000g, 15 minutes, 4°C) for phase separation. Topmost aqueous layer was pipetted out into a new tube. The RNA was precipitated using 100% isopropanol (20,000g, 15 minutes, 4°C). The isopropanol was removed from the RNA preparation by ice-cold 70% ethanol washes (2 washes; 10,000g, 10 minutes each, 4°C). The final pellet was air dried and resuspended in DEPC water and quantified spectrophotometrically. The RNA preparation was then treated with DNAseI (Invitrogen, Germany) for 15 minutes at room temperature to remove contaminating DNA fragments. The DNAse action was stopped by added EDTA to a final concentration of 0.25mM and an incubation at 65°C for 10 minutes.

Measuring DNA quality and concentration: RNA concentration was measured using spectophotometer (Bio-Tek Instruments, USA) according to manufacturer instructions. Absorption peaks indicated possible contamination of RNA. Ratios of absorption 260/280 or 260/230 were used as indicators of contamination for proteins and aromatic compounds, respectively. In particular, preparations with 260/280 ratio of 1.8 – 2.0 and 260/230 ratio greater than 2.0 were considered of good quality, and used for further analysis. RNA was stored at -20°C for short term, or at -80°C for long time.

cDNA preparation: For cDNA synthesis, 1µg of total RNA was diluted cDNA Master Mix using reagents from cDNA systhesis kit (Applied Biosystems, UK). cDNA was stored at -20°C.

Master Mix per reaction	
10X RT Buffer	2 µl
25X dNTP Mix	0.8 µl
10X RT Random Primers	2 µl
Reverse Transcriptase	1 µl
RNase Inhibitor	1 µl
Nuclease-free H_2O	3.2 µl
Total per Reaction	10 µl

PCR conditions	
25°C C °C	10 minutes
37°C	120 minutes
85°C	5 minutes
4°C	pause

Table 12: cDNA synthesis reaction set up and temperature conditions

Quantitative real time PCR: Relative expression of target genes was measured by quantitative real time PCR (qRT-PCR) using the Lightcycler 480 real-time PCR system (Roche, Germany). The qRT-PCR was performed in a 96 well plate in duplicates. Lightcycler 480 SYBR green I Master (Roche, Germany) containing FastStart Taq DNA Polymerase and DNA double-strand-specific was used for product detection and characterization. Primers specific to gene analysed are listed in the 2.1.9 Section. The reaction mix and PCR conditions are given below in table 1.

Master Mix per reaction	
dH_2O	7.2 µl
10 µM Forward primer	0.4 µl
10 µM Forward primer	0.4 µl
SYBR green Mix	10 µl
cDNA	2 µl
Total per Reaction	10 µl

PCR conditions		
Stage1	95°C	3 minutes
Stage2	95°C	10 seconds
	60°C	20 seconds
	70°C	1 seconds
Stage3	95°C	5 seconds
	65°C	1 minute
	97°C	continuous
	40°C	Melt curve

Table 13: qPCR reaction set up and temperature conditions

Analysis: To calculate the relative expression of a gene of interest (GOI), the ΔCt method was used, which normalizes the cycle of threshold (Ct) measured for the GOI to the Ct measured for a housekeeping gene (HKG) taking into account the primer efficiency. One of the samples was used as internal reference for the fold induction calculation of the transcript level of the other samples. The calculation can be summarized in the following formula:

$$\frac{Efficiency_{GOI}^{Ct\,(reference\,(GOI))\,-Ct\,(sample\,(GOI))}}{Efficiency_{REF}^{Ct\,(reference\,(REF))\,-Ct\,(sample\,(REF))}} = Fold\ induction$$

Primer specificity was evaluated by analysis of the melting curve and by including appropriate controls. Actin or 18srRNA was used as the housekeeping gene for normalization, and the mean of fold induction was calculated.

2.2.3 Cell culture methods

(a) AtT20 cell culture

AtT20 (Sigma-aldrich, USA) is a cell line is a POMC expressing cell line, established after alternate passage of mouse pituitary tumor cells as tumors in animals and in cell culture. These are suspension cells; are round and grow in aggregates. The cells were cultured in Ham's F10 medium, 82.5%; horse serum, 15%; FBS, 2.5%, 1%Penicillin-streptomycin, 1% AmphotericinB, 1% L-Glutamine).

The cells were grown in T-25 culture flasks at 37°C, 5% CO2. For sub-culturing, the clusters were allowed to settle and all but 2 ml medium was removed. The clusters were gently transferred to new flasks and fresh medium was added. A subcultivation ratio of 1:2 was always used.

(b) CRH response assay

In this assay, AtT20 cells were exposed to increasing glucose concentrations in presence and absence of Corticotropin Releasing Hormone (CRH) and then harvested to quantifiy POMC mRNA levels.

AtT20 cells, in their log phase, were collected in a conical flask and centrifuged at 150g for 5 minutes at room temperature. The pellet was resuspended in PBS and divided equally into tubes per exposure condition. The tubes were centrifuged (150g, 5 minutes) and the pellet was resuspended in 6mM, 20mM or 40mM glucose medium with reduced sera (0.5% horse serum and FCS). 20mM and 40mM Sorbitol controls were included to exclude effects on POMC expression due to osmotic changes. Half of the cells per tube were exposed to CRH (10^{-7}M), while the other half were not. The cells were plated in 6 well plate (10^{6} cells per well) in triplicates for each condition at 37°C, 5% CO_2.

After 12 hours of exposure, the cells were harvested, washed twice with PBS and the pellet was resuspended in Trizol reagent. mRNA was extracted as described in section 2.2.2(f). POMC mRNA expression was quantified and normalized with actin (house keeping gene) for each condition using the q-RTPCR.

(c) Western blotting

Cell exposure conditions: AtT20 cells, in their log phase, were pooled, pelleted and washed with PBS. The pellet was then equally divided and exposed to either 6mM or 20mM glucose in reduced sera culture medium. The cells were plated in quadruplicates per exposure condition, as 10^6 cells per well. After 12 hour-long exposure, the cells were pelleted and washed twice with PBS and proceeded for nuclear lysate preparation.

Nuclear lysate preparation: The pellets were resuspended in Buffer A and incubated on ice for 10 minutes. The nuclei were pelleted by centrifugation (20,000g, 5 minutes, 4°C) and resuspended in Buffer C. The suspension was further incubated on ice for 20 minutes and finally centrifuged(20,000g, 5 minutes, 4°C) to pellet the debris. The supernatant containing nuclear proteins was collected and quantified using Bradford assay.

Immunoblotting: Equal amount of protein from each sample was loaded onto an SDS polyacrylamide gel. The blotted proteins were probed with either of the NK-kB subunit antibodies- p65, p50, p52, cRel. Histone H3 antibody was used as the loading control. The protocol is described in section 2.2.2(a).

(d) Electromobility Shift Assay (EMSA)

AtT20 nuclear lysates were prepared as given in 2.2.3(c). A radioactively labeled DNA probe, consisting of NF-kB consensus sequence was prepared by incubating the NF-kB oligonucleotide with radioactive P32 isotope along with T4 polynucleotide kinase overnight at 4ºC. The enzyme activity was terminated using 0.5M EDTA and the labeled DNA probe was then precipitated with 70% ethanol and sodium acetate. The probe was dissolved in ddH2O and stored at 4ºC for 48 hours.

For EMSA reactions 10ug AtT20 nuclear lysates were mixed in a 20µL reaction with 66.7nM of probe, 0.1mg/mL BSA, and EMSA Buffer (10mM Tris-Cl pH 7.4, 50mM KCl, 0.5mM MgCl2, 0.1mM EDTA, 5% glycerol) for 30 minutes at room temperature. Reactions were then loaded onto a pre-electrophoresed 6% acrylamide/bis (37.5:1) gel in 0.5xTBE and run at 100V at 4ºC. The gels were dried and analyzed by exposing them to photographic film.

(e) Chromatin Immunoprecipitation (ChIP)

AtT20 cells in their log phase were selected for performing ChIP assay such that there were 10^6 cells per IP reaction. The cells were centrifuged and resuspended in either 6mM or 20mM glucose medium with reduced serum. Post 12 hours or exposure to low and high glucose, the cell were crosslinked. The rest of the procedure was same as described in section 2.2.2(e)

(f) DRG (primary) culture

DRGs from 6 week old female WT mice were dissected and dissociated using 0.3% collagenase and then by 0.05% trypsin at 37°C for 45 minutes per treatment. The DRGs were then mechanically dissociated using Pasteur pipette and trypsin reaction was stopped by adding FCS to the tubes. The cell suspension was then centrifuged at 300g for 3 minutes and washed with PBS twice. The pellet was resuspended in the culture medium and placed into wells of 12-well plate coated with (0.01%) and laminin (25µg/ml) drop by drop. The cells were allowed to attach by incubating the plate at 37°C for 15 minutes. 1 ml of medium was added to each well gently and the cells were incubated overnight at 37°C at 5% CO2. Selection medium containing cytosine arabinoside (AraC;10µM) and NGF (50ng/ml) to inhibit dividing non-neuronal cells and to promote neuronal growth. The cells were incubated with selection medium for 24 hours and then replaced with normal DRG cell culture medium.

(g) Transfection and live cell staining of DRG cells

Transfection of primary cells: The DRGs were dissected and dissociated as above. After washing with PBS post dissociation, the cells pellet was resuspended in R buffer. The suspension was then divided equally into number tubes required for live cell staining conditions. 2µg of Flag-MOR-mCherry construct was added per tube except for the 'untransfected control'. The cells then were electroporated using the Neon transfection system with 2 pulses at1300V, 20 seconds each. The transfected cells were seeded on poly-L-ornithine and laminin coated coverslips and incubated overnight at 37°C at 5% CO2. Selection medium was added 12 hours post transfection. After 24 hours of transfection, the cells were incubated with either of the following medium: low glucose medium (17mM), low glucose + PKC inhibitor (1µM), high glucose (40mM) or high glucose+ PKC inhibitor. These media contained AraC and NGF. The same media (without

AraC and NGF) were refreshed after 24 hours of exposure. 48 hours post exposure conditions, the cells were staining live with Flag antibody

Live cell staining: To each well, wheat germ agglutinin conjugated to FITC (5µg/ml) was directly added to the cells and incubated at 37°C for 10 minutes. The cells were washed thrice with PBS and fixed with 4% paraformaldehyde for 20 minutes. The cells were washed thrice with PBS, stained for DAPI and then mounted using Permaflour mountant medium. The stained cells were imaged using LSM 710 or LSM 700 confocal microscope.

(h) Immunocytochemistry

DRGs cells seeded on coverslips were fixed with 4% paraformaldehyde and immunostained as follows. The fixe cells were washed with PBS, permeabilized with PBS+0.2%TritonX100 and Blocked with PBS+10%FCS for 1 hour. Appropriate dilution of primary antibodies was then added to each well, except secondary antibody control. The cells were incubated at 4°C overnight and then washed with PBST (PBS+o.2%TritonX100) and probed with appropriate secondary antibodies. The unbound antibodies were washed with PBST. Finally, the cells were stained with DAPI and mounted using Permaflour mountant medium and imaged using confocal microscope.

2.2.4 Molecular biology methods

(a) PCR amplification of Flag-MOR

N terminally tagged Flag-MOR construct was kind gift provided by Dr. Manojkumar Puthenveedu, Carnegie Mellon University, USA. Primers specific for the 5' and 3' terminus of the construct, containing restriction enzyme overhangs were generated (EcorI overhang in the forward and SacII in the reverse primer). Amplification of DNA sequences was performed using these specific primer sets. For each PCR amplification, a 50µl reaction was set as below in table... A non-template control (ddH2O added instead of plasmid) was included to determine primer specificity Reaction mixtures were loaded into an automated DNA thermal cycler to undergo amplification.

Master Mix per reaction	
10X Thermopol Buffer	5 µl
10mM dNTP Mix	1 µl
10µM F+R Primers	2 µl
Flag-MOR construct (100ng)	1 µl
dd H_2O	40µl
DeepVent DNA Polymerase	1 µl
Total per Reaction	50 µl

PCR conditions		
94°C C °C	230 seconds	
94°C	60 seconds	30 cycles
67°C	60 seconds	
72°C	110 seconds	
72°C	320 seconds	
72°C	pause	

Table 14: PCR reaction set up and temperature conditions for cloning

The sample was loaded onto 0.8% agarose gel to check the molecular weight of the amplified product. The reaction mix was then purified using PCR purification kit (Qiagen, Germany). The samples were mixed with 5 volumes of Column Binding Buffer and loaded into a matrix-containing column. The columns were centrifuged at 13,000g, 1 minute, 25°C. The column was washed with Washing Buffer (13,000g, 1 minute, 25°C) and the dry spun for 2 minutes (13,000g, 25°C). 30 µl Elution Buffer was directly added on to the column, incubated for 1 minute at room temperature and the centrifuged at 13,000g, 1 minute, 25°C into a clean tube.

(b) Restriction digestion of vector and insert

A sequential digestion of purified PCR product (insert) and the vector pmCherryN1 (Clonetech), was performed at 370C using restriction enzymes indicated for the two primers in 1X compatible buffer. The reaction was performed as per the table 2. The reaction tubes were then incubated at 37oC for 6 hours for each enzyme and were then analyzed for digestion. After digestion with the first enzyme, EcoRI, the vector and insert were PCR purified as described in 2.2.4.(a) and then the second digestion as set.

EcoRI digestion	
DNA (vector or insert)	Upto 30 µl
Buffer H (Promega)	5 µl
EcoRI (Promega)	1 µl
dd H_2O	14µl
Total per Reaction	50 µl

SacII digestion	
DNA (vector or insert)	Upto 30 µl
Buffer C (Promega)	5 µl
SacII (Promega)	1 µl
dd H_2O	14µl
Total per Reaction	50 µl

Table 15: Restriction digestion reaction set up and temperature conditions

(c) Gel purification of desired DNA fragments

The completion of restriction digestion was analysed by loading the vector and insert using on 1% agarose gel electrophoresis. The intense band of correct size was excised using a disposable sharp scalpel. The excised DNA band was weighed on a tarred balance and processed as per the instruction manual of GenElute Gel extraction kit (Sigma- Aldrich, USA). Briefly the gel slice was melted in 3V of gel solublization solution and Incubated on dry bath maintained at 56oC. Meanwhile, the DNA Binding column was prepared by using 500ul of column preparation solution. Once the gel slice is melted, then one gel volume was added (100mg of gel= 100ul of gel volume) of Iso-propanol. The solublized gel mix was then loaded onto the binding column, followed by centrifugation at maximum speed for 1 minute. After binding of DNA, the column was washed using 500ul of Column wash buffer. Finally, DNA was eluted with pre-warmed (56°C) 10mM Tris-Cl (pH=8.0). The concentration of eluted DNA was checked using spectrophotometer at 260nm and the quality of elution was analyzed by agarose gel electrophoresis.

(d) DNA ligation of vector and insert

The purified vector and insert DNA was further used for T4 DNA ligase mediated DNA ligation. The DNA Ligation was set up as per the table 3. Three different molar ratios of vector: insert for DNA ligation (1:3 and1:5) were used along with a vector alone as negative control. The insert molar ratios were calculated as described as follows,
For a ration of 3:1,

$$\frac{ng\ of\ Vector\ x\ kb\ size\ of\ Insert}{kb\ size\ of\ Vector}\ x\frac{3}{1} = ng\ of\ Insert$$

Components	**1:3**	**1:5**	**-ve control**
10X DNA ligation buffer	2 ul	2 ul	2 ul
Vector (digested)	50ng	50ng	50ng
Insert (Digested)	39 ng	64 ng	0.0 ul
T_4 DNA Ligase	1.0ul	1.0ul	1.0ul
dH_2O upto	10ul	10ul	10ul

Table 16: Ligation reaction for restriction digestion fragments of vector (pmCherryN1) and insert (MOR)

The reaction mix was then incubated at 16 degree centigrade for 16 hours. After incubation the whole ligation mix was transformed into E.Coli XL1 Blue (endA1 gyrA96(nalR) thi-1 recA1 relA1 lac glnV44 F'[::Tn10 proAB+ lacIq Δ(lacZ)M15] hsdR17(rK- mK+)). The recovered cells were then plated onto Luria-Bertani (LB) agar plate containing kanamycin. The plated cells were then incubated at bacteriological incubator maintained at 37°C for 16–18 hours. The well grown colonies were used for screening by inoculating 3.0 ml of LB medium containing Kanamycin (30ug/ml) were grown individually for 16 hours and the well grown culture was then used for the mini preparation of plasmid DNA using Qiagen mini-prep kit. A selected number of clones were further confirmed using restriction digestion and PCR amplification using specific primers. The positive clones were, then sequence verified using vector specific primers from MWG (Eurofins MWG, Germany). Only the positive clones were selected for protein expression by transfection in HEK 293 cells using electroporation method. The clone best expressing the protein of interest was sequenced and selected for further experiments.

3. Results

3.1 Neuronal cells in the DRG are the major contributors of endogenous opioids during diabetes

3.1.1 Immune cell population in diabetic sciatic nerves

Immune cells infiltrating the sciatic nerves of mice with nerve injury have previously been shown to be the primary source of endogenous opioids in the PNS. To investigate the presence of endogenous opioids, the immune cell population in the sciatic nerves of diabetic mice was first studied. Every fifth section of sciatic nerves of mice 8, 16 and 24 weeks post STZ induction were stained for the immune cell markers CD45 (leukocyte marker) and MHCII (antigen presenting immune cell marker). It was found that after 8 weeks post STZ induction the number of $MHCII^+$ leukocytes (Mean positive cells per section ± S.E.M.) were not significantly different from the age-matched control mice (1.8±0.25 in control vs. 2.4 ±0.49 in diabetic). However, at 4 months post induction, the number of $MHCII^+$ leukocytes had increased by 2.6 fold in the diabetic sciatic nerves (3.6 ± 0.73 in control vs. 9.36±1.0 in diabetic). The number of double-positive ($CD45^+MHCII^+$) immune cells had decreased as compared to the 4 months diabetic mice, but still remained significantly higher than the control group (6.75 ± 2.71 in control vs. 12.15±1.3 in diabetic) (Figure5a). The immune cell population was also increased in the control mice as the age increased, but the increase in the immune cell number in the diabetic nerves was always higher than in the control nerves. The $CD45^+MHCII^+$ population in the nerves had peaked at 4 months post induction indicating a possibility of immune cell infiltration at this time point post STZ treatment.

Since macrophages are one of the antigen presenting cells known to infiltrate the nerves post injury, the diabetic nerves of 4 months mice were examined for an increase in the macrophage population by co-staining for CD68 and MHCII markers. A significant increase in the $CD68^+$ macrophage population was observed in the diabetic nerves (2.2±0.4 in control vs. 6.0±0.4 in diabetic) (Figure 1b). No T cell ($CD3^+$) infiltration was observed in the nerves in control or in diabetic mice.

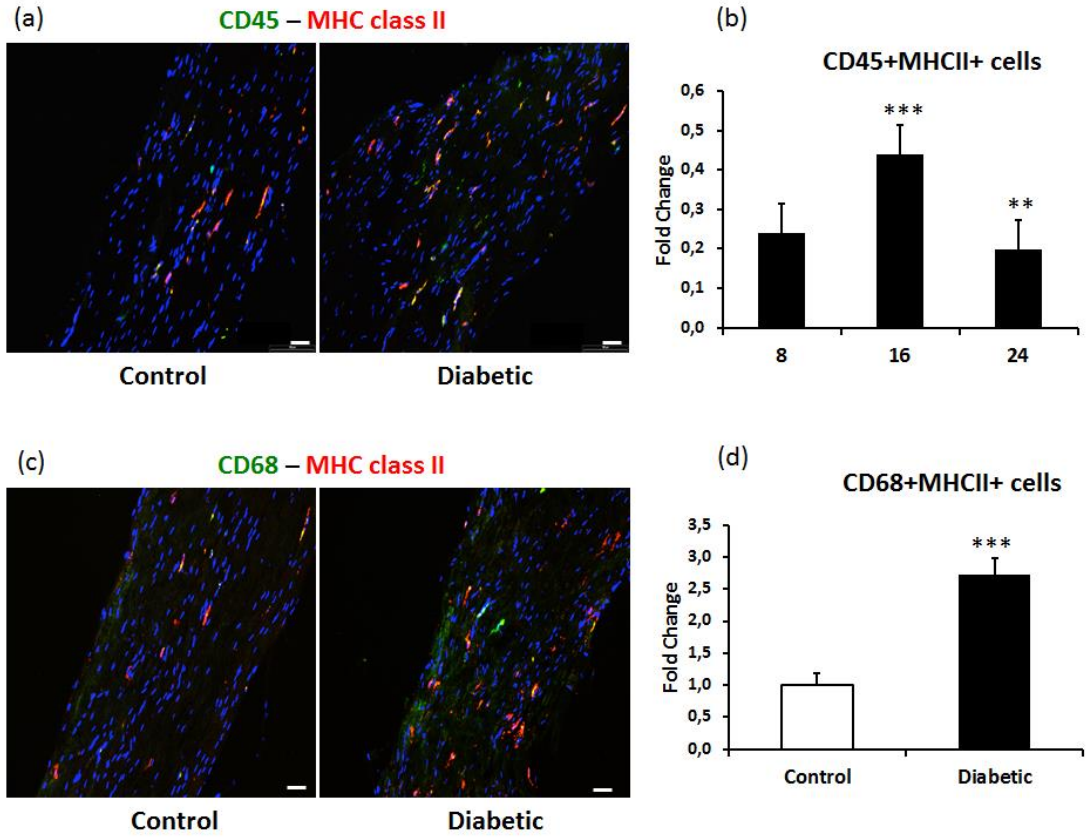

Figure 5 (a-d): Immune cell populations in control and diabetic sciatic nerves (a) Representative double immunoflourescence figures for CD45+(green) - MHCII+ (red) leukocytes in 16 weeks post STZ induction and age-matched controls. (b) A 2.6 fold increase was seen in MHCII+ leukocytes (CD45+ cells) at 16 weeks post STZ induction. (c, d) A subset of the increased immune cell population is the CD68+(green) – MHCII+(red) macrophages, which were also increased by 2.6 fold compared to the control mice. Dotted line represents the mean number of immune cells in age-matched controls. Data represented as Mean positive cells per section+/- SEM; Student's t-test **p<0.01, ***p<0.001. Scale bar =50 µm.

3.1.2 Expression of endogenous opioids in the PNS of diabetic mice

As the $CD45^{+}$ leukocyte population in the diabetic nerves was increased at 4 months, sections from these nerves were subsequently co-stained for opioid content, using a pan-opioid antibody and CD45. Surprisingly, no colocalization was observed between the two markers (Figure 6a). Therefore, the nerves were co-stained for a pan neuronal marker, ß tubulin III (Tuj1). The maximum opioid staining colocalized with Tuj-1 stained axons in the sciatic nerve. (Figure 6b).

Axons of the neurons carry the proteins expressed in the cell bodies of the neurons. The axons present in sciatic nerves have their cell bodies in lumbar DRG. Hence, sections of lumbar DRG were subsequently stained for opioid content, leukocytes (CD45), neurons (Tuj1) and the glial cell marker, CD11b. Consistent with the findings in the sciatic nerve,

opioid contents colocalized with the neuronal cell bodies, although some signal was also found to colocalize with the glial and immune cells present in the DRG. (Figure 6c, d).

It can therefore be concluded that although there was an increase in the immune cell population in the nerves of diabetic mice, these immune cells did not express endogenous opioids.

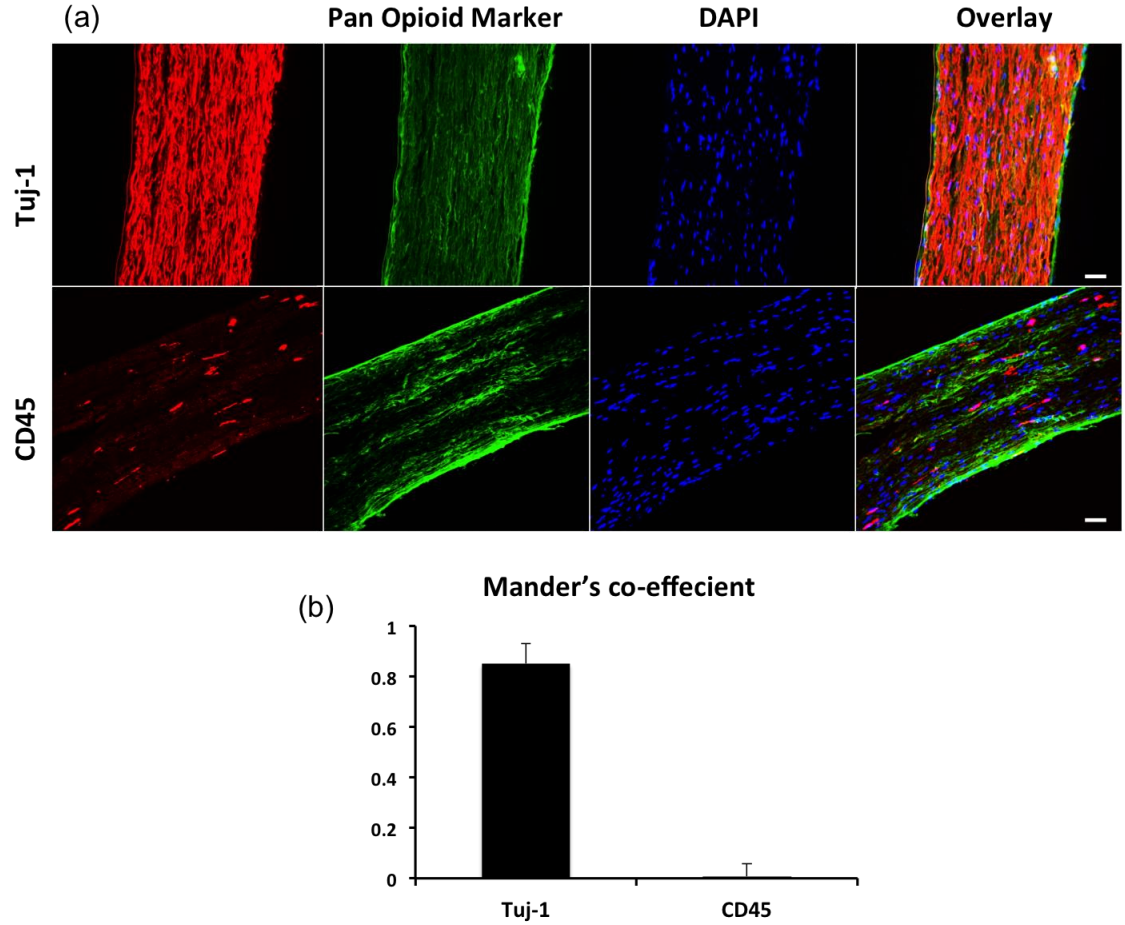

Figure 6 (a, b): Cells expressing endogenous opioids in PNS of 4 months diabetic mice (a) Co-staining of sciatic nerve sections of diabetic mice with cell specific markers for neurons (Tuj-1) and immune cells (CD45) with pan opioid marker showed presence of opioids in the axons rather than immune cells. (b) Calculation of Mander's co-efficient for each marker showed maximum colocalization between Tuj-1 stained axons and pan opioid marker. Scale bar=50 µm.

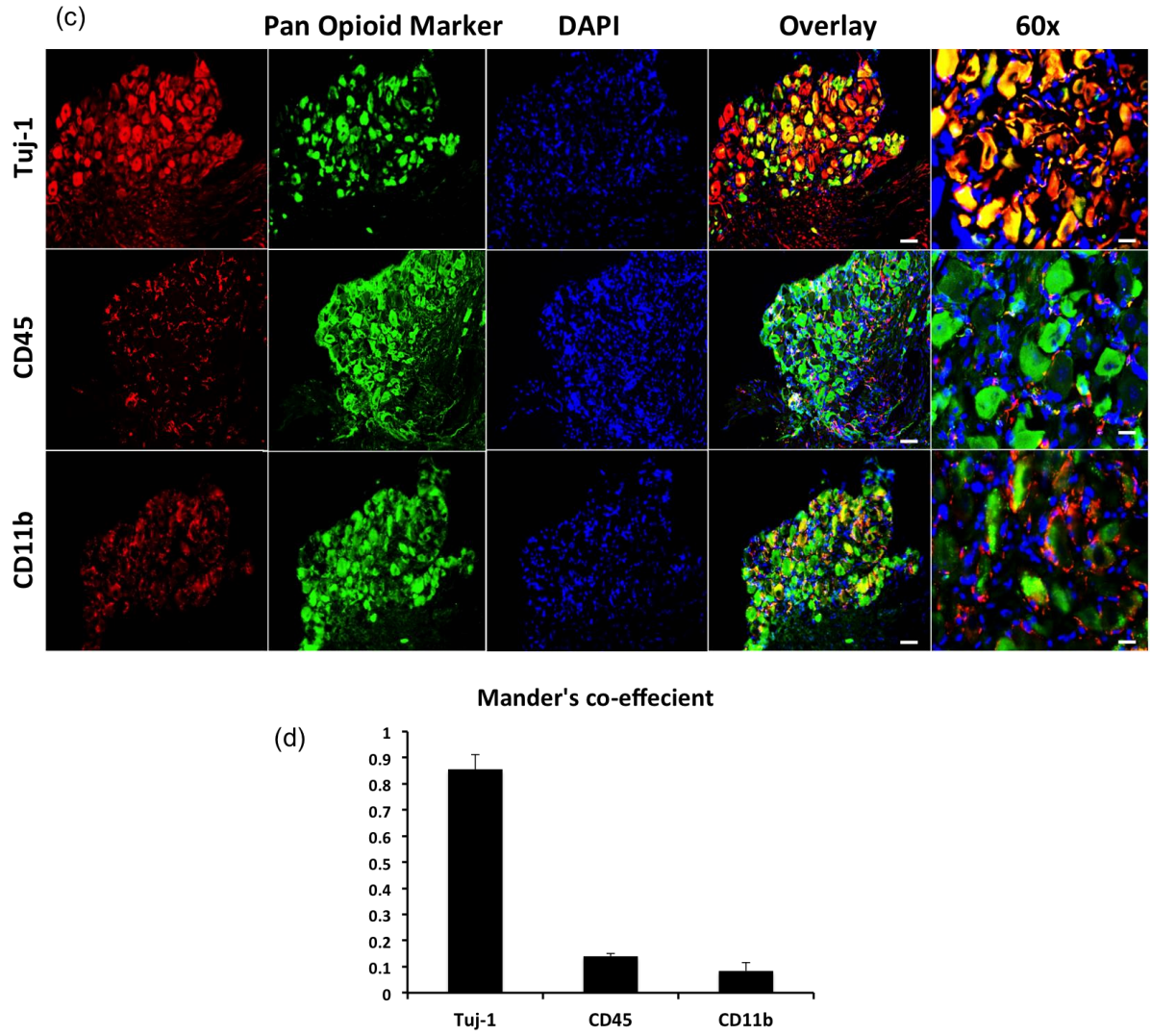

Figure 6 (c, d): Cells expressing endogenous opioids in PNS of 4 months diabetic mice (c) Co-staining of DRG sections of diabetic mice with cell specific markers for neurons (Tuj-1), immune cells (CD45) and glial cells (CD11b) with pan opioid marker showed presence of opioids in neuronal cell bodies. (d) This was confirmed by calculating Mander's correlation co-efficient Highest colocalization was seen between between Tuj1 and pan opioid marker. Scale bar =50 µm.

3.2 Expression of endogenous opioids changes during the course of diabetes

Since in DPN, DRG neurons were identified to be the most relevant cell type to study the endogenous opioid system, it was important to understand the changes occurring in these cells post STZ induction.

3.2.1 Pain phenotype profiling post STZ induction

Pain is the foremost functional consequence that the endogenous opioids in the PNS can influence. Thermal hyperalgesia was measured using the hotplate (50°C) in the control

and diabetic mice at 2, 4, 8 and 12 weeks post STZ induction. Shorter response times indicating increased pain sensitivity was observed 2 weeks after STZ treatment. However, after 4 weeks, the mice recovered from the initial hypersensitivity until the 8th week. This is in accordance with previous reports showing early thermal hyperalgesia caused due to STZ injection and its reversal between 5-6 weeks [112,113]. After the initial response to STZ, and following recovery, a significant hyperalgesia was again observed at week 12 (Figure 7). Whether diabetes induced changes in endogenous opioids could be associated with the observed hypersensitivity needed to be further investigated. Therefore week 12 was marked as the endpoint of the time course study for endogenous opioids.

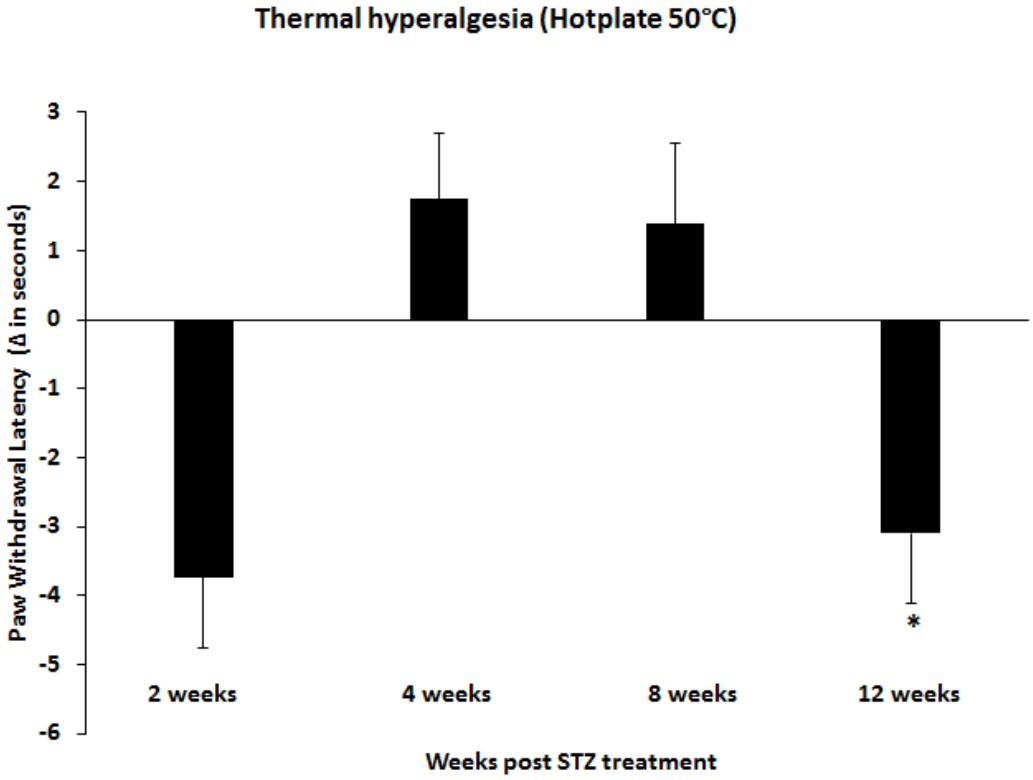

Figure 7 Thermal hyperalgesia post STZ induction STZ induced diabetic mice (n=12) and age matched controls (n=12) were measured using hotplate method until 12 weeks at which time point the diabetic mice showed significant increased pain sensitivity. Data represented as Mean +/- SEM; Student's t-test *p<0.05.

3.2.2 Alteration in endogenous opioids post STZ treatment: a time course study

(a) Diabetic parameters of mice

To understand the changes occurring in the endogenous opioids post STZ treatment, 4, 8 and 12 weeks post induction were chosen as time points of interest. At each time point the STZ induced mice showed significantly higher blood glucose levels and Hba1c content, while body weight were significantly decreased indicting the mice were

diabetic. As the majority of the opioid content was observed within the neuronal cell bodies of lumbar DRG, the transcription and expression of the specific opioid subtypes was studied further at each of the stated time points.

Weeks post STZ induction		Blood sugar (mg/dL)	Hba1c (%)	Body weight (g)
4 weeks	Control	97.25	3.3	22.85
	Diabetic	401.5***	9.7***	16.12***
8 weeks	Control	145.25	3.5	27.2
	Diabetic	407.8***	11.3***	17.64***
12 weeks	Control	122.5	3.2	26.02
	Diabetic	370.5**	9.8***	19.37**

Table 17: Diabetic Parameters of mice Data represented as Mean +/- SEM; Student's t-test **p<0.01, ***p<0.001.

(b) Gene expression of endogenous opioids in lumbar DRG

POMC mRNA showed a 98% decrease at 4 weeks, a 75% decrease at 8 weeks ($p<0.01$) and remained significantly downregulated by 90% till 12 weeks ($p<0.001$) post STZ treatment. Interestingly, a PENK and PDYN mRNA did not show a pattern of change similar to POMC mRNA, suggesting that the three different opioid genes are regulated differently after STZ treatment. At 4 weeks, mRNA levels of PENK were increased by 50%, while no change was observed in PDYN mRNA level. At 8 weeks, along with POMC mRNA, PENK and PDYN mRNA levels were decreased significantly. At 12 weeks, the PENK and PDYN levels were recovered, unlike the POMC, which remained significantly downregulated (Figure 8).

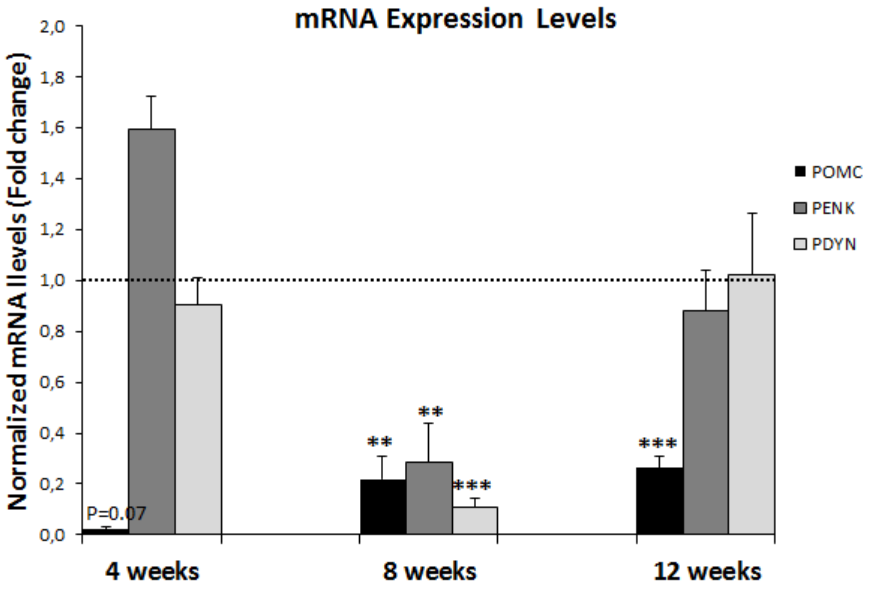

Figure 8: Gene expression of POMC, PENK and PDYN in lumbar DRG Quantification of mRNA levels and their normalization with actin revealed a sustained downregulation in POMC gene expression until 12 weeks post STZ treatment. The PENK and PDYN mRNA levels, however, showed only a transient decrease at 8 weeks and were restored to normal levels at 12 weeks. The dotted line represents the mRNA level in control. Data represented as Mean +/- SEM; Student's t-test **p<0.01, ***p<0.001.

(c) Opioid peptide levels in lumbar DRG

At 4 weeks, the levels of POMC, PENK and PDYN were significantly increased in lumbar DRG ($p<0.001$ for all opioids). The increased POMC and PDYN peptide did not corroborate with the mRNA levels at 4 weeks. This suggested that the increased POMC and PDYN peptide content in the DRG must have been due to an increase in the mRNA level prior to the 4^{th} week. At 8 weeks, the peptide levels of all three opioids were decreased, consistent with the mRNA levels. By 12 weeks, PENK and PDYN peptide levels were normalized as compared to the controls, consistent with the mRNA levels. However, the POMC peptide level was significantly decreased, again consistent with the mRNA levels (Figure 9, 10).

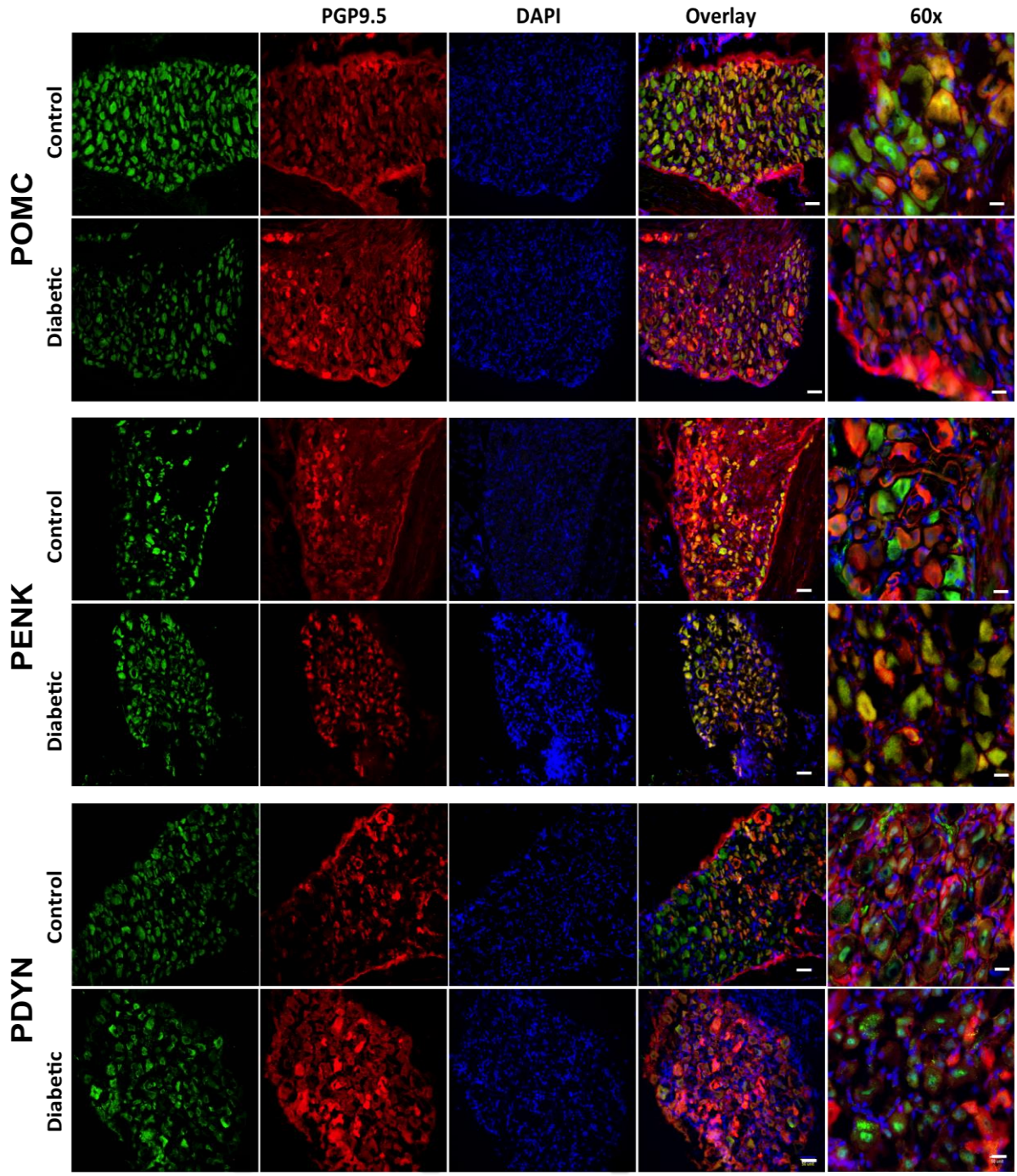

Figure 9: Endogenous opioid staining in lumbar DRG of 12 weeks STZ and control mice Representative double immunofluorescence staining of the opioids and pan neuronal marker PGP9.5 showed a decreased POMC staining, no change in dynorphin and an increased signal intensity for enkephalin at 12 weeks. Scale bar =50 µm.

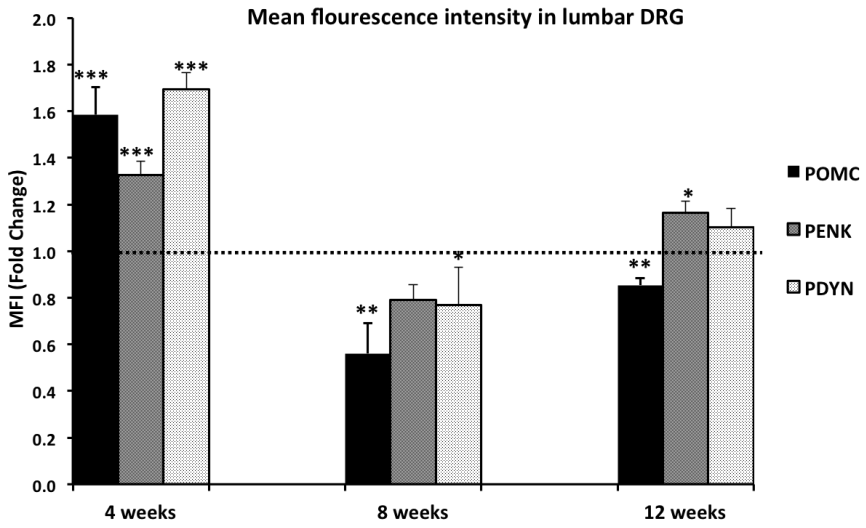

Figure 10: Mean Fluorescence Intensities (MFI) calculation for opioid peptide staining Signal intensities (MFI) for each DRG section stained for opioids were calculated for 4, 8 and 12 weeks post STZ and compared with those of age-matched controls. The dotted line represents the level in control. All three opioids had increased intensities at 4 weeks and showed a transient decrease at 8 weeks. The PENK and PDYN level recovered at 12 weeks, but POMC level in the DRG remained significantly downregulated at 12 weeks. Data represented as Mean +/- SEM; Student's t-test *p<0.05, **p<0.01, ***p<0.001.

In summary, the temporal changes observed in the gene expression and consequently peptide levels were not similar between the three opioids. The opioid peptide levels were associated with the changes in pain sensitivity post STZ induction. For instance, recovery from previously increased pain sensitivity was seen at 4 weeks, perhaps as a consequence of increased opioids. There onwards, as the opioid levels decreased, the pain sensitivity too increased and failed to recover at 12 weeks even when the PENK and PDYN levels are returned to normal level. The overt hyperalgesic phenotype at 12 weeks was associated with decreased POMC content in DRG at 12 weeks.

This data would suggest that at 12 weeks, the hyperalgesic phenotype observed is associated with a decrease in POMC content in the DRGs, and that the regulation of POMC level is most relevant in the context of painful diabetic neuropathy

3.3 Downregulation of POMC in 12 weeks diabetic mice

3.3.1 Decrease of POMC and ß-endorphin peptide levels in DRG, sciatic nerves and footpads

To further investigate POMC in diabetic neuropathy, peptide levels were measured in the lumbar DRGs, sciatic nerves and footpads of 12 weeks STZ-diabetic mice by western

blotting. The diabetic mice had significantly increased blood glucose (mg/dL; 112.6 ± 3.03 vs. 319.2 ± 34.4; Student's t-test p<0001) and HbA1c (%; 3.02 ± 0.08 vs. 12.24 ± 0.78; Student's t-test p<0001) and decreased body weight (g; 25.8 ± 0.28 vs. 19 ± 1.09; Student's t-test p<0001). There was a significant decrease of approximately 50% in the ~28Kda band of POMC precursor peptide in the total protein lysates of all three tissues (Figure 11a, b). This decrease was confirmed in the DRGs by immunofluorescence double staining of POMC and Tuj1. It was found that the POMC signal intensity in the DRG was decreased in the diabetic DRG, but also the number of neurons expressing POMC had decreased by 5% per section (Figure 11c, d, e). The downregulation of POMC in the footpads was also confirmed by immunofluorescence double staining of POMC and PGP9.5, a marker for nerve fibers. There was a significant decrease in the number of PGP9.5 nerve fibers also expressing POMC from 66% in control to 44% in the diabetic mice. (Figure 11 f, g). Lastly, POMC is a precursor to the 3.5 KDa active opioid peptide, ß endorphin. Hence, ß-endorphin peptide levels were quantified (ng per mg protein) in the DRG, sciatic nerves and the footpads using an ELISA. There was a significant decrease in the sciatic nerves of diabetic mice (3.7 ± 1.17 in control vs 0.94 ± 0.79 in diabetic; Student's t-test p>0.05) and the footpads (6.55 ± 0.02 in control vs 1.35 ± 0.55; Student's t-test p<0.05). No change was observed in ß-endorphin levels in the DRG of control and diabetic mice (1.66 ± 1.28 in control vs 1.7 ± 1.19; Student's t-test p<0.05) (Figure 11h).

It is noteworthy that ß-endorphin level in the DRG is 4 fold lower than those in the footpads and more than 2 fold lower compared to the sciatic nerves in the control mice. This suggests that processing of POMC occurs majorly in the nerve endings in the footpads and to some extent in the sciatic nerves.

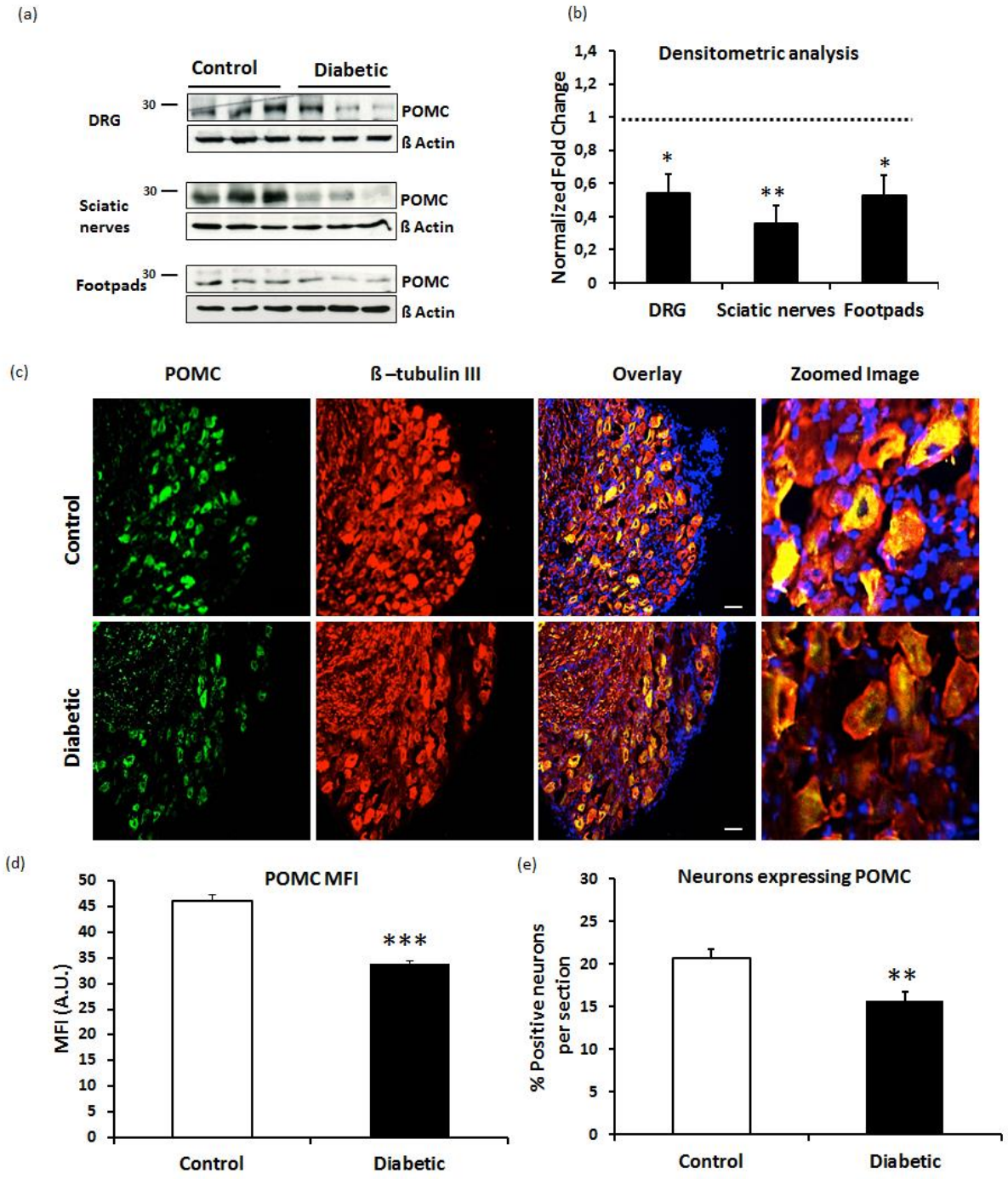

Figure 11: POMC expression in the lumbar DRG of control and diabetic mice (a) POMC peptide levels were compared between control and diabetic (n=6 each) in the lumbar DRG, sciatic nerves and footpads using western blot. (b) Upon densitometric quantification of the ~28Kda POMC band, a significant decrease of 46% was observed in the diabetic DRG and footpads, while the level in sciatic nerves had decreased by 62%. (c, d) Double immunofluorescence staining of POMC and Tuj1(pan neuronal marker) revealed a ~30% decrease in the Mean Fluorescence intensity (MFI) of the POMC signal. (e)Also, the number of neurons expressing POMC had decreased by 5% per section. Data represented as Mean +/- SEM; Student's t-test **p<0.01, ***p<0.001. Scale bar =50 µm.

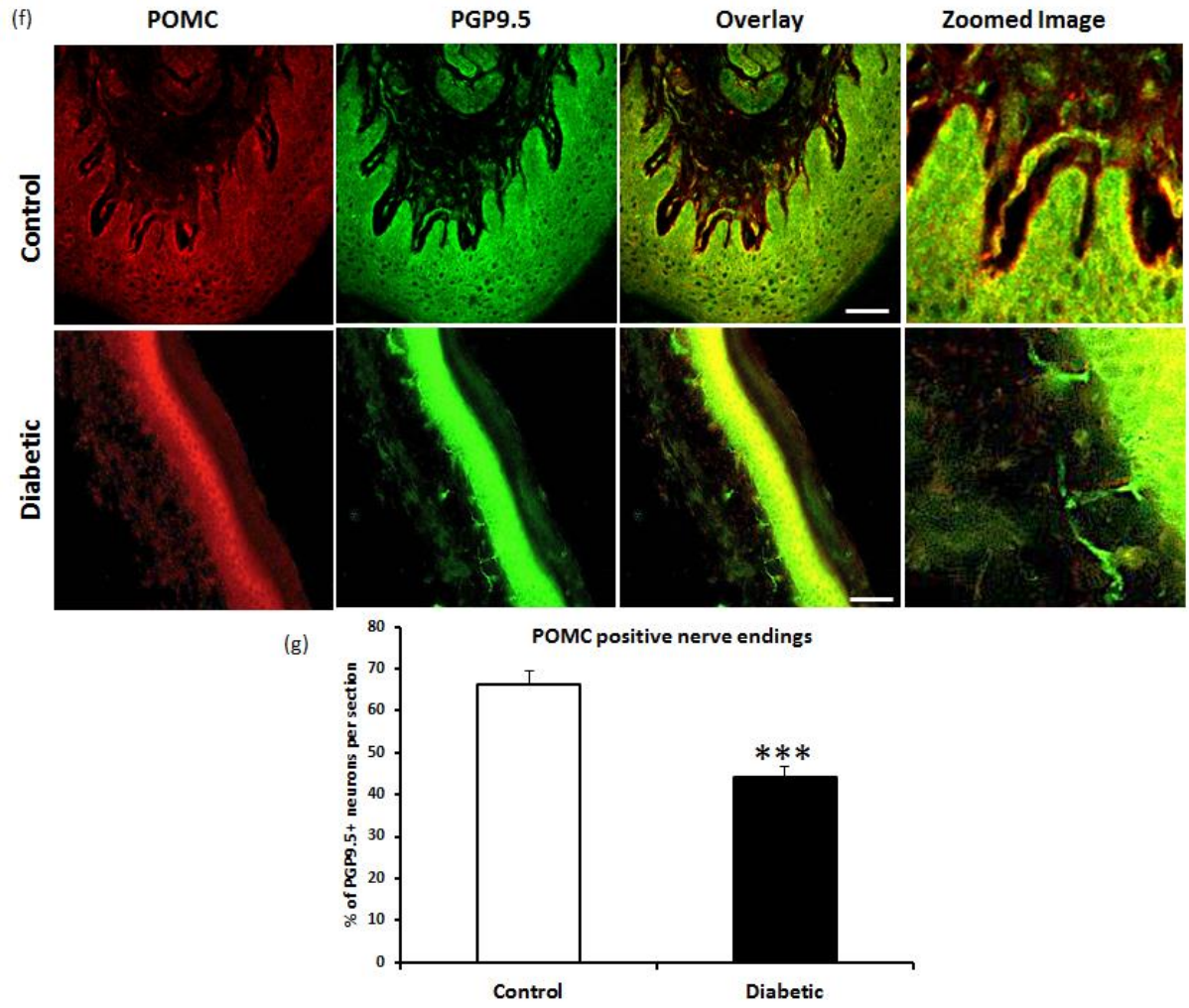

Figure 11: (f, g): POMC expression in the nerve endings of control and diabetic mice Co-staining of PGP9.5 (pan neuronal marker) with POMC in the footpad sections of control and diabetic mice (n=6 each) revealed that there was a significant decrease in the number of PGP9.5 positive nerve endings expressing POMC in the diabetic footpads. Data represented as Mean +/- SEM; Student's t-test ***p<0.001. Scale bar =50 µm.

(h)

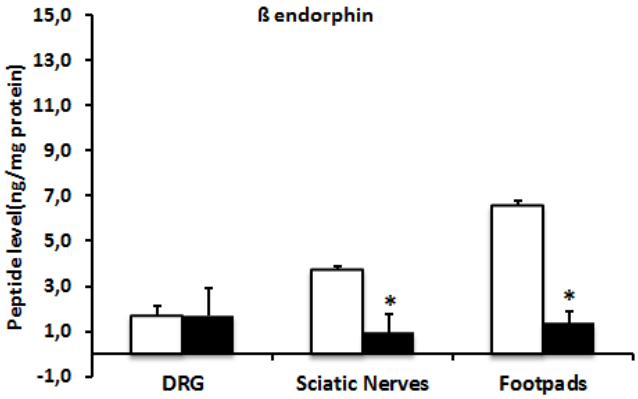

Figure 11(h): ß-endorphin levels in control and diabetic mice ß-endorphin peptide levels were measured in control and diabetic (n=6 each) mice using ELISA. A significant decrease was found in the diabetic sciatic nerves and footpads compared to the controls, in the ß-endorphin in the DRGs remained unchanged indicating POMC processing must be taking place in the sciatic nerve exons and nerve endings in the footpads.

3.3.3 Decrease in POMC mRNA expression

To confirm whether the decrease in ß-endorphin and POMC was due to decreased gene expression, POMC mRNA levels were quantified in the DRG, sciatic nerves and footpads. A decrease of 80%was observed in the diabetic DRGs as compared to the control DRGs. No changes were detected in the POMC mRNA level in the sciatic nerves or footpads (Figure 12). In fact the gene expression in sciatic nerves and footpads was significantly lower as compared to the DRGs, reasserting the fact that the source of POMC and hence ß-endorphin in the PNS is the neurons present in the lumbar DRG.

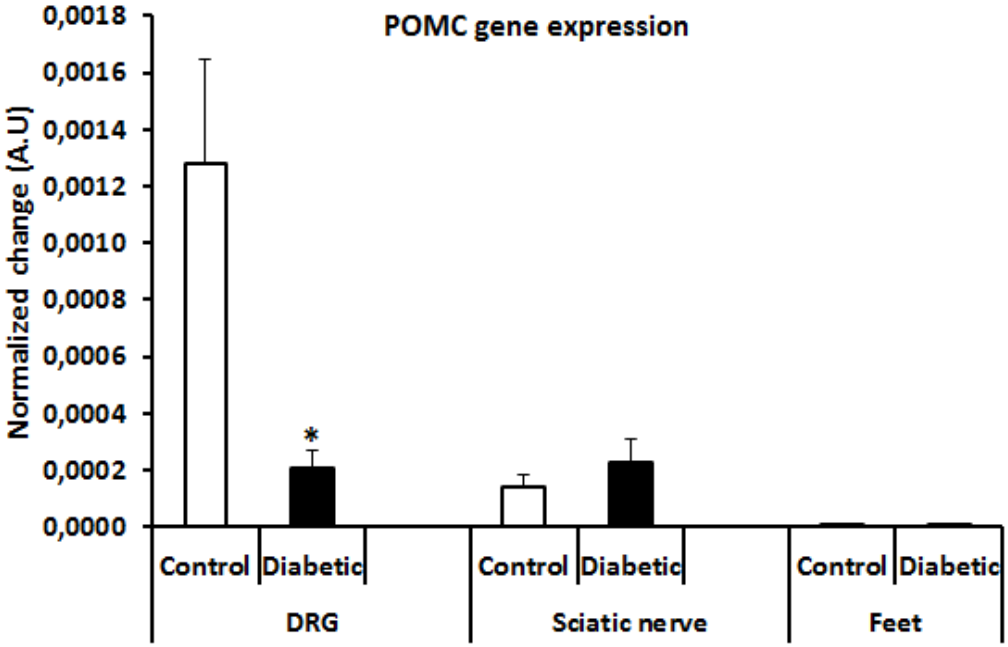

Figure 12: POMC gene expression in DRG, sciatic nerves and footpads POMC gene expression was majorly present in control DRG, while sciatic nerves and footpads showed negligible expression. An 80% decrease in diabetic lumbar DRG was found upon comparing with control lumbar DRG and normalization with 18srRNA (house-keeping gene). Data represented as Mean +/- SEM; Student's t-test *p<0.05.

3.4 Significant downregulation of MOR in 12 weeks diabetic mice

An anti-nociceptive signaling is only triggered when ß-endorphin binds its cognate receptor MOR. From the above data it is evident that one arm of this anti-nociceptive pathway is defective due to decreased ß-endorphin level during diabetes. From a therapeutic point of view, it is therefore important to understand whether the other key component, MOR, is functional during diabetes.

The MOR protein levels in control and diabetic lumbar DRG, sciatic nerves and footpads were determined using western blot. Surprisingly, the protein level of MOR was

decreased in the diabetic DRG by 78%; in the sciatic nerves by 45% and in the footpads by 65% as compare to the control tissues (Figure 13 a, b). This finding was confirmed by microscopic image analysis of the DRG sections (MOR signal intensity quantification; Figure 13 c, d) and in the foot sections which showed a 23 % decreases in PGP9.5 nerve endings, immunoreactive for MOR in the diabetic mice (Figure 13 e, f)

Interestingly, the decrease in MOR protein level in the PNS of diabetic mice was not due to decreased MOR gene expression (Figure 13 g). This implied that MOR protein was synthesized equally in control and diabetic DRG, but was potentially undergoing degradation in the diabetic DRG.

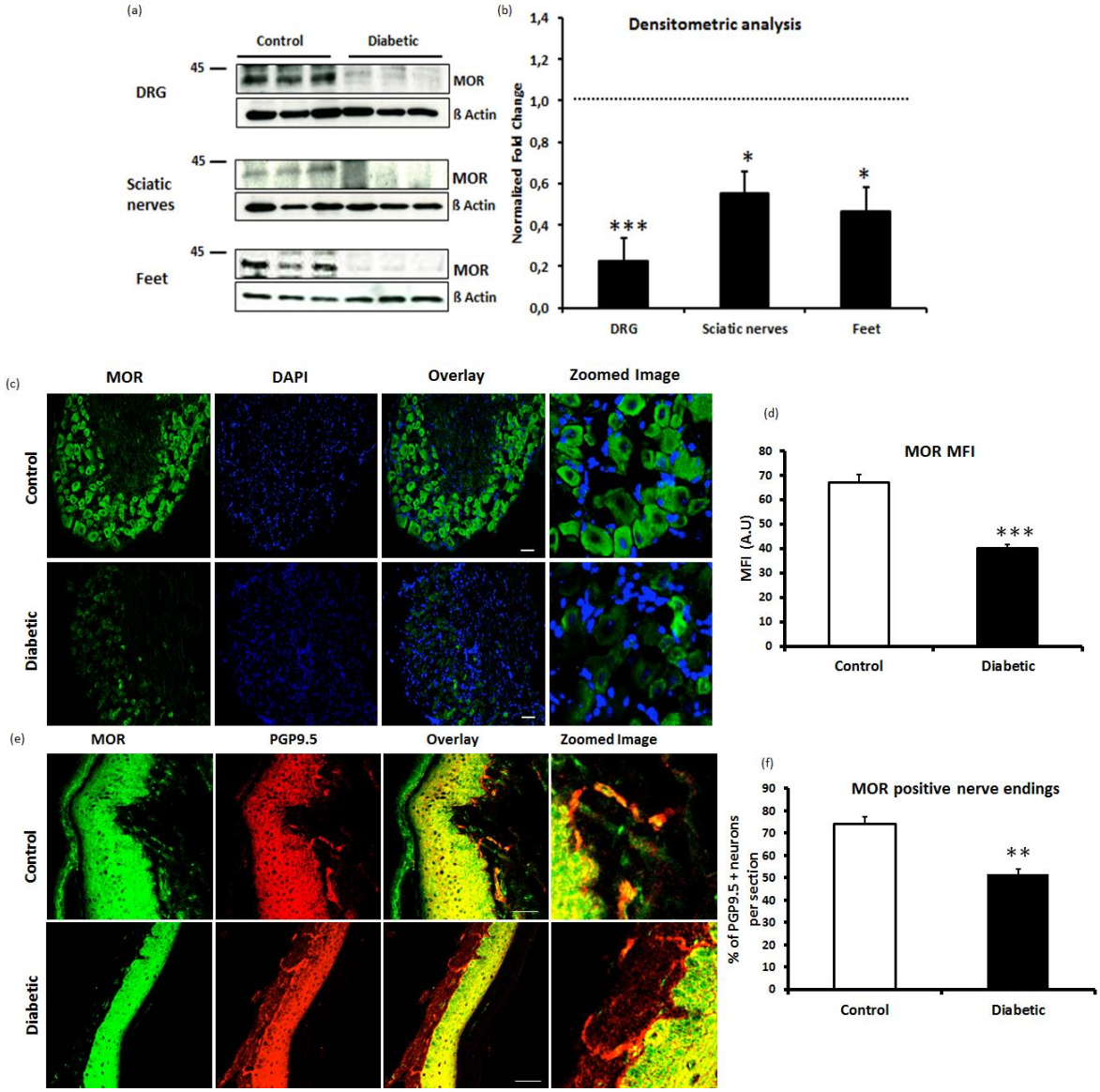

Figure 13 (a-f): MOR protein level in control and diabetic mice (a) MOR protein levels were compared between control and diabetic (n=6 each) in the lumbar DRG, sciatic nerves and footpads using western blot. (b) Upon densitometric quantification of the ~42Kda band, a significant decrease by 78% was observed in the diabetic

DRG, 45% decrease in the sciatic nerves and 65% decrease in the footpads. (c, d) Immunofluorescence staining of MOR in the DRG revealed a 40% decrease in the Mean Fluorescence intensity (MFI) of the MOR signal. (e, f) Also, the number of neurons expressing MOR had decreased by 23% per section. Data represented as Mean +/- SEM; Student's t-test **p<0.01, ***p<0.001. Scale bar =50 µm.

(g)

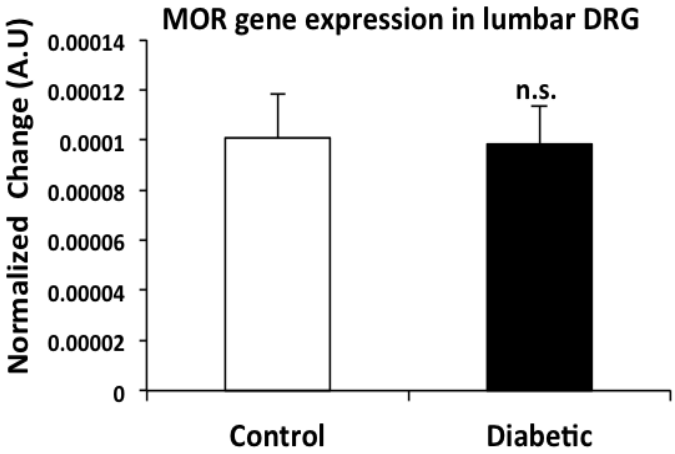

Figure 13 (g): MOR gene expression in the DRG of control and diabetic mice No significant difference was observed in the MOR mRNA level in the DRG of control and diabetic mice (n=6 each). 18s rRNA was used as the house-keeping gene for normalization. Data represented as Mean +/- SEM; Student's t-test n.s. p>0.05

3.5 Downregulated POMC and MOR associate with increased pain sensitivity

In order to understand the contribution of POMC-MOR pathway in pain sensitivity during diabetes, responses of mice to heat and mechanical stimulation were measured. The comparison of values showed that the diabetic mice were much more susceptible to pain than the control (Figure 14). Interestingly, this increase in pain sensitivity was associated with the decreased POMC and MOR levels in the mice.

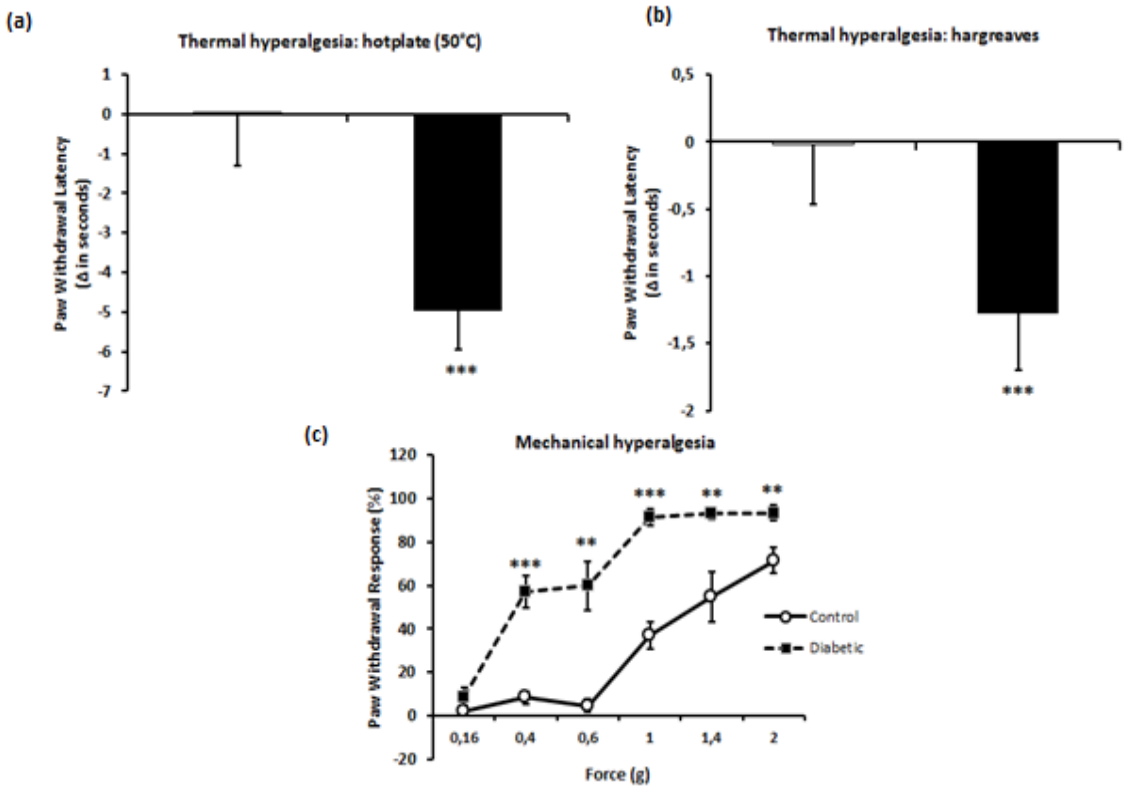

Figure 14(a-c): Increased thermal and mechanical hyperalgesia in diabetic mice Heat (a, b) and mechanical pain sensitivity(c) was found to be significantly increased in STZ mice 12 weeks post induction of diabetes (n=25 per group). Data represented as Mean +/- SEM; Student's t-test **p<0.01, ***p<0.001.

3.6 High glucose triggered NF-kB activation suppresses POMC expression

3.6.1 High glucose triggered POMC suppression

In order to understand the mechanism behind reduced POMC transcription in diabetes, *in vitro* studies were performed in AtT-20 cells. AtT-20 is a mouse pituitary cell line, routinely used to study POMC promoter, because of its high POMC expression levels. The effect of increasing glucose concentrations on POMC promoter was studied in presence or absence of POMC promoter agonist, corticotropin releasing hormone (CRH). It was found that POMC mRNA level was decreased under high glucose conditions. The presence of CRH during the exposure significantly increased POMC mRNA level under normal glucose conditions, but failed to do so at 20mM and 40mM glucose conditions. This effect was not due to a change in osmolarity as the effect of either 20mM or 40mM sorbitol exposure conditions was equal to the change in expression observed at 5mM glucose (Figure 15).

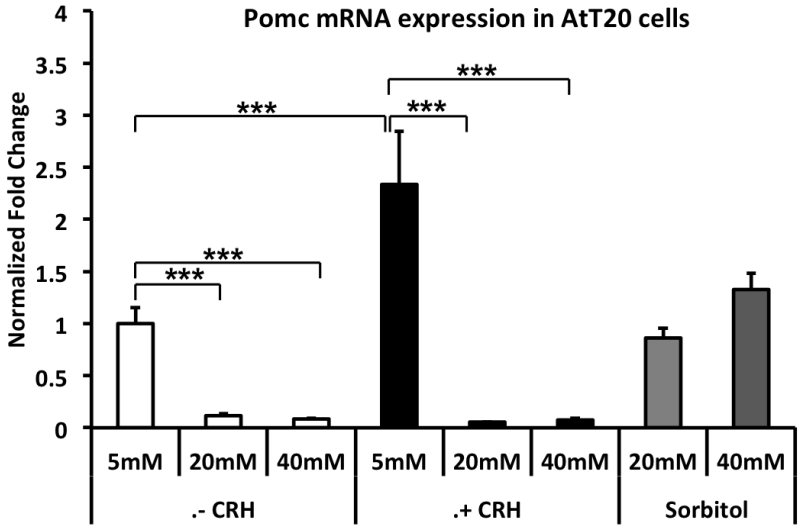

Figure 15: High glucose inhibits POMC gene expression POMC mRNA level were quantified and normalized using 18s rRNA in AtT20 cells. Exposure to high glucose concentrations for 12 hours inhibited POMC gene expression, even in the presence of POMC promoter agonist (CRH). Sorbitol control show that this effect is not caused due to increase in osmolarity. Data represented as Mean +/- SEM; 2 way ANOVA test and Bonferonni post hoc test ***p<0.001.

3.6.2 High glucose activates NF-kB in AtT20 cells

As the presence of CRH could not increase POMC gene expression this would suggest that high glucose was activating some factor, capable of binding to the POMC promoter, which antagonizes the effect of CRH. *In silico* analysis of the mouse POMC promoter region showed the presence of a NF-kB binding region (-125 to -83) ahead of the CRH binding region (-173 to -160) as predicted in the literature[114]. Studies have shown the inhibitory effect of NF-kB and its ability to block CRH mediated activation of POMC promoter [27,115]. However, it has also been shown that NF-kB is able to activate the POMC promoter[116].

Stimulation of AtT20 cells with increasing concentrations of glucose lead to increased activation of NF-kB (Figure 16a). Using supershift EMSA technique, p50 was identified as the major NF-kB subunit being activated (Figure 16b). This finding was supported by the increased p50 protein levels in the cells exposed to 20mM glucose for 12 hours as compared to those exposed to 5mM glucose (Figure 16c).

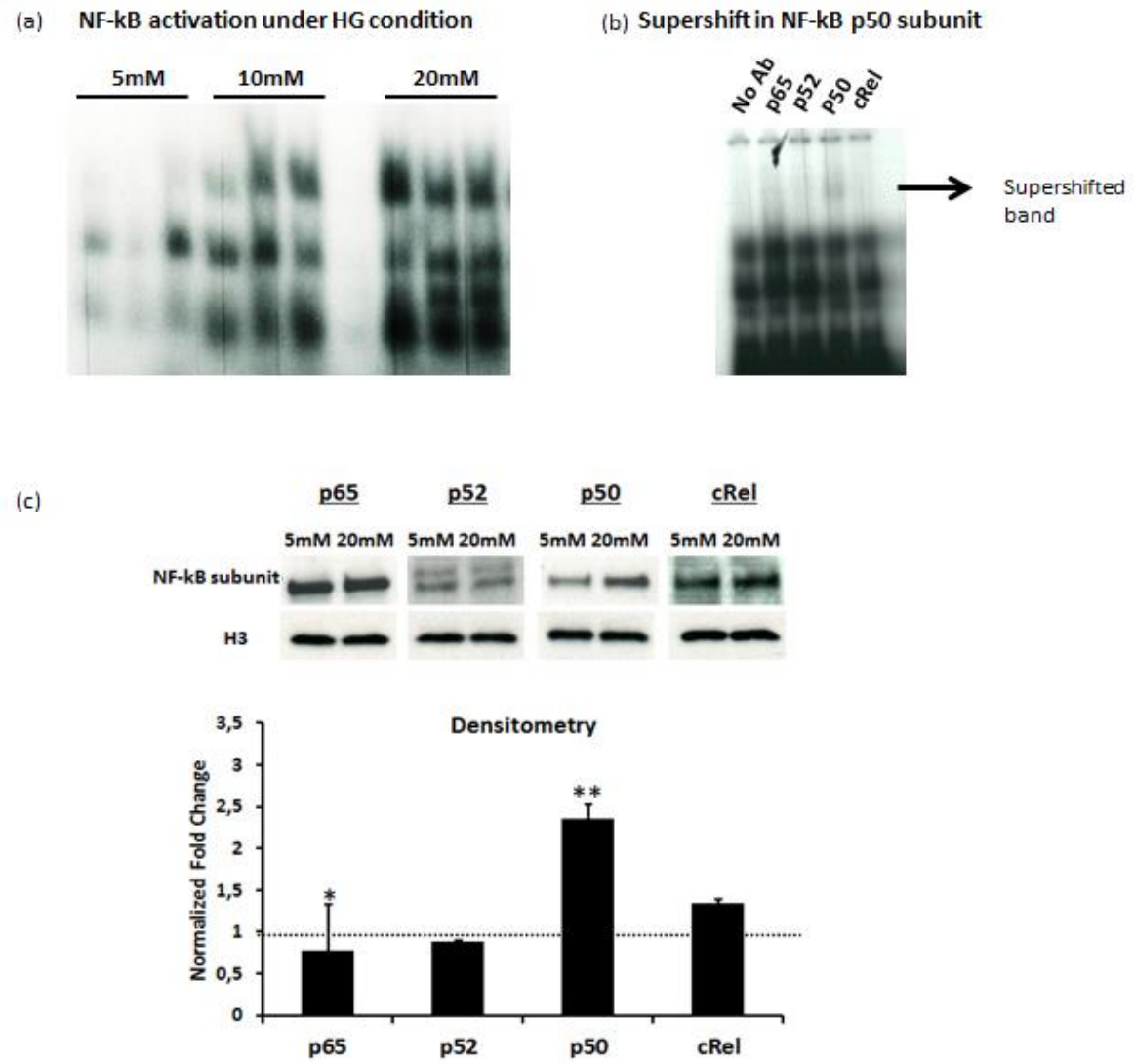

Figure 16 (a-c): High glucose induces NF-kB activation in AtT20 cells (a) Exposure of AtT20 cells to increasing glucose concentrations for 12 hours, induces NF-kB activation in an increasing order. Arrow denotes the band representing NF-kB (b) Supershift EMSA showed that p50 subunit was activated in AtT20 cells exposed to 20mM glucose for 12 hours. (c) The increased p50 activation is supported by increased p50 protein levels in the AtT20 nuclear lysates harvested at 12 hours. Data represented as Mean +/- SEM; Student's t-test **p<0.01.

3.6.3 NF-kB activated during hyperglycaemia suppresses POMC promoter

The direct evidence for the binding of glucose activated NF-kB to the POMC promoter was shown by ChIP assay. It was found that after 12hrs of high glucose (20mM) stimulation the POMC promoter was significantly more occupied by p50 NF-kB subunit (Figure 16a). There also was an increased binding of cRel to POMC promoter under high glucose condition, suggesting that the POMC promoter was either bound by p50 homodimer or p50-cRel heterodimer. Since p50 was the common subunit of the NF-kB complex binding to the POMC promoter, ChIP assay for p50 subunit was repeated in

control and diabetic DRG (n=5 each). A significant increase in p50 binding to POMC promoter was noted in the DRG (Figure 16b). Upon co-staining of the control and diabetic DRG sections with NF-kB p50 subunit and POMC, it was found that the neuronal cell bodies in which an increased p50 expression was seen, the POMC expression was decreased and vice versa (Figure 16c). This data would suggest that high glucose triggers NF-kB activation, particularly the p50 subunits in the AtT20 and the lumbar DRG. The p50 subunits most likely form a homodimer and bind to the POMC promoter leading to suppression of promoter and decreased POMC mRNA and peptide levels (Figure 17).

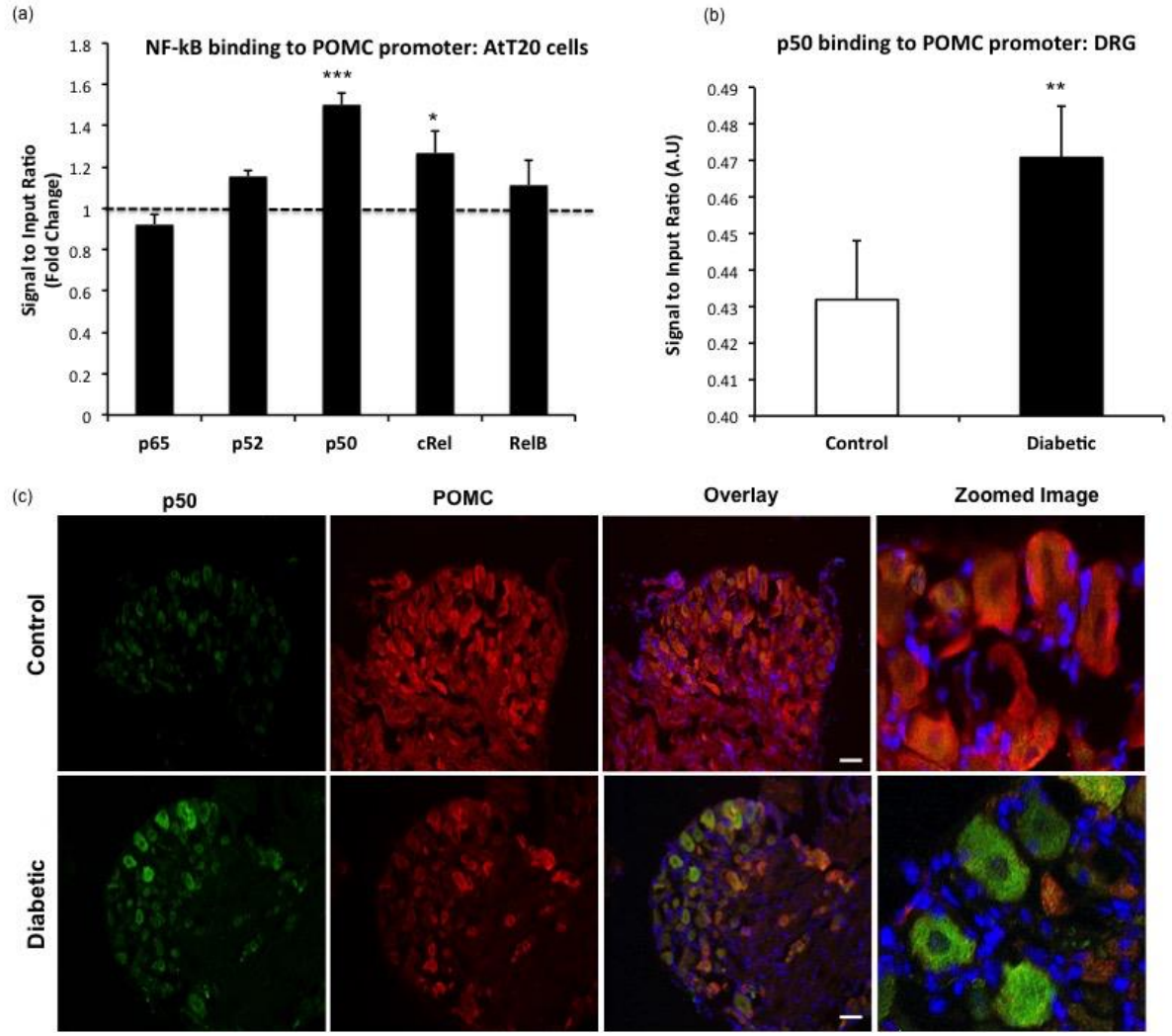

Figure 17 (a-c): NF-kB binding to POMC promoter (a) Two individual ChIP experiments were analysed together to investigate which NF-kB subunit binds POMC promoter under high glucose condition (20mM). Binding of p50 and cRel was significantly increased in the AtT20 cells (b) ChIP assay only for p50 binding showed significant occupancy of POMC promoter by p50 in diabetic DRG (c) Double immunostaning for POMC and p50 showed that increased p50 signal was localized to those neuronal cell bodies in the diabetic DRG where the POMC signal was decreased. Data represented as Mean +/- SEM; Student's t-test *p<0.05, **p<0.01, ***p<0.001. Scale bar =50 µm.

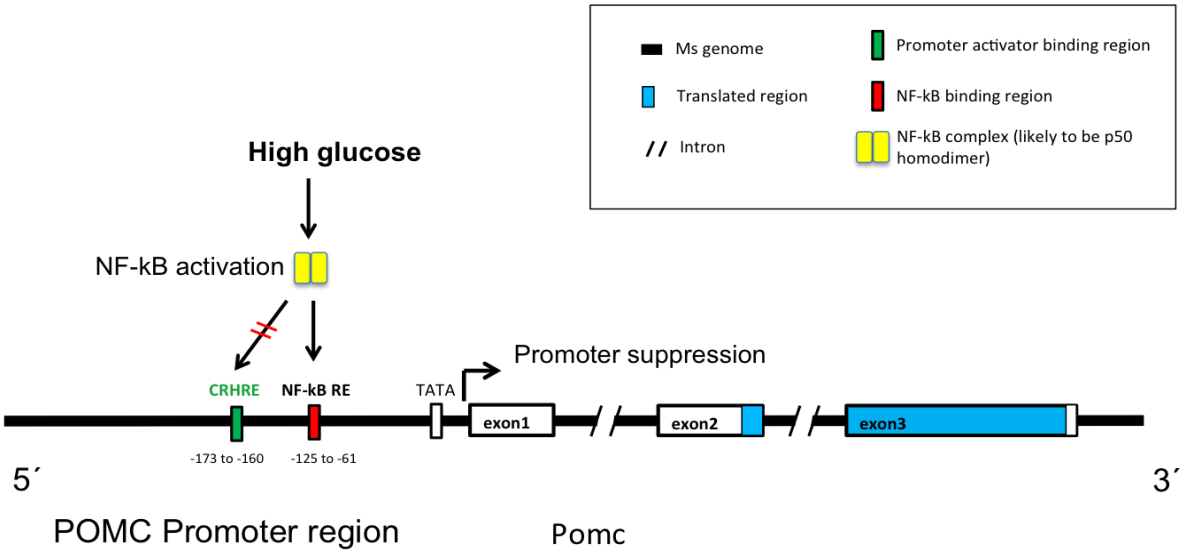

Figure 18 Schematic representation for decreased POMC expression during diabetes NF-kB is activated during hyperglycaemia, and the NF-kB complex (likely to be p50 homodimer) translocated into the nucleus where is binds to the POMC promoter region inhibiting the expression of POMC gene. This leads to decreased POMC mRNA and protein levels in the PNS. NF-kB binding to POMC promoter blocks the effects of CRH on POMC expression.

3.7 High glucose triggered PKC activation causes MOR degradation

3.7.1 Increased PKC activation in DRG during hyperglycaemia

There are two possible pathways that MOR can be degraded: agonist-dependent and agonist-independent. As the most potent endogenous MOR agonist, ß-endorphin, was deceased during diabetes, it was likely that MOR underwent degradation via the agonist-independent pathway. In the agonist-independent pathway, MOR is phosphorylated by PKC. Several studies have shown chronic PKC activation during diabetes, however, it was first necessary to establish increase in PKC activation during diabetes. Total protein lysates from lumbar DRG of control and diabetic mice were assessed using the kinase assay for PKC activation. Indeed, a significant increase in the PKC activation was noted in the diabetic DRG (Figure19 a). Whether the activation of PKC in the DRG was triggered due to hyperglycaemia, was assessed by exposing DRG cells to low and high glucose *in vitro.* Activation of PKC was determined by subcellular localization of PKC. In the DRG culture exposed to low glucose (17.5mM), PKC signal was observed within the PGP9.5 stained neuronal cell body. While, high glucose exposed DRG neurons showed increased association of PKC signal with wheat germ agglutinin (WGA), a dye used to define the plasma membrane. This activation within the

DRG neurons was inhibited in presence of PKC inhibitor, seen by diffuse signal not associated with cell membrane (Figure 19b,c).

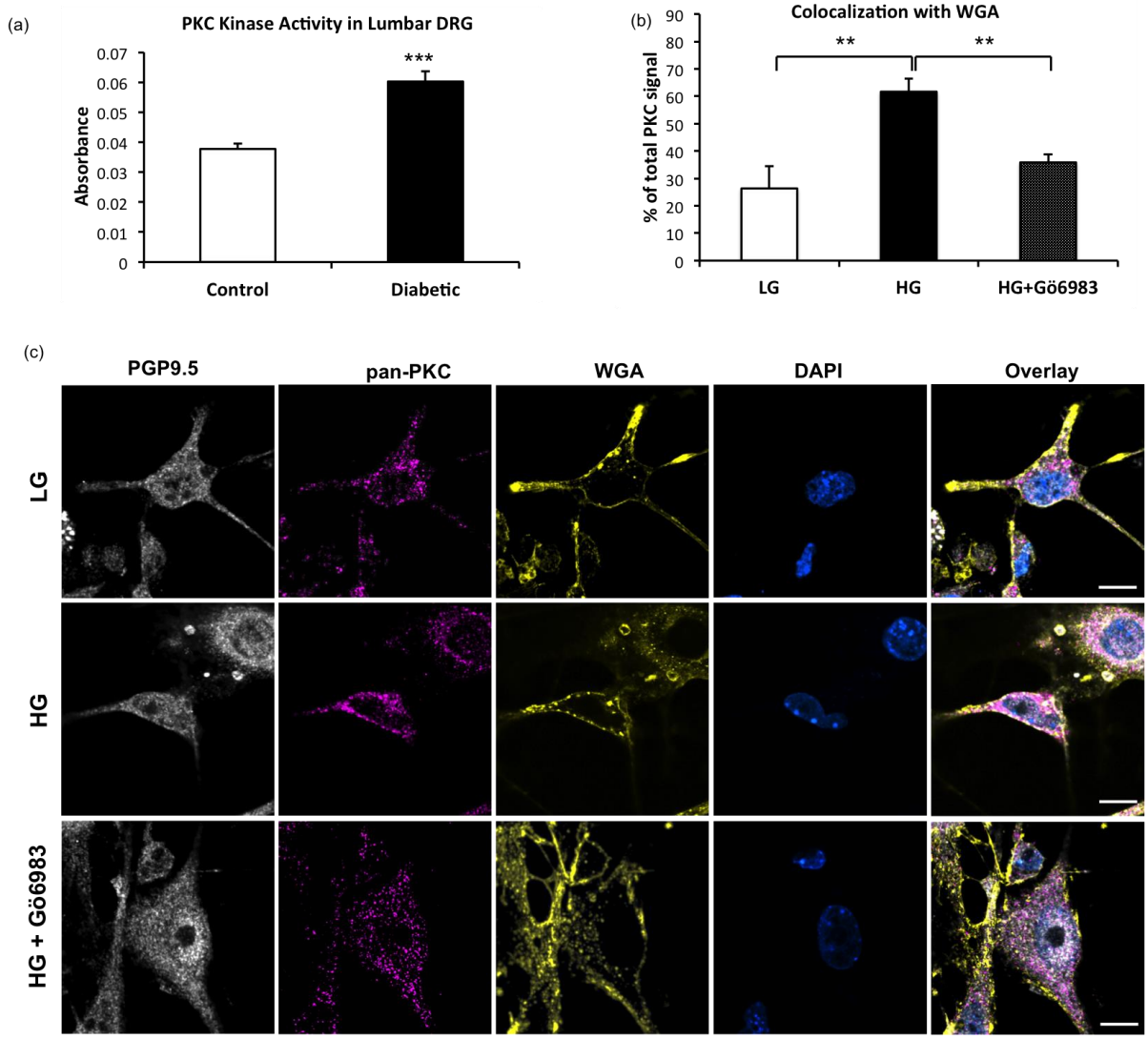

Figure 19: Increased PKC activation under hyperglycaemic conditions (a) PKC activity was increased in the DRG of diabetic mice compared to the non-diabetic mice DRG. (b,c) A similar activation of PKC was also observed when DRG culture was exposed to high glucose (HG; 40mM) compared to the DRG culture exposed to low glucose (LG; 17.5 mM) for 48 hours. The increase in activity was determined by subcellular distribution of PKC. In active state, PKC was present within the neuronal cell body, while upon activation in HG exposure, the PKC signal was present at the cell membrane determined by Wheat Germ Agglutinin (WGA) staining. In presence of PKC inhibitor(Gö6983), PKC signal was relocalized within the neuronal cell body. Data represented as Mean +/- SEM; Student's t-test *p<0.05, **p<0.01, ***p<0.001. Scale bar =10 µm.

3.7.2 Hyperglycaemia induced PKC activation is necessary and sufficient for MOR internalization

To establish whether PKC activation under hyperglycemic conditions able to induce internalization of MOR, DRG cells were transfected with Flag-MOR-mCherry construct and exposed to low and high glucose conditions in presence and absence of a PKC inhibitor. After 48 hours it was found that in cells exposed to either low glucose or low glucose + PKC inhibitor, the mCherry/MOR signal was associated with the WGA signal which denoted the plasma membrane. However, when the cells were exposed to high glucose, mCherry/MOR signal was found to be within the cells rather than being associated with cell membrane. The internalization of MOR, was therefore found to be reduced in presence of the PKC inhibitor. This suggests that PKC mediated phosphorylation is capable of internalizing MOR (Figure 20a, b).

A control to verify whether the neuronal cells of the DRGs were transfected with the construct, was set by co-staining with PGP9.5 and mCherry antibodies. 70% of the total cells were neuronal cells indicating a largely homogenous neuronal population was present in the cultured DRG cells. (Figure 20).

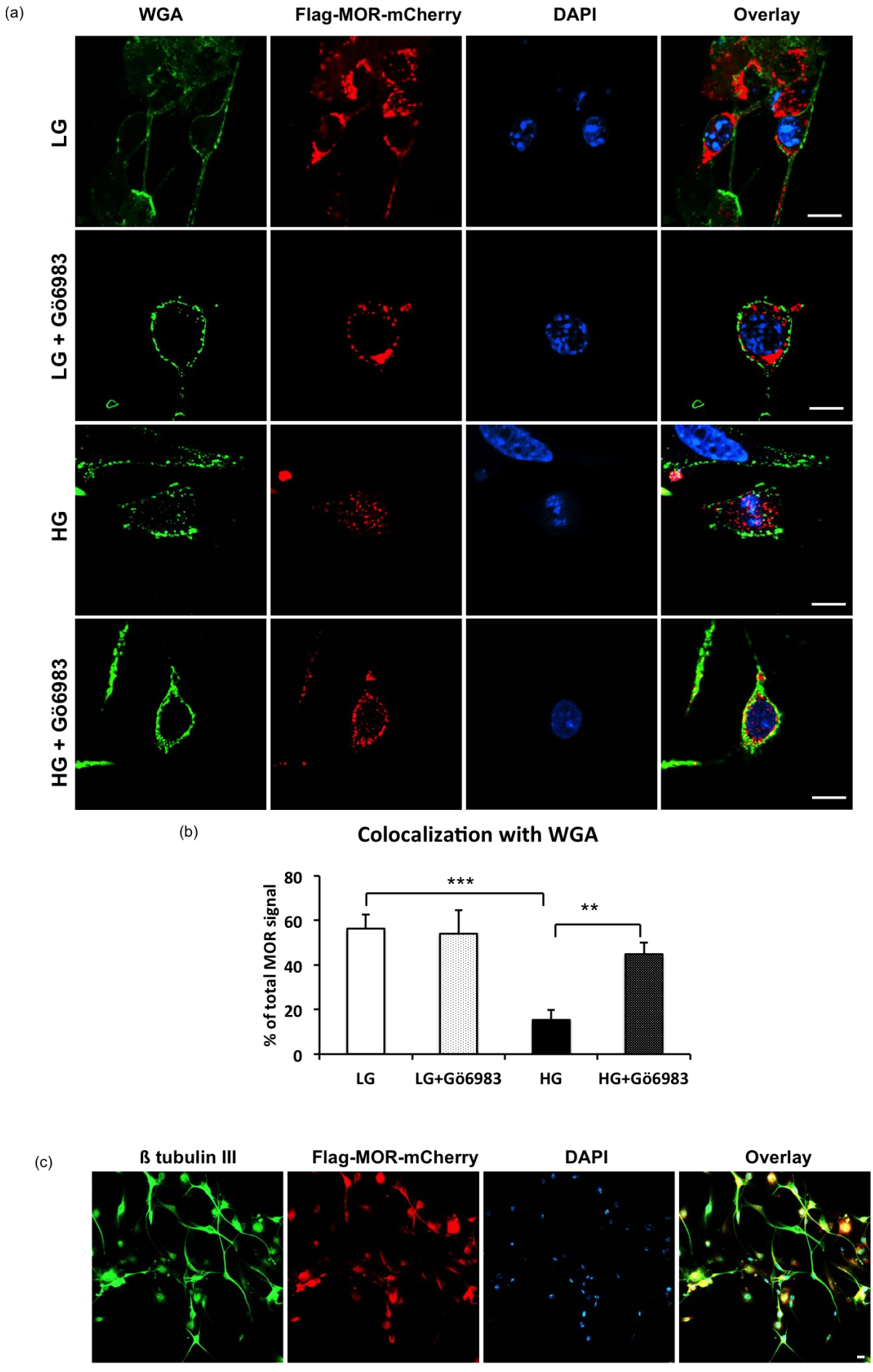
(a)
WGA
Flag-MOR-mCherry
DAPI
Overlay
LG
LG + Gö6983
HG
HG + Gö6983
(b)
Colocalization with WGA
% of total MOR signal
80
60
40
20
0
***
**
LG
LG+Gö6983
HG
HG+Gö6983
(c)
ß tubulin III
Flag-MOR-mCherry
DAPI
Overlay

Figure 20: Hyperglycaemia induction PKC activation causes MOR internalization (a) Flag-MOR-mCherry transfected WT primary DRG cells were exposed to low (LG; 17.5mM) or high (HG; 40mM) glucose in presence and absence of PKC inhibitor (Gö6983). After 48 hours of exposure and live staining with wheat germ agglutinin (WGA) revealed internalization of MOR under high glucose condition, which was reversed significantly in presence of PKC inhibitor. (b) Presence MOR signal on cell surface or within the cell was determined by % colocalization of MOR with WGA (c) The DRG culture was stained with ßtubulin III, neuronal marker. 70% of the total cell population was neuronal cells. Data represented as Mean +/- SEM; unpaired Student's t-test * **p<0.01, ***p<0.001. Scale bar =10 µm.

3.7.3 MOR is trafficked to lysosomal degradation pathway during diabetes

To determine whether MOR is trafficked to the lysosomal degradation pathway, DRG sections from control and STZ-diabetic mice were co-staining for MOR and the lysosomal marker, Lamp1. There was a significant increase in the colocalization in the STZ-diabetic DRG, providing evidence that the MOR was indeed being degraded in the lysosomes in STZ-diabetic DRG (Figure 21a, b).

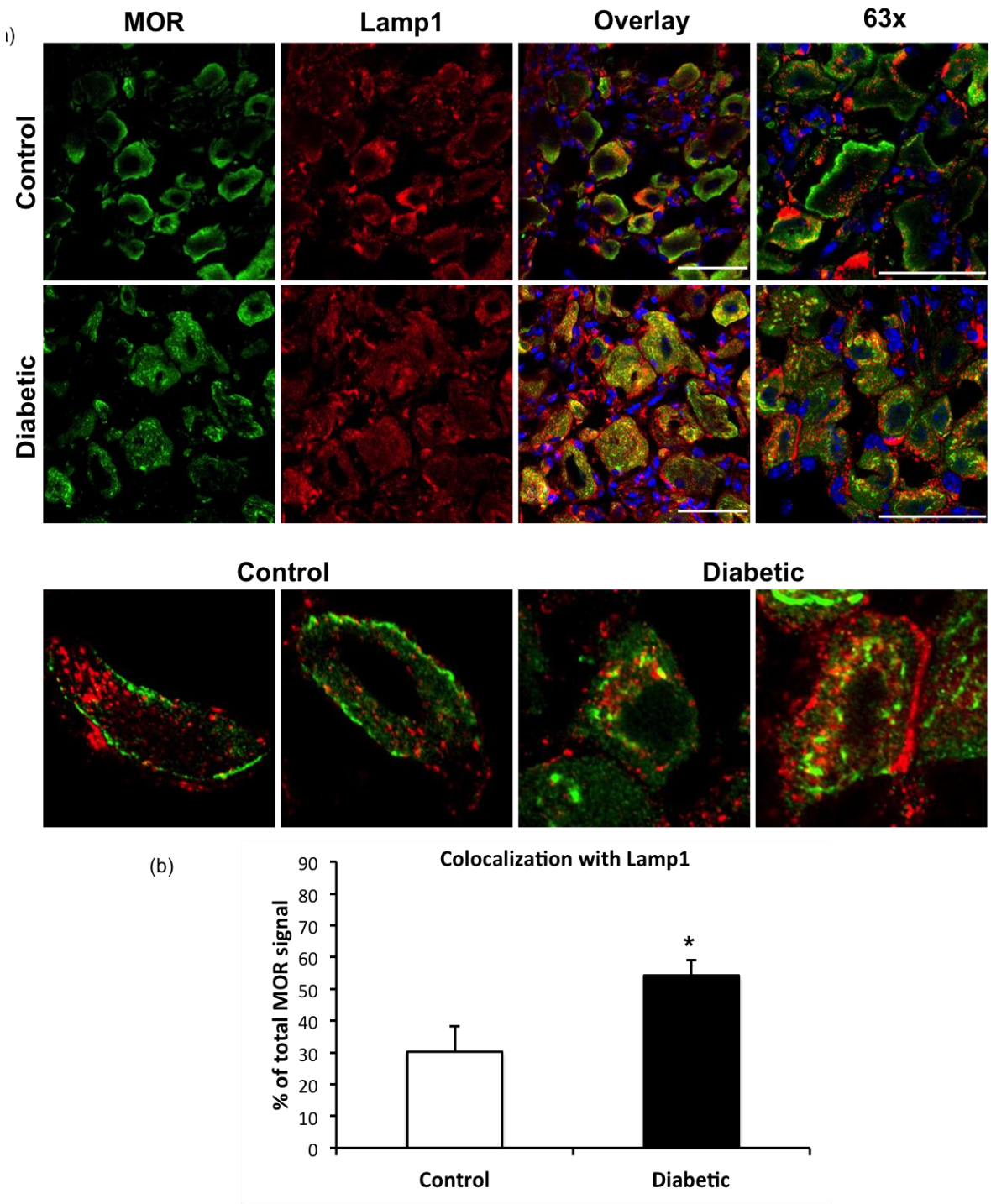

Figure 21: Lysosomal degradation of MOR during diabetes MOR immunoreactivity was predominantly seen within the cytoplasm of DRG neuronal cells during diabetes and was colocalized with lysosomal marker indicating the trafficking of MOR into the lysosomal degradation pathway. The DRG neurons in the control mice showed MOR immunoreactivity on the cell surface and no colocalization with lysosomal marker.

In summary, the hyperglycemia induced chronic PKC activation is partly responsible for sustained MOR internalization and therefore its trafficking to the lysosomal degradation pathway during diabetes (Figure 22).

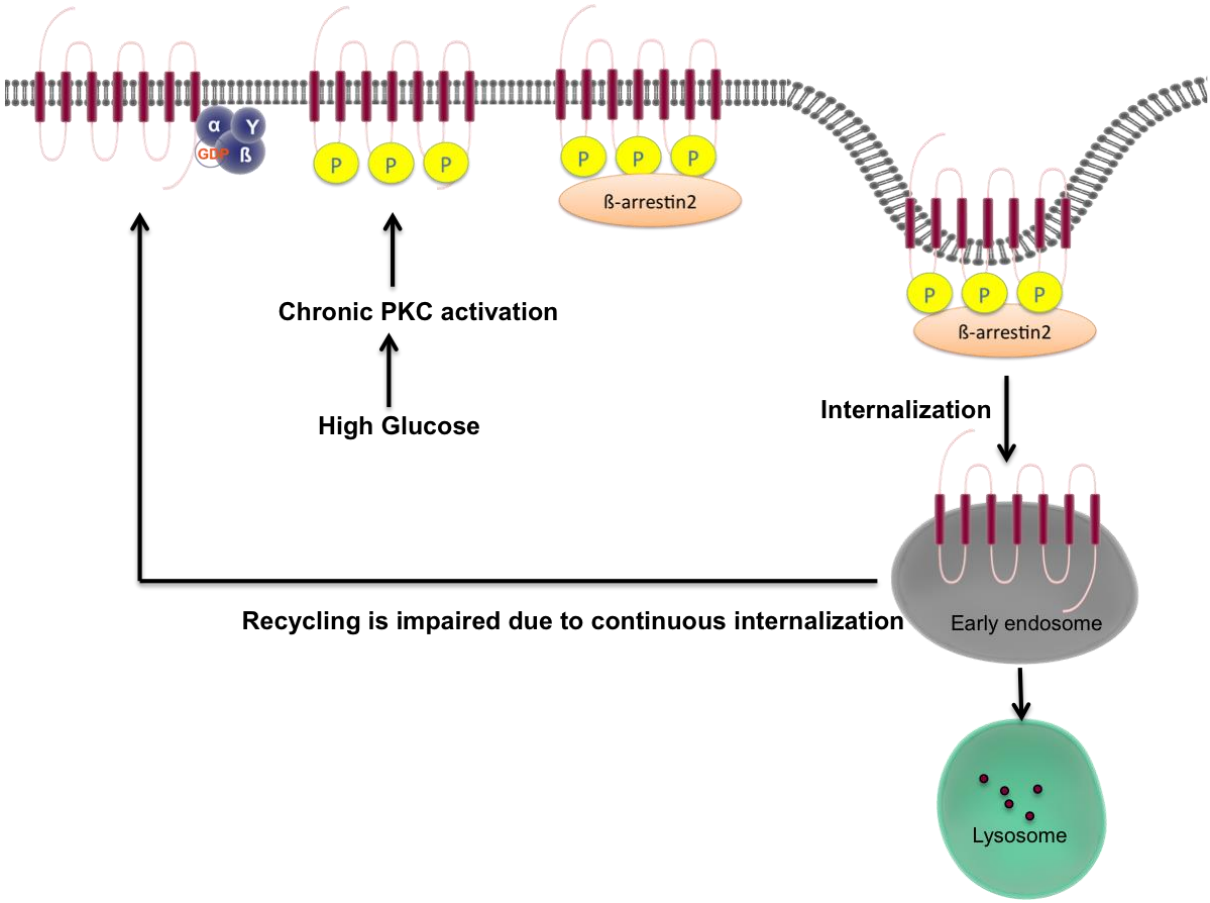

Figure 22 Schematic representation of MOR downregulation during diabetes MOR is persistently internalized due to chronic PKC mediated phosphorylation. As a result, the failure of recycling event occurs which destines the receptor into degradation pathway.

4. Discussion

Diabetic peripheral neuropathy (DPN) is a highly debilitating complication affecting the quality of life of diabetic patients severely. Current treatments for DPN such as opioid analgesics are ineffective while others namely; pregabalin, duloxetin etc. have adverse side effects[11]. Thus, in search of mechanisms underlying pain sensation anomalies in DPN, expression of the endogenous opioid peptides in the PNS of STZ induced mice was studied.

The present study found that POMC, ß endorphin and MOR were decreased in the lumbar dorsal root ganglia, sciatic nerves and footpads of STZ treated mice, as compared to the untreated mice. While, downregulation of MOR seemed to be due to its lysosomal degradation induced by activated PKC, POMC promoter suppression seemed to be partly mediated by high glucose induced NF-kB. Interestingly, the downregulated POMC-MOR levels associated with increased thermal and mechanical pain sensitivity of the STZ mice. Taken together, this data indicates that POMC-MOR proteins are involved in the hyperalgesia experienced during diabetic peripheral neuropathy.

Given that major opioid expression occurs in CNS, opioid peptide-opioid receptor pain signaling has been extensively studied in the CNS. For instance, Havlicek *et al* found that intracerebral injection of endorphin is able to induce a general state of anesthesia[117]. Decreases in ß-endorphin in the central nervous system results in chronic pain state[118]. Activation of DOR through enkephalin is of less consequence in acute pain state and more towards chronic pain in rodent CNS[119]. Dynorphin-KOR system results in analgesia partly due to direct inhibition of pain pathways and partly by its engagement in stress pathways[120] However, such opioid signaling modulates the central and supraspinal mechanisms of pain.

Whereas in the PNS, the endogenous opioids have been primarily studied in the mice with nerve injury as models of neuropathic pain. Peripheral nerve damage is associated with an activation of immune cells and their infiltration at the site of injury. The evidence for expression of opioids within the immune cells has prompted several

researchers to investigate the importance of immune cell-derived opioids in alleviation of injury induced heat and mechanical hyperalgesia[72,82,121,122]. However, the modulation of peripheral analgesic pathways in neuropathic models in the absence of a direct injury, such as DPN, has not been studied. Indeed, there are microstructural alterations in the sciatic nerves during diabetes, but they have been shown to occur in patients with advanced diabetic neuropathy. For instance, Pham *et al*, reported presence of lesions in the sciatic nerves of patients having diabetes for ca.20 years[123]. Yet, symptoms of increased pain sensitivity are shown even by pre-diabetic and patients with early diabetes [3]. It is, therefore, important to identify pathogenetic mechanisms occurring in the early stages to prevent the progression of DPN. In this light, the contribution of endogenous opioid system to the pathogenesis of early DPN (until 12 weeks) was studied in STZ induced mice.

Since, infiltrating immune cells were reported to be the primary source of opioids in the PNS of neuropathic pain models, the STZ induced diabetic mice were studied for immune cell infiltration. An increasing number of leukocytes and macrophages were found in the diabetic nerves. Interestingly, these immune cells were not found to express opioid peptides. There are two possible explanations to this finding. First, the identified macrophages were pro-inflammatory. Pannell *et al* (2016) showed that only the anti-inflammatory M2 macrophages express and release opioids[121]. Second, immune cells express negligible opioids under normal physiological condition[124–126]. The presence of CRH can upregulate opioid expression in the immune cells and releases the peptides. CRH is expressed in the nerve upon injury, but not otherwise[127]. As such, the immune cells were identified as not being the primary source of opioids in the diabetic nerves. The neuronal cells of lumbar DRG expressed the endogenous opioids in diabetic and non-diabetic mice. These results are in line with previous studies showing presence of neuron derived opioids in the PNS[69,71,128]. It was clear from this data that the pathobiology of DPN mouse model was different from the mouse models of nerve injury.

The STZ mouse model used in the study has some limitations. Since the mice are induced diabetes chemically, it is important to determine whether the changes seen are due to hyperglycemia and not STZ. For this purpose a time course study was carried out

until 12 weeks post STZ treatment. The effect of STZ induced diabetes on DRG neurons was measured as a function of opioid expression and pain sensitivity at intervals of 4 weeks. It was found that the mice showed an initial hyperalgesia, presumably as an effect of the STZ followed by a phase of recovery. This observation in agreement with other studies reporting the effect of STZ on pain sensitivity due to sudden increase in oxidative stress and inflammation[112,113]. The neuron-derived opioids, too, underwent transient changes in this period showing that STZ had a temporary effect on the DRG neurons, which was gone by 12 weeks post STZ treatment. There exist few studies on the harmful effect of STZ on the neuronal cells. For example, Genrikhs *et al*, reported the neurotoxic effects of STZ in cultured neuronal cells [129]. However, the effects were monitored 48 hours post STZ exposure. Our data shows that though STZ does have some effect on the DRG neurons, they are not long lasting. This finding is supported by another study by Davidson *et al*,which showed that STZ has no direct effects on the peripheral nerves at 12 weeks post induction, using two different mouse strains and performing experiments in two different laboratories[130].

At 12 weeks post STZ treatment, Freeman *et al*, reported a dramatic increase in glucose and polyol pathway intermediates in lumbar DRG and sciatic nerves[131]. The authors reported a striking failure of energy homeostasis and oxidative stress in the sciatic nerves and argued that most severe molecular consequences were restricted to this region during diabetes. Although the metabolic dysregulation was severe in the nerves, the fact that there was a 14.6 fold increase in glucose and in sorbitol, fructose level in the DRG, shows that the pathogenic mechanisms occurring in DRG cannot be overlooked. There also were significant changes in levels of proteins involved in various pathways, namely, acute phase response, ER stress response, glycogen metabolism, ketogenesis and activation of LXR/RXR activation, which is known to affect POMC levels[132]. Although, the number of altered proteins were greater in the sciatic nerves, the changes occurring in the diabetic DRGs are more relevant to the endogenous opioid system in the PNS.

At 12 weeks once the potential for non-specific STZ effects had gone and overt hyperglycemia was present, the opioid levels of PENK and PDYN did not show significant changes. POMC, however, was significantly downregulated. This was also

reflected by decreased a ß-endorphin level in the diabetic mice. There are only two studies to date, which have looked at basal endogenous opioid levels in the PNS of diabetic animal models. Kou *et al*, showed a decrease in the non-classical opioid endomorphin 2 in the lumbar DRG[133]. These measurements were carried out 72 hours post STZ treatment, making it likely to be an STZ effect rather than diabetes mediated mechanism. Jolivalt *et al*, reported increased dynorphin levels in diabetic rats at 8 weeks post STZ treatment. The authors also showed that this increased endogenous dynorphin in the DRG contributed to hyperalgesia by activating the NMDA receptors in the peripheral nerves[71]. However, in the STZ mice model used in the present study, an upregulation of dynorphin and concomitant hyperalgesia was only observed at 4 weeks, which was considered to be a response to STZ. The disparity in the findings could be due to use of different animal models (rats and mice) which may show effects on a different time scales post diabetes induction.

As such, the current study is the only one to have reported changes in basal expression of POMC in the DRG during diabetes. There have been a few contradictory studies, which have shown changes in POMC and ß-endorphin peptide levels in the CNS and blood during diabetes. The most recent study was in 1999 by Cheung *et al*, which showed decreased ß-endorphin in the anterior pituitary and neurointermediate lobe after 1 week of STZ injection[98]. A direct effect of STZ was ruled out in this case since the STZ injection was not given intracerebrovetricularly. Tsigos *et al* showed that diabetic patients had lower ß-endorphin levels in the CSF. Lowering of ß-endorphin and POMC in diabetic patients would suggest that similar decrease observed in the mice was not merely an STZ effect. Interestingly the CSF levels of ß-endorphin did not correlate with symptoms of pain in the patients[134]. This suggests that diabetes causes a systemic downregulation of POMC and ß-endorphin, but only the decrease in the PNS is relevant to painful DPN.

The decrease in POMC was consistently found in the diabetic DRG, sciatic nerves and footpads. According to the classical model of opioid precursor processing, the precursors are synthesized in the cell bodies of neurons and then packaged into vesicles. They undergo proteolytic cleavage within these vesicles in the cell bodies to form mature opioid peptides, which are then transported, via axons, to the nerve

endings. Yakovleva *et al* challenged this model showing that the PDYN precursor peptides are only proteolytically cleaved in the nerve endings following an excitatory stimulus[100]. The data from this study would support the concept of the POMC peptide being synthesized in the neuronal cell bodies, located in the DRG, undergoing axonal transport, and subsequent cleavage to ß-endorphin in the nerve endings present in the footpads, but also to some extent in the sciatic nerves. This is evident from the amount of ß-endorphin found in each of the tissues; maximum ß-endorphin level (ng per mg protein) was found in the footpads of control mice (6.5 ±0.02) compared to sciatic nerves (3.7 ±1.17) and DRG (1.6 ± 1.28). This finding seems to partly agree with the classical model and partly with the non-conventional model.

Despite a few articles reporting the downregulation of the POMC peptide during diabetes, there exists very little information on the mechanism for this downregulation . It was found that decreased POMC gene expression in the diabetic mice was the reason for lower peptide levels. There are few known negative regulators of POMC promoter. Activated glucocorticoids receptor complex can inhibit the POMC promoter by directly binding to a region within the promoter and was first shown by Drouin *et al* [26]. This was the only known negative feedback mechanism for POMC expression until recently when Ma *et al*, showed that FoxO1 is activated during diet induced leptin, and is able to restrict STAT3 mediated POMC activation[135]. The promoter repression by Smad heterodimers is suggested to play a role during early development and organogenesis[136]. NF-kB is a contested regulator of promoter regulation. Jang *et al* showed that NF-kB p65 subunit was activated and increased POMC expression in hypothalamus of mice injected with LPS or HIV-1 Tat protein. An infection associated inflammatory environment was mimicked in the mice to show and NF-kB mediated POMC activation is associated with a decrease in food intake, causing anorexia and weight loss in infectious diseases [28]. This was supported by the study of Takayasu et al, which demonstrated that *in vitro* exposure of mouse pituitary cells AtT20 to pro-inflammatory cytokines TNF-α and IL-1ß caused translocation of p65 subunits to nucleus and binding to POMC promoter leading to promoter activation[137]. These two datasets indicated that acute inflammation caused p65 subunit to activated POMC promoter under acute inflammatory condition. Asaba *et al* reported that high glucose triggered NF-kB activation was responsible for POMC promoter activation in AtT20

cells[116]. Conversely, Shi *et al* showed that in chronic low-grade inflammation (high fat diet fed mice model) p65 is not able to activate the POMC promoter in hypothalamic neurons because of increased DNA methylation in the NF-kB binding region in the promoter. The free p65 subunit actually suppressed POMC promoter by inhibiting STAT3 signaling pathway[138]. A direct role for inhibitory activity of NF-kB has been described by Karalis *et al* [27]. It was shown that NF-kB can bind directly to the POMC promoter and suppression of CRH mediated activation. This finding was reproduced by Zbytek *et al* in human melanocytes[115]. These studies would indicate that NF-kB has the capacity to activate or suppress POMC gene expression depending on the mechanism/pathway behind the activation of NF-kB activation as well as the possibly cell/tissue type.

NF-kB activation is shown to be present in the DRG of STZ induced rats. NF-kB activation has been linked with painful DPN, by showing direct binding of NF-kB to the promoter of purinergic P2X3R (ion channel upregulated during neuropathic pain) gene. In this particular study, p65 subunit was activated in DRG[139]. In this study, it was also shown that NF-kB was activated in the DRGs of diabetic mice and its role in enhancing the painful symptoms of DPN by lowering POMC gene expression. However, the subunit identified to suppress the POMC promoter was p50, (p50 homodimer or p50-cRel). Homodimers of p50 subunit have been known to transcriptionally repressive[140,141]. The p50 homodimers are upregulated during inflammation and suppress the NF-kB target genes such as the pro-inflammatory cytokines TNF-α[142] and IL-2[143]. Anti-inflammatory role of p50 homodimers was asserted by showing p50 knock-out mice were susceptible to inflammatory bowel disease[144]. This could indicate that NF-kB activation is triggered in the diabetic DRG due to hyperglycaemia associated inflammation, but suppression of POMC is an unwanted side-effect. Although Djurik et al showed an anti-inflammatory activity of cRel containing subunits[145], p50-cRel heterodimers have only been shown to occur in mature B lymphocytes previously[146]. This data confirms a negative regulatory role for NF-kB for POMC gene under hyperglycaemic condition. However, this result is contradictory to the data shown by Asaba *et al* mentioned above which argues for NF-kB activation of POMC under high glucose condition. However, unlike the mentioned report, the present study has shown direct evidence for binding of p50 subunit and lowering of POMC mRNA *in vitro* as well as *in vivo* in diabetic mice.

NF-kB mediated downregulation of POMC rendered one arm of the ß-endorphin-MOR anti-nociceptive pathway dysfunctional. It was important to understand whether the other arm, MOR and its signaling was still functional. It was found that MOR protein level, too, was decreased during diabetes. Since the MOR mRNA level remained unchanged, the receptor was hypothesized to undergo degradation. MOR is reported to undergo degradation in presence of excessive amounts of the agonist or presence of the agonist for longer duration of time (several hours at the minimum)[147]. Its most potent endogenous agonist, ß-endorphin, was found in this study to be significantly decreased. The next most potent agonist for MOR, enkephalin was also found not to be elevated at 12 weeks in diabetic DRGs. Yet, MOR was found to co-localize with the lysosomal marker. This is consistent with a previous study in the DRGs of STZ induced rats[104]. Given the circumstances of decreased endogenous agonists, the occurrence of MOR degradation was curious. A research article published by Illing *et al* showed that MOR could be phosphorylated by PKC in an agonist-independent manner[59]. Phosphorylation is a prerequisite of MOR internalization. The hypothesis of agonist-independent phosphorylation, internalization and degradation seemed to be a probable scenario in the present study. Therefore, PKC kinase activity was assessed and a significant increase was observed in the diabetic DRGs. Mousa *et al* described the role of PKC in MOR phosphorylation in diabetic DRGs, usinga PKC inhibitor *in vivo* to show that PKC activation was responsible for uncoupling of MOR from the G proteins, causing desensitization of the receptor. PKC was shown to be activated in a RAGE dependent manner[11133]. Desensitization of MOR is usually followed by resensitization. Mousa *et al* indicated that in early diabetes, desensitization-resensitization event was still functional, since no reduction in MOR protein was found. In the current study, however, it was observed that high glucose mediated activation of PKC for 48 hours was capable of completely internalizing the MOR in DRG neurons *in vitro, a* step occurring after uncoupling from G proteins. An internalized receptor is reported to retain its functionality and signaling for few hours before being recycled back to the surface. But in the hyperglycaemic condition, even if the receptor was recycled back to the surface, chronic activation of PKC will internalize the receptor again, leading to futile loop event. The impairment of successful recycling results in lysosomal targeting of MOR[147]. The current study shows not just PKC mediated MOR internalization, but also an association

between chronic PKC activation and MOR lysosomal degradation. Further studies are required to determine the role of RAGE in the PKC mediated internalization during hyperglycaemic condition is using the RAGE$^{-/-}$ mice[148].

There have been numerous studies which have looked at MOR protein levels and whether its downstream signaling is functional in diabetes[104,106,149]. However, all of them have looked singularly at MOR expression and signaling during diabetes and therefore has given insufficient information on mechanistic details of this phenomenon. In this study, endogenous opioid system within the PNS has been comprehensively studied and was able to suggest an agonist-independent degradation of MOR as a possible mechanism for reduction in MOR protein.

In summary, the POMC- MOR anti-nociceptive pathway was shown to contribute to painful diabetic neuropathy. In order to study the changes in the endogenous opioid system, female mice were chosen for study. This was because firstly, multiple observations supporting presence of sexual dimorphism in response of the endogenous opioid systems [150]; secondly, there are reports showing analgesics against peripheral neuropathic pain are less effective in females than in males [151,152] making females a more interesting model to study. In order to understand whether the findings of this study are gender specific, similar experiments in male mice could be performed. Also, to add more credibility to the findings, restoration of POMC and MOR levels in the diabetic mice and then examining their pain sensitivity would be a confirmatory proof. Although the impairment of the POMC-MOR pathway is affected due to hyperglycaemia, this data is restricted to the type 1 diabetic mouse model. Repeating the experiments in animal models of type 2 diabetes, such as dbdb mice or ZDF rats, will ascertain the role of this anti-nociceptive pathway in DPN. Since the alteration in POMC-MOR pathway is described in PNS, the study also raises the question whether such a defect might exist in other tissues known to express both proteins. Of course, in other tissues, if such a defect does exist, the effect may not be on pain sensitivity. But given the numerous roles of POMC and its derived peptides such an anomaly if in CNS, GI tract, heart or blood-borne immune cells (section 1.3), may have far reaching consequences in diabetes and therefore deserves further investigation.

In conclusion, this study, for the first time, emphasizes the importance of endogenous POMC and MOR pathway in the PNS in context of painful diabetic neuropathy. It provides a platform for development of new therapies to counter painful symptoms by boosting the endogenous POMC synthesis and prevention of MOR degradation. Administration of POMC promoter agonists such as CRH (usually administered in the patients with Cushing's disease of POMC defeciency[153]) into the spinal cord may be one of the few alternatives to enhance ß-endorphin production in the peripheral nerves during diabetes. Use of gene delivery techniques would also be a potential therapeutic in the future for patients with painful DPN. More importantly, metformin, a commonly used anti-diabetic drug has been recently shown to lower POMC levels [132]. It becomes all the more necessary to develop strategies to boost POMC-MOR expression in the PNS while using metformin to treat diabetes and preventing exacerbation of DPN. Further studies are therefore required to establish whether the targeting of POMC-MOR pathway could be a valid therapeutic opinion in the treatment of diabetic neuropathy.

Summary

Diabetic peripheral neuropathy (DPN) is a highly debilitating complication affecting the quality of life of diabetic patients severely. Current treatments for DPN such as opioid analgesics are ineffective while others namely; pregabalin, duloxetin etc. have adverse side effects. Thus, in search of mechanisms underlying pain sensation anomalies in DPN, expression of the endogenous opioid peptides in the PNS of STZ induced mice was studied.

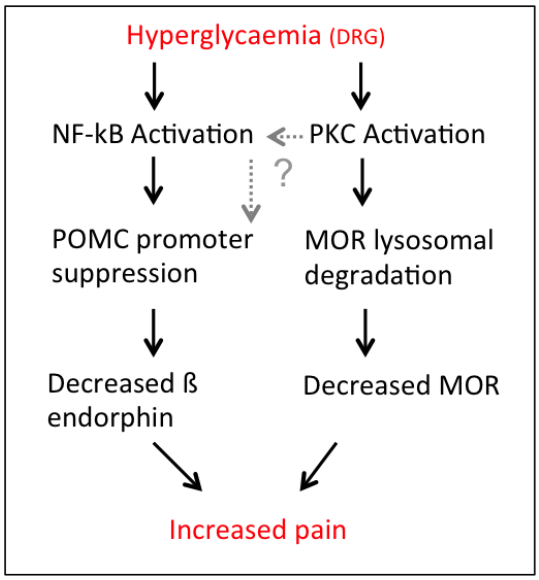

To this end, immune cell population, previously shown to be opioid source in injured nerves were studied in the diabetic sciatic nerves. Though there was a significant increase in the number of leukocytes and macrophages in the sciatic nerves, a negligible number of these immune cells expressed opioid peptides. Instead, the opioids present in the sciatic nerves were derived from the neuronal cells present in the lumbar DRG. The neuronal cells of DRG were susceptible to STZ and exhibited transient changes in the opioid expression following STZ induction. However, at 12 weeks post induction, effect of STZ had subsided and opioid levels were restored. At this time point, although the PENK and PDYN peptide level had returned to normal, POMC peptide level in the DRG, sciatic nerves and footpads remained significantly downregulated. A downregulation in ß-endorphin and its receptor MOR was also observed in the diabetic mice. While, downregulation of MOR seemed to be due to its lysosomal degradation induced by activated PKC, POMC promoter suppression seemed to be partly mediated by high glucose induced NF-kB. Interestingly, the downregulated POMC-MOR levels correlated with increased thermal and mechanical pain sensitivity of the STZ mice. Taken together, this data indicates that POMC-MOR proteins are involved in the hyperalgesia experienced during diabetic peripheral neuropathy and restoring their normal level may endogenous levels may prove to be a novel therapeutic strategy against painful diabetic neuropathy.

Zussamenfassung

Periphere diabetische Neuropathie (PDN) ist eine belastende Komplikation, welche die Lebensqualität von diabetischen Patienten stark beeinflusst. Aktuelle Behandlungen für PDN wie opioide Analgetika sind ineffektiv, während andere namentlich Pregabalin, Duloxetin etc. negative Nebeneffekte haben. Daher wurde zur Erforschung der zugrundeliegenden Mechanismen der Anomalien bei der Schmerzwahrnehmung in PDN die Expression von endogenen Opioidpeptiden in STZ induzierten Mäusen mit DPN untersucht.

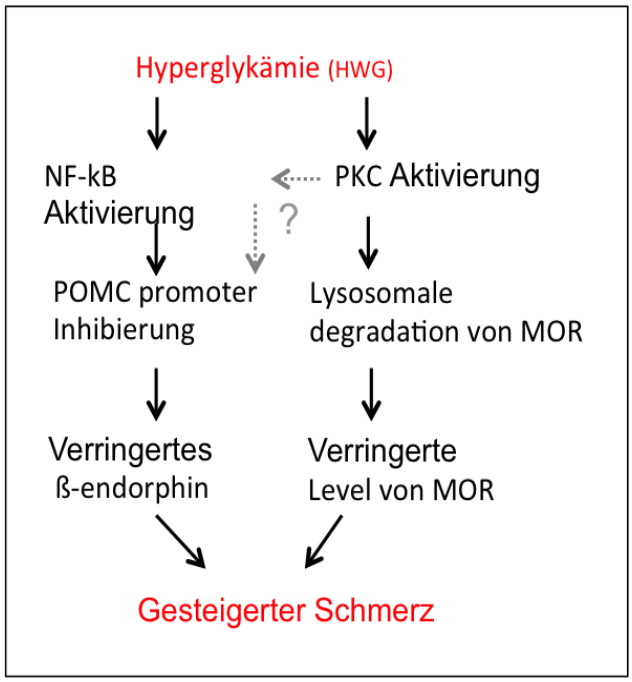

Dazu wurden Immunzellpopulationen, welche als Quelle von Opioiden in verletzten Nerven identifiziert wurden, in diabetischen Ischiasnerven untersucht. Trotz eines signifikanten Anstiegs in der Anzahl der Leukozyten und Makrophagen exprimierte nur eine vernachlässigbare Anzahl dieser Zellen Opioidpeptide. Stattdessen wurden die nachweisbaren Opioide in Ischiasnerven von den neuronalen Zellen der lumbalen Hinterwurzelganglien (HWGs) exprimiert. Die neuronalen Zellen der HWG waren anfällig für STZ und zeigten nach der Behandlung mit STZ kurzzeitige Veränderungen in der Opioidexpression. 12 Wochen nach der Induktion klangen diese Effekte ab und die Opioidlevel normalisierten sich. Obwohl die Level von PENK und PDYN sich normalisierten, blieben die Level des POMC Peptides in HWGs, Ischiasnerven und Fußsohlen signifikant verringert. Außerdem waren ß-Endorphin und sein Rezeptor MOR in diabetischen Mäusen runter reguliert. Das verringerte Level von MOR scheint in dessen lysosomaler Degradation, induziert durch aktivierte PKC, begründet zu sein. Die geringeren POMC Level scheinen ihre Ursache teilweise in erhöhter Glukose und daraus resultierender Inhibierung des POMC Promoters durch NF-kB zu haben. Interessanterweise korrelieren die verringerten POMC-MOR Level mit gesteigerter thermaler und mechanischer Schmerzempfindlichkeit bei den mit STZ induzierten

Mäusen. Zusammengenommen deuten diese Daten darauf hin, dass die POMC-MOR Proteine an der Hyperalgesie bei peripherer diabetischer Neuropathie beteiligt sind und die Normalisierung des endogenen Levels eine mögliche therapeutische Strategie gegen schmerzhafte diabetische Neuropathie sein könnte.

References

1. Danaei, G. *et al.* National, regional, and global trends in fasting plasma glucose and diabetes prevalence since 1980: systematic analysis of health examination surveys and epidemiological studies with 370 country-years and 2·7 million participants. *Lancet Lond. Engl.* **378,** 31–40 (2011).
2. WHO | Diabetes. *WHO* Available at: http://www.who.int/mediacentre/factsheets/fs312/en/. (Accessed: 16th February 2017)
3. Callaghan, B. C., Little, A. A., Feldman, E. L. & Hughes, R. A. C. Enhanced glucose control for preventing and treating diabetic neuropathy. *Cochrane Database Syst. Rev.* CD007543 (2012). doi:10.1002/14651858.CD007543.pub2
4. Duby, J. J., Campbell, R. K., Setter, S. M., White, J. R. & Rasmussen, K. A. Diabetic neuropathy: an intensive review. *Am. J. Health-Syst. Pharm. AJHP Off. J. Am. Soc. Health-Syst. Pharm.* **61,** 160-173-176 (2004).
5. Ziegler, D., Papanas, N., Vinik, A. I. & Shaw, J. E. Epidemiology of polyneuropathy in diabetes and prediabetes. *Handb. Clin. Neurol.* **126,** 3–22 (2014).
6. Boulton, A. J. in *Endotext* (eds. De Groot, L. J. et al.) (MDText.com, Inc., 2000).
7. van Baal, J., Hubbard, R., Game, F. & Jeffcoate, W. Mortality associated with acute Charcot foot and neuropathic foot ulceration. *Diabetes Care* **33,** 1086–1089 (2010).
8. Ismail-Beigi, F. *et al.* Effect of intensive treatment of hyperglycaemia on microvascular outcomes in type 2 diabetes: an analysis of the ACCORD randomised trial. *Lancet Lond. Engl.* **376,** 419–430 (2010).
9. Duckworth, W. *et al.* Glucose Control and Vascular Complications in Veterans with Type 2 Diabetes. *N. Engl. J. Med.* **360,** 129–139 (2009).
10. Gæde, P., Lund-Andersen, H., Parving, H.-H. & Pedersen, O. Effect of a Multifactorial Intervention on Mortality in Type 2 Diabetes. *N. Engl. J. Med.* **358,** 580–591 (2008).
11. Ziegler, D. & Fonseca, V. From guideline to patient: a review of recent recommendations for pharmacotherapy of painful diabetic neuropathy. *J. Diabetes Complications* **29,** 146–156 (2015).
12. Tesfaye, S. *et al.* Duloxetine and pregabalin: high-dose monotherapy or their combination? The 'COMBO-DN study'--a multinational, randomized, double-blind, parallel-group study in patients with diabetic peripheral neuropathic pain. *Pain* **154,** 2616–2625 (2013).
13. Cohen, K., Shinkazh, N., Frank, J., Israel, I. & Fellner, C. Pharmacological Treatment Of Diabetic Peripheral Neuropathy. *Pharm. Ther.* **40,** 372–388 (2015).
14. Gibbons, C. H. & Freeman, R. Treatment-induced neuropathy of diabetes: an acute, iatrogenic complication of diabetes. *Brain* **138,** 43–52 (2015).
15. Vincent, A. M., Callaghan, B. C., Smith, A. L. & Feldman, E. L. Diabetic neuropathy: cellular mechanisms as therapeutic targets. *Nat. Rev. Neurol.* **7,** 573–583 (2011).
16. Benarroch, E. E. Endogenous opioid systems Current concepts and clinical correlations. *Neurology* **79,** 807–814 (2012).
17. Fichna, J., Janecka, A., Costentin, J. & Do Rego, J.-C. The endomorphin system and its evolving neurophysiological role. *Pharmacol. Rev.* **59,** 88–123 (2007).
18. Reinscheid, R. K. *et al.* Orphanin FQ: a neuropeptide that activates an opioidlike G protein-coupled receptor. *Science* **270,** 792–794 (1995).
19. Tegeder, I. & Geisslinger, G. Opioids As Modulators of Cell Death and Survival—Unraveling Mechanisms and Revealing New Indications. *Pharmacol. Rev.* **56,** 351–369 (2004).
20. Nakanishi, S., Taii, S., Hirata, Y., Matsukura, S. & Imura, H. A large product of cell-free translation of messenger RNA coding for corticotropin. *Proc. Natl. Acad. Sci.* **73,** 4319–4323 (1976).
21. Takahashi, H. *et al.* Complete nucleotide sequence of the human corticotropin-beta-lipotropin precursor gene. *Nucleic Acids Res.* **11,** 6847–6858 (1983).
22. Nakanishi, S. *et al.* Isolation and characterization of the bovine corticotropin/beta-lipotropin precursor gene. *Eur. J. Biochem.* **115,** 429–438 (1981).

23. Drouin, J., Chamberland, M., Charron, J., Jeannotte, L. & Nemer, M. Structure of the rat pro-opiomelanocortin (POMC) gene. *FEBS Lett.* **193,** 54–58 (1985).
24. Notake, M. *et al.* Isolation and characterization of the mouse corticotropin-beta-lipotropin precursor gene and a related pseudogene. *FEBS Lett.* **156,** 67–71 (1983).
25. Jin, W. D. *et al.* Characterization of a corticotropin-releasing hormone-responsive element in the rat proopiomelanocortin gene promoter and molecular cloning of its binding protein. *Mol. Endocrinol. Baltim. Md* **8,** 1377–1388 (1994).
26. Charron, J. & Drouin, J. Glucocorticoid inhibition of transcription from episomal proopiomelanocortin gene promoter. *Proc. Natl. Acad. Sci. U. S. A.* **83,** 8903–8907 (1986).
27. Karalis, K. P., Venihaki, M., Zhao, J., van Vlerken, L. E. & Chandras, C. NF-kappaB participates in the corticotropin-releasing, hormone-induced regulation of the pituitary proopiomelanocortin gene. *J. Biol. Chem.* **279,** 10837–10840 (2004).
28. Jang, P.-G. *et al.* NF-kappaB activation in hypothalamic pro-opiomelanocortin neurons is essential in illness- and leptin-induced anorexia. *J. Biol. Chem.* **285,** 9706–9715 (2010).
29. Cawley, N. X., Li, Z. & Loh, Y. P. 60 YEARS OF POMC: Biosynthesis, trafficking, and secretion of pro-opiomelanocortin-derived peptides. *J. Mol. Endocrinol.* **56,** T77–T97 (2016).
30. Feldberg, W. & Smyth, D. G. C-fragment of lipotropin—an endogenous potent analgesic peptide. *Br. J. Pharmacol.* **60,** 445–453 (1977).
31. Foley, K. M. *et al.* β-Endorphin: Analgesic and hormonal effects in humans. *Proc. Natl. Acad. Sci. U. S. A.* **76,** 5377–5381 (1979).
32. Al-Fayoumi, S. I. *et al.* Identification of stabilized dynorphin derivatives for suppressing tolerance in morphine-dependent rats. *Pharm. Res.* **21,** 1450–1456 (2004).
33. Sokolov, O. Y. *et al.* Half-life of leu-enkephalin in the serum of infants of the first year of life on different types of feeding: relationship with temperament. *Bull. Exp. Biol. Med.* **137,** 342–344 (2004).
34. Jones, B. N. *et al.* Structure of two adrenal polypeptides containing multiple enkephalin sequences. *Arch. Biochem. Biophys.* **204,** 392–395 (1980).
35. Kley, N. & Loeffler, J. P. in *Opioids* (eds. Herz, P. D. med A., Akil, D. med H. & Simon, D. med E. J.) 379–392 (Springer Berlin Heidelberg, 1993). doi:10.1007/978-3-642-77460-7_16
36. Guitart, X., Thompson, M. A., Mirante, C. K., Greenberg, M. E. & Nestler, E. J. Regulation of cyclic AMP response element-binding protein (CREB) phosphorylation by acute and chronic morphine in the rat locus coeruleus. *J. Neurochem.* **58,** 1168–1171 (1992).
37. Sonnenberg, J. L., Rauscher, F. J., Morgan, J. I. & Curran, T. Regulation of proenkephalin by Fos and Jun. *Science* **246,** 1622–1625 (1989).
38. Rosen, H., Krichevsky, A., Polakiewicz, R. D., Benzakine, S. & Bar-Shavit, Z. Developmental regulation of proenkephalin gene expression in osteoblasts. *Mol. Endocrinol. Baltim. Md* **9,** 1621–1631 (1995).
39. Geracioti Jr., T. D., Strawn, J. R., Ekhator, N. N., Wortman, M. & Kasckow, J. in *Hormones, Brain and Behavior (Second Edition)* (eds. Pfaff, D. W., Arnold, A. P., Etgen, A. M., Fahrbach, S. E. & Rubin, R. T.) 2541–2599 (Academic Press, 2009). doi:10.1016/B978-008088783-8.00082-6
40. Breslin, M. B. *et al.* Differential processing of proenkephalin by prohormone convertases 1(3) and 2 and furin. *J. Biol. Chem.* **268,** 27084–27093 (1993).
41. Paletzki, R. F. *et al.* Inhibiting AP-1 activity alters cocaine induced gene expression and potentiates sensitization. *Neuroscience* **152,** 1040–1053 (2008).
42. Naranjo, J. R., Mellström, B., Achaval, M. & Sassone-Corsi, P. Molecular pathways of pain: Fos/Jun-mediated activation of a noncanonical AP-1 site in the prodynorphin gene. *Neuron* **6,** 607–617 (1991).
43. Bakalkin, G., Yakovleva, T. & Terenius, L. Prodynorphin gene expression relates to NF-κB factors. *Mol. Brain Res.* **24,** 301–312 (1994).
44. Huang, M. *et al.* Ptf1a, Lbx1 and Pax2 coordinate glycinergic and peptidergic transmitter phenotypes in dorsal spinal inhibitory neurons. *Dev. Biol.* **322,** 394–405 (2008).
45. Day, R. *et al.* Prodynorphin processing by proprotein convertase 2. Cleavage at single basic residues and enhanced processing in the presence of carboxypeptidase activity. *J. Biol. Chem.* **273,** 829–836 (1998).

46. Khachaturian, H., Lewis, M. E., Schäfer, M. K.-H. & Watson, S. J. Anatomy of the CNS opioid systems. *Trends Neurosci.* **8,** 111–119 (1985).
47. Williams, J. Basic Opioid Pharmacology. *Rev. Pain* **1,** 2–5 (2008).
48. Gomes, I., Filipovska, J., Jordan, B. A. & Devi, L. A. Oligomerization of opioid receptors. *Methods San Diego Calif* **27,** 358–365 (2002).
49. Liu, X.-Y. *et al.* Unidirectional cross-activation of GRPR by MOR1D uncouples itch and analgesia induced by opioids. *Cell* **147,** 447–458 (2011).
50. Connor, M. & Kitchen, I. Has the sun set on kappa3-opioid receptors? *Br. J. Pharmacol.* **147,** 349–350 (2006).
51. Gold, M. S. & Levine, J. D. DAMGO inhibits prostaglandin E2-induced potentiation of a TTX-resistant Na+ current in rat sensory neurons in vitro. *Neurosci. Lett.* **212,** 83–86 (1996).
52. Chizhmakov, I. *et al.* Opioids inhibit purinergic nociceptors in the sensory neurons and fibres of rat via a G protein-dependent mechanism. *Neuropharmacology* **48,** 639–647 (2005).
53. Petraschka, M. *et al.* The absence of endogenous beta-endorphin selectively blocks phosphorylation and desensitization of mu opioid receptors following partial sciatic nerve ligation. *Neuroscience* **146,** 1795–1807 (2007).
54. Dang, V. C., Chieng, B., Azriel, Y. & Christie, M. J. Cellular morphine tolerance produced by βarrestin-2-dependent impairment of μ-opioid receptor resensitization. *J. Neurosci. Off. J. Soc. Neurosci.* **31,** 7122–7130 (2011).
55. Soohoo, A. L. & Puthenveedu, M. A. Divergent modes for cargo-mediated control of clathrin-coated pit dynamics. *Mol. Biol. Cell* **24,** 1725–1734, S1-12 (2013).
56. Roman-Vendrell, C., Yu, Y. J. & Yudowski, G. A. Fast Modulation of μ-Opioid Receptor (MOR) Recycling Is Mediated by Receptor Agonists. *J. Biol. Chem.* **287,** 14782–14791 (2012).
57. He, L., Fong, J., von Zastrow, M. & Whistler, J. L. Regulation of opioid receptor trafficking and morphine tolerance by receptor oligomerization. *Cell* **108,** 271–282 (2002).
58. Pfeiffer, M. *et al.* Heterodimerization of substance P and mu-opioid receptors regulates receptor trafficking and resensitization. *J. Biol. Chem.* **278,** 51630–51637 (2003).
59. Illing, S., Mann, A. & Schulz, S. Heterologous regulation of agonist-independent μ-opioid receptor phosphorylation by protein kinase C. *Br. J. Pharmacol.* **171,** 1330–1340 (2014).
60. Zhan, C. *et al.* Acute and long-term suppression of feeding behavior by POMC neurons in the brainstem and hypothalamus, respectively. *J. Neurosci. Off. J. Soc. Neurosci.* **33,** 3624–3632 (2013).
61. Mechling, A. E. *et al.* Deletion of the mu opioid receptor gene in mice reshapes the reward–aversion connectome. *Proc. Natl. Acad. Sci.* **113,** 11603–11608 (2016).
62. Motanis, H., Maroun, M. & Barkai, E. Learning-induced bidirectional plasticity of intrinsic neuronal excitability reflects the valence of the outcome. *Cereb. Cortex N. Y. N 1991* **24,** 1075–1087 (2014).
63. Khakpai, F. The effect of opiodergic system and testosterone on anxiety behavior in gonadectomized rats. *Behav. Brain Res.* **263,** 9–15 (2014).
64. Pradhan, A. A., Befort, K., Nozaki, C., Gavériaux-Ruff, C. & Kieffer, B. L. The delta opioid receptor: an evolving target for the treatment of brain disorders. *Trends Pharmacol. Sci.* **32,** 581–590 (2011).
65. Knoll, A. T. & Carlezon, W. A. Dynorphin, stress, and depression. *Brain Res.* **1314,** 56–73 (2010).
66. Pohl, M. *et al.* Expression of preproenkephalin A gene and presence of Met-enkephalin in dorsal root ganglia of the adult rat. *J. Neurochem.* **63,** 1226–1234 (1994).
67. Braz, J. *et al.* Therapeutic efficacy in experimental polyarthritis of viral-driven enkephalin overproduction in sensory neurons. *J. Neurosci. Off. J. Soc. Neurosci.* **21,** 7881–7888 (2001).
68. Obara, I. *et al.* Local peripheral opioid effects and expression of opioid genes in the spinal cord and dorsal root ganglia in neuropathic and inflammatory pain. *Pain* **141,** 283–291 (2009).
69. Höftberger, R. *et al.* Peroxisomal localization of the proopiomelanocortin-derived peptides beta-lipotropin and beta-endorphin. *Endocrinology* **151,** 4801–4810 (2010).

70. Merighi, A. *et al.* The immunocytochemical distribution of seven peptides in the spinal cord and dorsal root ganglia of horse and pig. *Anat. Embryol. (Berl.)* **181,** 271–280 (1990).
71. Jolivalt, C. G., Jiang, Y., Freshwater, J. D., Bartoszyk, G. D. & Calcutt, N. A. Dynorphin A, kappa opioid receptors and the antinociceptive efficacy of asimadoline in streptozotocin-induced diabetic rats. *Diabetologia* **49,** 2775–2785 (2006).
72. Liou, J.-T., Liu, F.-C., Mao, C.-C., Lai, Y.-S. & Day, Y.-J. Inflammation confers dual effects on nociceptive processing in chronic neuropathic pain model. *Anesthesiology* **114,** 660–672 (2011).
73. Liang, X., Liu, R., Chen, C., Ji, F. & Li, T. Opioid System Modulates the Immune Function: A Review. *Transl. Perioper. Pain Med.* **1,** 5–13 (2016).
74. Al-Hashimi, M., Scott, S. W. M., Thompson, J. P. & Lambert, D. G. Opioids and immune modulation: more questions than answers. *Br. J. Anaesth.* **111,** 80–88 (2013).
75. Forman, L. J., Estilow, S. & Hock, C. E. Localization of beta-endorphin in the rat heart and modulation by testosterone. *Proc. Soc. Exp. Biol. Med. Soc. Exp. Biol. Med. N. Y. N* **190,** 240–245 (1989).
76. Lang, R. E. *et al.* Evidence for the presence of enkephalins in the heart. *Life Sci.* **32,** 399–406 (1983).
77. Weihe, E., McKnight, A. T., Corbett, A. D. & Kosterlitz, H. W. Proenkephalin- and prodynorphin- derived opioid peptides in guinea-pig heart. *Neuropeptides* **5,** 453–456 (1985).
78. Feng, Y. *et al.* Current Research on Opioid Receptor Function. *Curr. Drug Targets* **13,** 230–246 (2012).
79. Holzer, P. Opioid receptors in the gastrointestinal tract. *Regul. Pept.* **155,** 11–17 (2009).
80. Slominski, A. On the role of the endogenous opioid system in regulating epidermal homeostasis. *J. Invest. Dermatol.* **135,** 333–334 (2015).
81. Schafer, M., Carter, L. & Stein, C. Interleukin 1β and Corticotropin-Releasing Factor Inhibit Pain by Releasing Opioids from Immune Cells in Inflamed Tissue. *Proc. Natl. Acad. Sci. U. S. A.* **91,** 4219–4223 (1994).
82. Machelska, H. & Stein, C. Leukocyte-derived opioid peptides and inhibition of pain. *J. Neuroimmune Pharmacol. Off. J. Soc. NeuroImmune Pharmacol.* **1,** 90–97 (2006).
83. Stein, C., Machelska, H., Binder, W. & Schäfer, M. Peripheral opioid analgesia. *Curr. Opin. Pharmacol.* **1,** 62–65 (2001).
84. Rittner, H. L., Machelska, H. & Stein, C. Leukocytes in the regulation of pain and analgesia. *J. Leukoc. Biol.* **78,** 1215–1222 (2005).
85. Zemel, M. B. & Shi, H. Pro-opiomelanocortin (POMC) deficiency and peripheral melanocortins in obesity. *Nutr. Rev.* **58,** 177–180 (2000).
86. Wiedermann, C. J. *et al.* Decreased beta-endorphin content in peripheral blood mononuclear leukocytes from patients with Crohn's disease. *Brain. Behav. Immun.* **8,** 261–269 (1994).
87. Halabe Bucay, A. Activation of the proopiomelanocortin gene with ketoconazole as a treatment for Parkinson's disease: a new hypothesis. *Ann. N. Y. Acad. Sci.* **1144,** 237–242 (2008).
88. Henderson-Smith, A. *et al.* Next-generation profiling to identify the molecular etiology of Parkinson dementia. *Neurol. Genet.* **2,** (2016).
89. Sandyk, R. The endogenous opioid system in neurological disorders of the basal ganglia. *Life Sci.* **37,** 1655–1663 (1985).
90. Walters, A. S., Ondo, W. G., Zhu, W. & Le, W. Does the endogenous opiate system play a role in the Restless Legs Syndrome? A pilot post-mortem study. *J. Neurol. Sci.* **279,** 62–65 (2009).
91. Gillman, M. A. & Sandyk, R. The endogenous opioid system in Gilles de la Tourette syndrome. *Med. Hypotheses* **19,** 371–378 (1986).
92. Corazziari, E. Role of opioid ligands in the irritable bowel syndrome. *Can. J. Gastroenterol. J. Can. Gastroenterol.* **13 Suppl A,** 71A–75A (1999).
93. Yakovleva, T. *et al.* Dysregulation of dynorphins in Alzheimer disease. *Neurobiol. Aging* **28,** 1700–1708 (2007).

94. Aleem, F. A. & McIntosh, T. Elevated plasma levels of beta-endorphin in a group of women with polycystic ovarian disease. *Fertil. Steril.* **42,** 686–689 (1984).
95. Gillberg, C., Terenius, L. & Lönnerholm, G. Endorphin activity in childhood psychosis. Spinal fluid levels in 24 cases. *Arch. Gen. Psychiatry* **42,** 780–783 (1985).
96. Forman, L. J., Marquis, D. E., Stevens, R., Adler, R. & Vasilenko, P. Diabetes induced by streptozocin results in a decrease in immunoreactive beta-endorphin levels in the pituitary and hypothalamus of female rats. *Diabetes* **34,** 1104–1107 (1985).
97. Forman, L. J., Estilow, S., Lewis, M. & Vasilenko, P. Streptozocin diabetes alters immunoreactive beta-endorphin levels and pain perception after 8 wk in female rats. *Diabetes* **35,** 1309–1313 (1986).
98. Cheung, C. Y. & Tang, F. The effect of streptozotocin-diabetes on beta-endorphin level and proopiomelanocortin gene expression in the rat pituitary. *Neurosci. Lett.* **261,** 118–120 (1999).
99. Greenberg, J. *et al.* Methionine-enkephalin and beta-endorphin levels in brain, pancreas, and adrenals of db/db mice. *Endocrinology* **116,** 328–331 (1985).
100. Timmers, K., Voyles, N. R., Zalenski, C., Wilkins, S. & Recant, L. Altered beta-endorphin, Met- and Leu-enkephalins, and enkephalin-containing peptides in pancreas and pituitary of genetically obese diabetic (db/db) mice during development of diabetic syndrome. *Diabetes* **35,** 1143–1151 (1986).
101. Berman, Y., Devi, L. & Carr, K. D. Effects of streptozotocin-induced diabetes on prodynorphin-derived peptides in rat brain regions. *Brain Res.* **685,** 129–134 (1995).
102. Fallucca, F., Tonnarini, G., Di Biase, N., D'Allessandro, M. & Negri, M. Plasma met-enkephalin levels in diabetic patients: influence of autonomic neuropathy. *Metabolism.* **45,** 1065–1068 (1996).
103. Juranek, J. K. *et al.* RAGE Deficiency Improves Postinjury Sciatic Nerve Regeneration in Type 1 Diabetic Mice. *Diabetes* **62,** 931–943 (2013).
104. Mousa, S. A. *et al.* Rab7 silencing prevents μ-opioid receptor lysosomal targeting and rescues opioid responsiveness to strengthen diabetic neuropathic pain therapy. *Diabetes* **62,** 1308–1319 (2013).
105. Mousa, S. A. *et al.* Protein kinase C-mediated mu-opioid receptor phosphorylation and desensitization in rats, and its prevention during early diabetes. *Pain* **157,** 910–921 (2016).
106. Shaqura, M. *et al.* Reduced number, G protein coupling, and antinociceptive efficacy of spinal mu-opioid receptors in diabetic rats are reversed by nerve growth factor. *J. Pain Off. J. Am. Pain Soc.* **14,** 720–730 (2013).
107. Stein, C. & Machelska, H. Modulation of peripheral sensory neurons by the immune system: implications for pain therapy. *Pharmacol. Rev.* **63,** 860–881 (2011).
108. Chen, S.-R. & Pan, H.-L. Antinociceptive effect of morphine, but not mu opioid receptor number, is attenuated in the spinal cord of diabetic rats. *Anesthesiology* **99,** 1409–1414 (2003).
109. Gunn, A., Bobeck, E. N., Weber, C. & Morgan, M. M. The Influence of Non-Nociceptive Factors on Hot Plate Latency in Rats. *J. Pain* **12,** 222–227 (2011).
110. Hargreaves, K., Dubner, R., Brown, F., Flores, C. & Joris, J. A new and sensitive method for measuring thermal nociception in cutaneous hyperalgesia. *Pain* **32,** 77–88 (1988).
111. Emery, M. A., Shawn Bates, M. L., Wellman, P. J. & Eitan, S. Hydrocodone is More Effective than Morphine or Oxycodone in Suppressing the Development of Burn-Induced Mechanical Allodynia. *Pain Med. Malden Mass* (2017). doi:10.1093/pm/pnx050
112. Bishnoi, M., Bosgraaf, C. A., Abooj, M., Zhong, L. & Premkumar, L. S. Streptozotocin-induced early thermal hyperalgesia is independent of glycemic state of rats: role of transient receptor potential vanilloid 1(TRPV1) and inflammatory mediators. *Mol. Pain* **7,** 52 (2011).
113. Pabbidi, R. M., Cao, D.-S., Parihar, A., Pauza, M. E. & Premkumar, L. S. Direct role of streptozotocin in inducing thermal hyperalgesia by enhanced expression of transient receptor potential vanilloid 1 in sensory neurons. *Mol. Pharmacol.* **73,** 995–1004 (2008).

114. Jenks, B. G. Regulation of Proopiomelanocortin Gene Expression. *Ann. N. Y. Acad. Sci.* **1163,** 17–30 (2009).
115. Zbytek, B., Pfeffer, L. M. & Slominski, A. T. CRH inhibits NF-κB signaling in human melanocytes. *Peptides* **27,** 3276–3283 (2006).
116. Asaba, K. *et al.* High glucose activates pituitary proopiomelanocortin gene expression: possible role of free radical-sensitive transcription factors. *Diabetes Metab. Res. Rev.* **23,** 317–323 (2007).
117. Havlicek, V., West, M., Kato, N. & Friesen, H. G. in *Endorphins and Opiate Antagonists in Psychiatric Research* (eds. Shah, N. S. & M.D, A. G. D.) 127–159 (Springer US, 1982). doi:10.1007/978-1-4684-1119-5_8
118. Bäckryd, E., Ghafouri, B., Larsson, B. & Gerdle, B. Do Low Levels of Beta-Endorphin in the Cerebrospinal Fluid Indicate Defective Top-Down Inhibition in Patients with Chronic Neuropathic Pain? A Cross-Sectional, Comparative Study. *Pain Med.* **15,** 111–119 (2014).
119. Basbaum, A. I. & Fields, H. L. Endogenous pain control systems: brainstem spinal pathways and endorphin circuitry. *Annu. Rev. Neurosci.* **7,** 309–338 (1984).
120. Taylor, A. M. W. *et al.* Anti-nociception mediated by a κ opioid receptor agonist is blocked by a δ receptor agonist. *Br. J. Pharmacol.* **172,** 691–703 (2015).
121. Pannell, M. *et al.* Adoptive transfer of M2 macrophages reduces neuropathic pain via opioid peptides. *J. Neuroinflammation* **13,** 262 (2016).
122. Celik, M. Ö. *et al.* Leukocyte opioid receptors mediate analgesia via Ca(2+)-regulated release of opioid peptides. *Brain. Behav. Immun.* **57,** 227–242 (2016).
123. Pham, M. *et al.* Magnetic resonance neurography detects diabetic neuropathy early and with Proximal Predominance. *Ann. Neurol.* **78,** 939–948 (2015).
124. Westly, H. J., Kleiss, A. J., Kelley, K. W., Wong, P. K. & Yuen, P. H. Newcastle disease virus-infected splenocytes express the proopiomelanocortin gene. *J. Exp. Med.* **163,** 1589–1594 (1986).
125. Buzzetti, R., McLoughlin, L., Lavender, P. M., Clark, A. J. & Rees, L. H. Expression of pro-opiomelanocortin gene and quantification of adrenocorticotropic hormone-like immunoreactivity in human normal peripheral mononuclear cells and lymphoid and myeloid malignancies. *J. Clin. Invest.* **83,** 733–737 (1989).
126. Ohta, K. *et al.* Thymic hyperplasia as a source of ectopic ACTH production. *Endocr. J.* **47,** 487–492 (2000).
127. Reinhold, A. K. *et al.* Differential Transcriptional Profiling of Damaged and Intact Adjacent Dorsal Root Ganglia Neurons in Neuropathic Pain. *PLoS ONE* **10,** (2015).
128. Gibbins, I. L., Furness, J. B. & Costa, M. Pathway-specific patterns of the co-existence of substance P, calcitonin gene-related peptide, cholecystokinin and dynorphin in neurons of the dorsal root ganglia of the guinea-pig. *Cell Tissue Res.* **248,** 417–437 (1987).
129. Genrikhs, E. E., Stelmashook, E. V., Golyshev, S. A., Aleksandrova, O. P. & Isaev, N. K. Streptozotocin causes neurotoxic effect in cultured cerebellar granule neurons. *Brain Res. Bull.* **130,** 90–94 (2017).
130. Davidson, E. *et al.* The Roles of Streptozotocin Neurotoxicity and Neutral Endopeptidase in Murine Experimental Diabetic Neuropathy. *Exp. Diabetes Res.* **2009,** (2009).
131. Freeman, O. J. *et al.* Metabolic Dysfunction Is Restricted to the Sciatic Nerve in Experimental Diabetic Neuropathy. *Diabetes* **65,** 228–238 (2016).
132. Cho, K. *et al.* Antihyperglycemic mechanism of metformin occurs via the AMPK/LXRα/POMC pathway. *Sci. Rep.* **5,** (2015).
133. Kou, Z.-Z. *et al.* Decreased Endomorphin-2 and μ-Opioid Receptor in the Spinal Cord Are Associated with Painful Diabetic Neuropathy. *Front. Mol. Neurosci.* **9,** 80 (2016).
134. Tsigos, C., Gibson, S., Crosby, S. R., White, A. & Young, R. J. Cerebrospinal fluid levels of beta endorphin in painful and painless diabetic polyneuropathy. *J. Diabetes Complications* **9,** 92–96 (1995).
135. Ma, W. *et al.* FoxO1 negatively regulates leptin-induced POMC transcription through its direct interaction with STAT3. *Biochem. J.* **466,** 291–298 (2015).

136. Nudi, M., Ouimette, J.-F. & Drouin, J. Bone Morphogenic Protein (Smad)-Mediated Repression of Proopiomelanocortin Transcription by Interference with Pitx/Tpit Activity. *Mol. Endocrinol.* **19,** 1329–1342 (2005).
137. Takayasu, S. *et al.* Involvement of Nuclear Factor-κB and Nurr-1 in Cytokine-Induced Transcription of Proopiomelanocortin Gene in AtT20 Corticotroph Cells. *Neuroimmunomodulation* **17,** 88–96 (2010).
138. Shi, X. *et al.* Nuclear factor κB (NF-κB) suppresses food intake and energy expenditure in mice by directly activating the Pomc promoter. *Diabetologia* **56,** 925–936 (2013).
139. Zhang, H.-H. *et al.* Promoted Interaction of Nuclear Factor-κB With Demethylated Purinergic P2X3 Receptor Gene Contributes to Neuropathic Pain in Rats With Diabetes. *Diabetes* **64,** 4272–4284 (2015).
140. Zhong, H., May, M. J., Jimi, E. & Ghosh, S. The Phosphorylation Status of Nuclear NF-KB Determines Its Association with CBP/p300 or HDAC-1. *Mol. Cell* **9,** 625–636 (2002).
141. Grundström, S., Anderson, P., Scheipers, P. & Sundstedt, A. Bcl-3 and NFκB p50-p50 Homodimers Act as Transcriptional Repressors in Tolerant CD4+ T Cells. *J. Biol. Chem.* **279,** 8460–8468 (2004).
142. Kastenbauer, S. & Ziegler-Heitbrock, H. W. NF-kappaB1 (p50) is upregulated in lipopolysaccharide tolerance and can block tumor necrosis factor gene expression. *Infect. Immun.* **67,** 1553–1559 (1999).
143. Kang, S. M., Tran, A. C., Grilli, M. & Lenardo, M. J. NF-kappa B subunit regulation in nontransformed CD4+ T lymphocytes. *Science* **256,** 1452–1456 (1992).
144. Erdman, S., Fox, J. G., Dangler, C. A., Feldman, D. & Horwitz, B. H. Typhlocolitis in NF-kappa B-deficient mice. *J. Immunol. Baltim. Md 1950* **166,** 1443–1447 (2001).
145. Djuric, Z. *et al.* Targeting Activation of Specific NF-κB Subunits Prevents Stress-Dependent Atherothrombotic Gene Expression. *Mol. Med.* **18,** 1375–1386 (2012).
146. O'Connor, S., Shumway, S. D., Amanna, I. J., Hayes, C. E. & Miyamoto, S. Regulation of Constitutive p50/c-Rel Activity via Proteasome Inhibitor-Resistant IκBα Degradation in B Cells. *Mol. Cell. Biol.* **24,** 4895–4908 (2004).
147. Williams, J. T. *et al.* Regulation of μ-Opioid Receptors: Desensitization, Phosphorylation, Internalization, and Tolerance. *Pharmacol. Rev.* **65,** 223–254 (2013).
148. Chavakis, T. *et al.* The pattern recognition receptor (RAGE) is a counterreceptor for leukocyte integrins: a novel pathway for inflammatory cell recruitment. *J. Exp. Med.* **198,** 1507–1515 (2003).
149. Chen, S.-R., Sweigart, K. L., Lakoski, J. M. & Pan, H.-L. Functional mu opioid receptors are reduced in the spinal cord dorsal horn of diabetic rats. *Anesthesiology* **97,** 1602–1608 (2002).
150. Gupta, D. S., von Gizycki, H. & Gintzler, A. R. Sex-/ovarian steroid-dependent release of endomorphin 2 from spinal cord. *J. Pharmacol. Exp. Ther.* **321,** 635–641 (2007).
151. Cicero, T. J., Nock, B. & Meyer, E. R. Gender-related differences in the antinociceptive properties of morphine. *J. Pharmacol. Exp. Ther.* **279,** 767–773 (1996).
152. Fillingim, R. B. & Gear, R. W. Sex differences in opioid analgesia: clinical and experimental findings. *Eur. J. Pain Lond. Engl.* **8,** 413–425 (2004).
153. Colao, A. *et al.* Corticotropin-releasing hormone administration increases alpha-melanocyte-stimulating hormone levels in the inferior petrosal sinuses in a subset of patients with Cushing's disease. *Horm. Res.* **46,** 26–32 (1996).